VOLUME 53, NO. 1 | **2020**
CHEMISTRY IN CHINA SPECIAL ISSUE (中国特刊)

MilliporeSigma

ALDRICHIMICA ACTA

CONTRIBUTORS TO THIS ISSUE (此特刊的贡献者)

Xiaoming Feng (冯小明), Sichuan University
Shu-Li You (游书力), SIOC, Chinese Academy of Sciences
Xuefeng Jiang (姜雪峰), East China Normal University
Wenjun Tang (汤文军), SIOC, Chinese Academy of Sciences

DEAR READER:

By most measures, China's transformation over the past half-century has been nothing short of spectacular, with its economy now ranked second in the world, an annual GDP north of USD 13 trillion, and 119 Chinese companies making it into Fortune magazine's Global 500 list.

Noteworthy also are China's commitment to, and remarkable advances in, basic and applied research in the natural sciences. Factors such as increased funding for scientific research, workforce qualification and size, and research output, quality, and innovation have propelled China to the #1 spot worldwide in terms of chemistry papers published,[1] and Chinese Universities to occupy 5 of the top 10 spots in chemistry research quality worldwide.[2]

At Merck KGaA, Darmstadt, Germany, we laud China's vigorous research efforts in chemistry and the life sciences, which we believe hold great promise for improving the quality of life for millions of people throughout the world. Moreover, we look forward to establishing strong collaborations with Chinese researchers to make their inventions more accessible worldwide to advance human health for all.

[1] *Nature* Index Country/Territory Outputs – Chemistry (https://www.natureindex.com/country-outputs/generate/Chemistry/global/All/n_article)

[2] *Nature* Index 2019 Tables: Institutions – Chemistry (https://www.natureindex.com/annual-tables/2019/institution/all/chemistry)

Sincerely yours,

Klaus-Reinhard Bischoff
Executive Vice President, MilliporeSigma
Head of Research Solutions
Global Business Unit

ALDRICHIMICA ACTA
VOL. 53, NO. 1 • 2020

Merck KGaA, Darmstadt, Germany
Frankfurter Strasse 250
64293 Darmstadt, Germany
Phone +49 6151 72 0

To Place Orders / Customer Service
Contact your local office or visit
SigmaAldrich.com/order

Technical Service
Contact your local office or visit
SigmaAldrich.com/techinfo

General Correspondence
Editor: Sharbil J. Firsan, Ph.D.
Sharbil.Firsan@milliporesigma.com

Subscriptions
Request your FREE subscription to the *Aldrichimica Acta* at **SigmaAldrich.com/Acta**

The entire *Aldrichimica Acta* archive is available at **SigmaAldrich.com/Acta**

Aldrichimica Acta (ISSN 0002-5100) is a publication of Merck KGaA, Darmstadt, Germany.

"PLEASE BOTHER US."

Dear Fellow Chemists,

Professor Xiaoming Feng of the College of Chemistry at Sichuan University kindly suggested that we offer Feng L_3-$PiPr_2$ (**904988**) and Feng L_3-$PrPr_2$ (**904961**) as chiral, *N*,*N*′-dioxide ligands for metals such as nickel(II), indium(III), scandium(III), cobalt(II), yttrium(III), and magnesium(II). The resulting stable complexes act as efficient catalysts for a number of important asymmetric transformations such as ring opening–cycloaddition, Michael addition–alkylation, 1,3-dipolar cycloaddition, and homologation of α-keto esters—leading to the desirable products in high yields and very high diastereo- and enantioselectivities.

(1) Zhang, H. et al. *Org. Lett.* **2019**, *21*, 2388. (2) Kuang, Y. et al. *Chem. Sci.* **2018**, *9*, 688. (3) Zhang, D. et al. *Chem. Commun.* **2017**, *53*, 7925. (4) Li, W. et al. *Angew. Chem., Int. Ed.* **2013**, *52*, 10883.

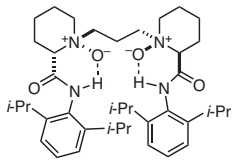

904988
Feng L_3-$PiPr_2$
(1*R*,1′*R*,2*S*,2′*S*)

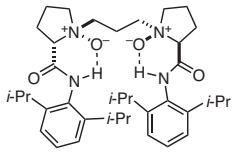

904961
Feng L_3-$PrPr_2$
(1*R*,1′*R*,2*S*,2′*S*)

904988	Feng L_3-$PiPr_2$, ≥95%	100 mg
904961	Feng L_3-$PrPr_2$, ≥95%	100 mg

We welcome your product ideas. Email your suggestion to **techserv@sial.com**.

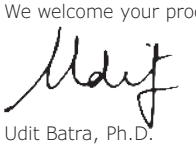

Udit Batra, Ph.D.
CEO, Life Science

TABLE OF CONTENTS

ABOUT OUR COVER

How did we in the West end up calling Zhōngguó (中国), China? Several theories exist, but what is making the "Central State" a critical player on the world stage today is not fine china, silk, or tea; rather, it is the breathtaking advances it has made in the past few decades, particularly in science and technology. We, of course, are mostly interested in the life science and physical science advances there. What better to illustrate these advances than the small selection of world-class chemical research that we are featuring in this issue—research that is being carried out at some of the most prestigious Chinese institutions. We hope this gets you as excited about the promise of chemistry research in China and its benefit to mankind as it does us.

Detail from ***One Hundred Flowers***. Photo courtesy The Metropolitan Museum of Art, New York, NY.

One Hundred Flowers (ink and color on silk, 41.9 x 649 cm) is an unattributed, fine handscroll composed during the Qing Dynasty after the style of the well-known Chinese artist Yun Shouping (1633–1690). It depicts a recurring theme in earlier Chinese paintings—flowers in bloom in a seemingly natural setting. This, however, is clearly a composite scene of blooming peonies* with other blossoming flowers, not unlike the still-life-with-flowers genre in western paintings.

This painting is a bequest of John M. Crawford Jr. to the Metropolitan Museum of Art, New York, NY.

** Peonies appear in many Chinese paintings of the past. What could the reason be? To find out, visit* ***SigmaAldrich.com/Acta***

MilliporeSigma

Find your Lead

Leverage DNA-encoded library technology for drug discovery

Accelerate your drug discovery with the DNA-encoded library (DEL) technology, an alternative approach to high-throughput screening (HTS) compound libraries for effective hit and lead discovery.

Learn more about the DyNAbind off-the-shelf DNA-encoded library, visit **SigmaAldrich.com/DEL**

Sigma-Aldrich®
Lab & Production Materials

Asymmetric Catalysis Enabled by Chiral *N,N'*-Dioxide–Nickel(II) Complexes


Prof. Z. Wang


Prof. X. H. Liu


Prof. X. M. Feng

Zhen Wang, Xiaohua Liu,* and Xiaoming Feng*

Key Laboratory of Green Chemistry and Technology
Ministry of Education
College of Chemistry
Sichuan University
29 Wangjiang Road, Jiuyan Bridge
Chengdu, Sichuan 610064, China
Email: xmfeng@scu.edu.cn; liuxh@scu.edu.cn

Keywords. asymmetric catalysis; chiral *N,N'*-dioxide ligand; nickel(II) complex; rearrangements; ene-type reactions; Friedel–Crafts reaction; allylboration; Mannich reaction; Michael reaction; bioactive compounds.

Abstract. The development of efficient catalysts and ligands bearing novel chiral backbones plays a crucial role in asymmetric catalysis. Our group has developed conformationally flexible, C_2-symmetric *N,N'*-dioxide amide compounds as a new class of privileged ligands, which form complexes with a number of metal salts leading to efficient catalysts for a number of asymmetric reactions. In this review, we highlight important asymmetric reactions that are promoted by chiral *N,N'*-dioxide–Ni(II) complexes, and shed some light on their mode of action.

Outline

1. Introduction

Catalytic asymmetric reactions have been recognized as fundamental synthetic methods for the construction of optically active compounds.[1–5] Impressive progress has been achieved by using sets of privileged synthetic chiral catalysts that include ligand–metal complexes and organocatalysts.[3,5] In enantioselective coordination catalysis and organometallic catalysis, ligand–metal interactions play a key role in almost every event.[6] An important property of the metal species is their ability to bind the substrate molecules via redistribution of electron density or cleavage in a specific array that is beneficial to high regio- and/or stereoselectivity. Meanwhile, the nature of the chiral ligands plays a crucial role in constructing the three-dimensional structures of the complexes and determining their catalytic activity and specificity.

Over the past two decades, our group has developed a class of C_2-symmetric amine oxide ligands, which are easily prepared from optically active amino acids and amines (aliphatic or aromatic) (**Figure 1**). The two *N*-oxide amide units are linked in such a way that conformation-flexible, straight-chain alkanes [–$(CH_2)_{2,3,4,5...}$–] are used. The structure is similar to nunchucks, pronounced "*Shuangjie Gun*" in Chinese, a weapon in Kungfu fighting. There are four oxygen donor groups in *N,N'*-dioxide ligands, all of which can simultaneously bond to the metal center, resulting in very stable complexes. The metal cations derive from main-group metals, transition metals, and rare-earth metals. Our extensive investigations have shown that the resulting chiral *N,N'*-dioxide–metal complexes exhibit excellent reactivity and enantiocontrol in more than 50 types of reactions with wide substrate scopes under mild reaction conditions. Their discovery, structure information, and some applications have been described in several accounts,[7] and will not be discussed in details herein. This mini-review focuses on the catalytic aspects of the chiral *N,N'*-dioxide–nickel(II) complexes in asymmetric reactions.

Nickel(II) forms a large number of complexes with complicated stereochemistry, encompassing coordination numbers 4, 5, and 6, and belonging to all the main structural types. On the other hand,

nickel(II)–*N,N'*-dioxide complexes have a relatively simple distorted octahedral 20-electron arrangement.[8] The powders of such nickel(II) complexes—formed from $Ni(BF_4)_2$ or $Ni(ClO_4)_2$—are characteristically green, and their X-ray crystal structures show that the chelating tetradentate ligands of the chiral *N,N'*-dioxides provide increased stability and a higher degree of control over the chiral coordination environment around the nickel center. The data related to the bite angles generated by coordination of the two carbonyl and the two amine oxide groups to nickel (i.e., the O^c-Ni-O^c angle and the O^N-Ni-O^N angle) indicates that the fine conformation of the catalysts could be tuned by varying the length of the linker between the two amine oxide units (e.g., L_2-PiPr$_2$ vs L_3-PiPr$_2$ vs L_4-PiPr$_2$), the amino acid backbone (L_3-PiPr$_2$ vs L_3-RaPr$_2$), and/or the substituent on the amide nitrogen (L_3-PiPr$_2$ vs L_3-PiCHPh$_2$, or L_3-RaPr$_2$ vs L_3-Ra*m*Bu$_2$).

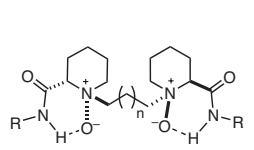

Label	R	n
L_2-PiPr$_2$	2,6-*i*-Pr$_2$C$_6$H$_3$	0
L_3-PiMe$_2$	2,6-Me$_2$C$_6$H$_3$	1
L_3-PiEt$_2$	2,6-Et$_2$C$_6$H$_3$	1
L_3-PiPr$_2$	2,6-*i*-Pr$_2$C$_6$H$_3$	1
L_3-Pi*o*Br	2-BrC$_6$H$_4$	1
L_3-Pi*s*EPh	(*S*)-2-PhEt	1
L_3-PiCHPh$_2$	CHPh$_2$	1
L_4-PiPr$_2$	2,6-*i*-Pr$_2$C$_6$H$_3$	2

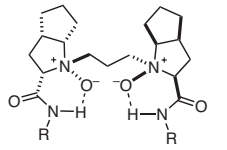

Label	R
L_3-RaEt$_2$	2,6-Et$_2$C$_6$H$_3$
L_3-RaPr$_2$	2,6-*i*-Pr$_2$C$_6$H$_3$
L_3-Ra*m*Bu$_2$	3,5-*t*-Bu$_2$C$_6$H$_3$
L_3-RaPr$_3$	2,4,6-*i*-Pr$_3$C$_6$H$_2$
L_3-RaPh	Ph

Figure 1. A Selection of C_2-Symmetric *N,N'*-Dioxide Ligands That Have Been Investigated by Our Group in the Featured Reactions.

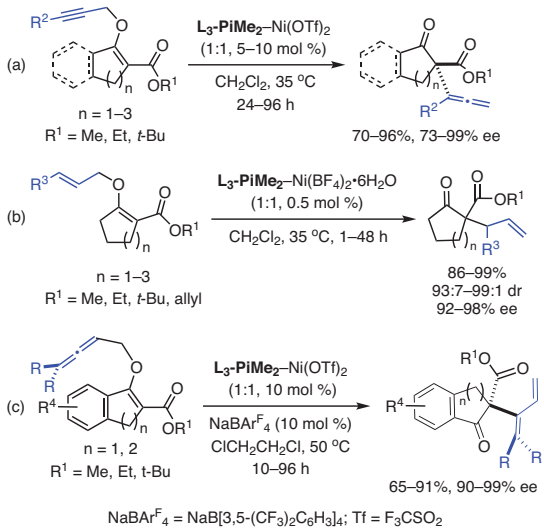

Scheme 1. The **L_3-PiMe$_2$** Enabled Propargyl, Allyl, and Allenyl Claisen Rearrangement. *(Ref. 10,11)*

This flexibility in tuning the ligand structure permits the resulting catalyst to satisfy the requirement of enantiocontrol in a variety of reactions. The chiral nickel coordination sphere can restrict how close the reactants can get to the center of the catalytic species by displacing the ancillary solvent or anion during the catalytic process.

2. Catalytic Asymmetric Rearrangement Reactions

2.1. Propargyl, Allyl, and Allenyl Claisen Rearrangement

The Claisen rearrangement and its variants are some of the most powerful stereoselective carbon–carbon bond-forming reactions.[9] If uncatalyzed, it usually requires higher reaction temperatures, while a Lewis acid catalyst might exert a positive influence on the reactivity. *N,N'*-Dioxide–nickel(II) salts offer several advantages in the Claisen rearrangement under mild reaction conditions. For instance, highly efficient and catalytic asymmetric propargyl and allyl Claisen rearrangements of *O*-propargyl and *O*-allyl β-keto esters were effected in the presence of the Ni(II) complexes of the three-carbon-linked *N,N'*-dioxide **L_3-PiMe$_2$**, prepared from L-pipecolic acid and 2,6-dimethylbenzenamine (**Scheme 1**, Parts (a) and (b)).[10] The enantioselective process gave a wide range of allenyl- or allyl-substituted all-carbon quaternary β-keto esters in good yields (up to 99%), high diastereoselectivities (up to 19:1 dr), and excellent enantioselectivities (up to 99% ee). The catalyst loading could be lowered to 0.5 mol % for the asymmetric allyl Claisen rearrangement without deterioration of the yields and stereoselectivities. Moreover, the chiral catalyst system was extended to the allenyl Claisen rearrangement to form branched 1,3-dienyl substituted β-keto esters with high enantioselectivity but at higher reaction temperatures (Scheme 1, Part (c)).[11]

The major pathway of the Claisen rearrangement proceeds via a cyclic chair conformation of the transition state (TS), whereas the minor pathway proceeds via a boat conformation of the TS. Because chiral starting materials could give Claisen rearrangement products of high optical purity, **L_3-PiMe$_2$**–Ni(OTf)$_2$ was successfully applied to the kinetic resolution of racemic propargyl vinyl ethers (**eq 1**).[12] This catalyst system showed a preference for the (*R*)-configured cyclic and linear propargyl vinyl ether through a bidentate bonding manner, leading to a diastereo- and enantioselective [3,3]-sigmatropic rearrangement. Complete central-to-axial chirality transfer occurs in the propargyl Claisen rearrangement, and the chirality of the newly formed stereogenic quaternary carbon is controlled, in some cases, by the chiral catalyst rather than by substrate induction. Moreover, the mismatched *S* isomer of the starting material could be recovered

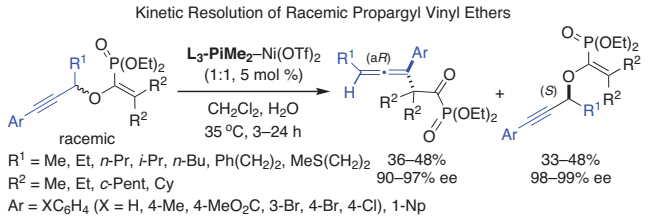

eq 1 *(Ref. 12)*

in high yield and enantiomeric excess. It is worth noting that enantioselective recognition enabled by chiral *N,N′*-dioxide–nickel(II) complexes has also been observed in visual or fluorescence sensing of chiral α-hydroxycarboxylic acids and *N*-Boc amino acids.[13]

2.2. [2,3]-Wittig Rearrangement

The [2,3]-Witting rearrangement proceeds via a five-membered cyclic transition state and provides a direct route to homoallyl alcohols and related compounds. Using progargylic ethers of oxindole derivatives as substrates, the reaction delivers allene-substituted alcohols, but the reactivity is low due to the distorted transition-state geometries arising from the alkyne sp center. By using **L$_3$-PiCHPh$_2$**–Ni(OTf)$_2$ as catalyst, a highly enantioselective variant was achieved (**eq 2**).[14] Interestingly, a low yield (18%) was obtained in the absence of the *N,N′*-dioxide ligand. Furthermore, kinetic resolution of racemic oxindole derivatives was also achieved with high efficiency and stereoselectivity.[14]

With respect to the modes of asymmetric catalysis of these chiral nickel complexes in the Claisen and [2,3]-Wittig rearrangements, it has been proposed that they occur by similar bidentate activations. The β-keto esters, phosphonates, and oxindoles are 1,4-dioxygen-type substrates, which could bond to the nickel(II) center with the ether oxygen and the carbonyl group, forming a stable five-membered cyclic transition state. The steric hindrance arising from the *N,N′*-dioxide ligand would then direct the subsequent rearrangement enantioselectively to generate the stereogenic center vicinal to the carbonyl group in the products.

2.3. Doyle–Kirmse Rearrangement

The unique electronic and steric properties of chiral *N,N′*-dioxide–metal complexes prompted us to design α-diazo pyrazoleamides for the asymmetric [2,3]-sigmatropic rearrangement of sulfonium ylides generated from α-diazo compounds and allyl sulfides. The control of enantioselectivity in this type of [2,3]-sigmatropic rearrangement relies on the formation of a metal-bonded ylide intermediate or discrimination of the heterotopic lone pairs on sulfur.[15] The chiral **L$_2$-PiPr$_2$**–Ni(II) complex efficiently catalyzed both the formation of the sulfide ylide intermediate and its subsequent enantioselective rearrangement. Moreover, a combination of **L$_2$-PiPr$_2$**, $NiCl_2$, and $AgNTf_2$ efficiently catalyzed the enantioselective Doyle–Kirmse reaction of a series of aryl- or vinyl-substituted α-diazo pyrazoleamides with allyl aryl sulfides (**Scheme 2**).[16] In most cases, the reactions were completed in 5–20 minutes in high yields and with excellent enantioselectivities (up to 99% yields and 96% ee's). There is an obvious ligand reaction-acceleration effect, as only a trace amount of the product was obtained without the chiral ligand. The introduction of a pyrazoleamide unit into the α-diazo compound enhances its electrophilicity, and facilitates the formation of the chiral Lewis acid bonded ylide intermediate and stereocontrol via bidentate coordination. The latter hypothesis has been supported by the reaction of C_2-symmetric diallyl sulfides with diazo pyrazoleamides, which led to the corresponding products with good enantioselecitivity.

2.4. [2,3]-Stevens and Sommelet–Hauser Rearrangements

The enantioselective [2,3]-Stevens and Sommelet–Hauser rearrangements of sulfonium ylides—generated from α-diazo compounds and thioacetates—are much more complicated in comparison with the asymmetric Doyle–Kirmse reaction. There are vicinal S- and C-stereogenic centers in the ylide intermediates, racemization or epimerization of ylide tautomers via 1,3-proton shifts, and a remote functionalization in the final [2,3]-rearrangement step.

The **L$_2$-PiPr$_2$**–Ni(II) complex catalyzed the asymmetric [2,3]-Stevens rearrangement of vinyl substituted α-diazo pyrazoleamides and aryl thioacetates. Initially, discrimination of the heterotopic lone pairs on sulfur affords the (*R*)-configured sulfonium ylide species **I**. Added 3-phenylpropanoic acid acts as a mild proton shuttle, enabling the slower diastereoselective tautomerization process to generate the (*R*,*R*)-ylide intermediate **II**, which undergoes an asymmetric [2,3]-rearrangement via an envelope transition state, leading to the desired products with a (*2R*,*3S*,*E*) configuration (**Scheme 3**).[17]

This same chiral nickel complex also efficiently catalyzed the asymmetric Sommelet–Hauser reaction of aryl-substituted α-diazo pyrazoleamides with (phenylthio)methylcarbamoates.[17] This rearrangement is potentially more challenging because dearomatization and rearomatization steps are involved in the process. The desired ortho-thioalkyl-substituted arylacetamides were isolated in 51–78% yield with 60–81% ee. The 1,3-proton shift results from a trace amount of water in the system, and the

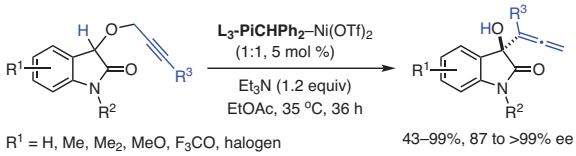

eq 2 *(Ref. 14)*

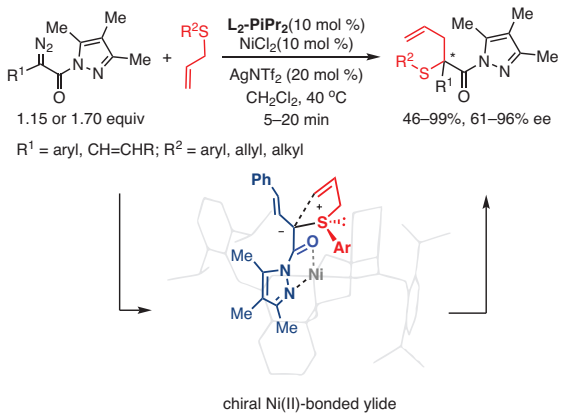

Scheme 2. Doyle–Kirmse Reaction Catalyzed by Ni(II)–*N,N′*-Dioxide Complexes. *(Ref. 16)*

[2,3]-rearrangement process is slow and difficult due to the high activation energy of the dearomatization step.

2.5. Allylboration/Oxy-Cope Rearrangement

Recently, the complex **L$_3$-RaPr$_2$**–Ni(OTf)$_2$ was used to catalyze an allylboration–oxy-Cope rearrangement sequence of β,γ-unsaturated α-keto esters with allylboronic acids under mild conditions (**Scheme 4**).[18] This protocol provides a facile and direct route to γ-allyl-α-keto esters in moderate-to-good yields (65–92%) and excellent enantioselectivity (90–99% ee). The 1,2-allylboration products could also be isolated in good yields and excellent diastereo- and enantioselectivities at lower reaction temperature. The general catalytic mechanism is based on coordination of the β,γ-unsaturated α-keto ester to the nickel center in a bidentate fashion,

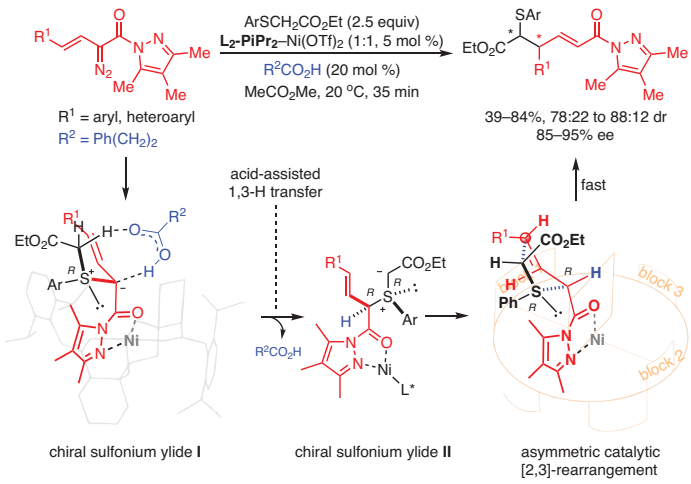

Scheme 3. Catalytic, Asymmetric [2,3]-Stevens Rearrangement Enabled by Ni(II)–*N,N'*-Dioxide Complexes. *(Ref. 17)*

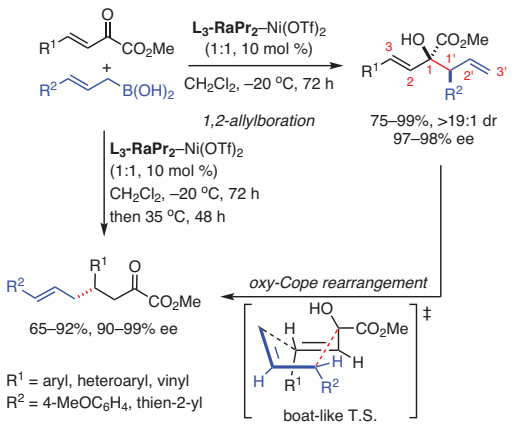

Scheme 4. Application of Ni(II)–*N,N'*-Dioxide Complexes as Catalysts for an Asymmetric Allylboration and Oxy-Cope Rearrangement Sequence. *(Ref. 18)*

which is suitable for the face-selective addition of the allylboronic acid. It was found that the subsequent enantioselective oxy-Cope rearrangement is induced by the optically enriched vinyl- and allyl-substituted alcohol intermediates, and the process could be accelerated by the chiral Lewis acid at higher reaction temperature. The chirality transfer in the oxy-Cope rearrangement is via a rare, boat-like transition state.

3. Asymmetric Catalytic Nucleophilic Addition Reactions

3.1. Ene-Type Reactions

Ene-type reactions can provide access to polyfunctionalized compounds that are synthetically versatile intermediates by the further transformation of the carbon–carbon double bond.[19] The asymmetric carbonyl–ene reaction of glyoxals and glyoxylates can be used to construct chiral γ,δ-unsaturated α-hydroxy carbonyl compounds. The chiral *N,N'*-dioxide–nickel(II) complexes can catalyze the asymmetric variant with remarkable results by employing glyoxals, α-keto esters, or isatins as the enophiles, and alkenes, enamides, vinylogous hydrazine, or 5-methyleneoxazolines as the nucleophiles. The common catalytic pathway involves bidentate coordination of the 1,2-dicarbonyl compounds to the nickel center, lowering the LOMO energy of the enophile. Subsequently, the ene component enantioselectively approaches the active carbonyl group via a cyclic transition state to yield the desired adduct.

For example, excellent enantioselectivities (up to >99% ee) were obtained in the **L$_3$-PiPr$_2$**–Ni(BF$_4$)$_2$ catalyzed carbonyl-ene reaction of glyoxals and glyoxylates with various alkenes.[20] The optically active allyl-substituted α-hydroxy carbonyl products can undergo a subsequent, FeCl$_3$–TBSCl catalyzed OH-selective Prins cyclization, leading to a broad range of substituted 4-hydroxytetrahydropyrans highly stereoselectively (**Scheme 5**, Part (a)).[21] The *N,N'*-dioxide–nickel(II) catalysts also show remarkable performance in the carbonyl-ene reaction of glyoxals and glyoxylates with a series of enamides[22] and 5-methyleneoxazolines[23] as nucleophiles. The hetero-ene reaction of glyoxal derivatives and 5-methyleneoxazoline worked well even at 0.5 mol % loading of the catalyst, providing 2,5-disubstituted oxazole derivatives in 60–99% yields and 95 to >99% ee's.

Similarly, the asymmetric ene-type reaction of α-keto esters with 5-methyleneoxazolines also works well under **L$_3$-PiPr$_2$**–Ni(BF$_4$)$_2$ catalysis.[23–24] Moreover, in the presence of **L$_3$-RaEt$_2$**–Ni(ClO$_4$)$_2$ as catalyst, a range of racemic β-halo-α-keto esters were efficiently converted into the chiral β-halo-α-hydroxy esters via dynamic kinetic asymmetric transformations. The corresponding ene products containing vicinal tri- and tetrasubstituted carbon centers were obtained in generally good yields and diastereoselectivity and excellent ee values (Scheme 5, Part (b)).[24]

The valuable nucleophile vinylogous hydrazine underwent an ene-type reaction with glyoxal derivatives. Subsequent treatment with magnesium monoperoxyphthalate hydrate (MMPP·6H$_2$O) gave the valuable, optically active 4-benzoyl-4-hydroxy-2-methylenebutanenitrile in 95% yield and 95% ee.[25] This vinylogous nitrile was elaborated in moderate yield and excellent ee into a bioactive compound that is a potentially cytotoxic agent against human leukemia HL-60 cells.[26] Furthermore, **L$_3$-RaPr$_2$**–Ni(OTf)$_2$

efficiently catalyzed the reaction of vinylogous hydrazine with isatins, and the product of the reaction was transformed in two steps into a spirocyclic lactone that is a potent antineoplastic agent against P-388 lymphocytic leukemia and human carcinoma of the nasopharynx (Scheme 5, Part (c)).[25]

In contrast to the preceding examples of the ene reaction, the asymmetric Alder–ene reaction using alkenes as enophiles remains a challenge due to the low reactivity of the olefins along with the required high activation energy of the ene reaction. Usually, stoichiometric amounts of chiral Lewis acids are required to achieve a satisfactory outcome.[27] In this regard, **L$_3$-RaPr$_2$**–Ni(NTf$_2$)$_2$ efficiently promoted the asymmetric intramolecular Alder–ene reaction, leading to a series of 3,4-disubstituted chromans, thiochromans, tetrahydroquinolines, and piperidines in high yields and with good-to-excellent diastereo- and enantioselectivities.[28]

3.2. Friedel–Crafts Reaction

The phenomenon of enantioselectivity reversal is interesting and has important applications in enantiodivergent synthesis.[29] Using the chiral pool and slightly modifying the amide moiety of the *N,N′*-dioxide ligand in chiral *N,N′*-dioxide–Ni(OTf)$_2$ complexes result in an enantiodivergent Friedel–Crafts-type reaction of β,γ-unsaturated α-keto esters with 2,5-dimethylpyrrole or 2-methylindole (**Scheme 6**).[30] For example, **L$_3$-RaPr$_2$**–Ni(OTf)$_2$ catalyzes the addition of 2,5-dimthylpyrrole to β,γ-unsaturated α-keto esters to give the dextran product, while **L$_3$-Ra*m*Bu$_2$**–Ni(OTf)$_2$ catalyzes the same reaction to yield the right-handed enantiomer. The strategy was also successfully implemented in an enantiodivergent synthesis of the corresponding indole adducts. The switch in enantioselectivity results from the markedly different spatial environments in the seesawed amide units of the two catalyst complexes. Steric hindrance around the enantiotopic face of the β,γ-unsaturated α-keto ester causes its differentiation upon bidentate coordination to the nickel center.

3.3. Michael and Mannich Reactions

Chiral *N,N′*-dioxide–Ni(II) complexes have also been used in classic addition reactions such as the oxa-Michael and Mannich reactions. For example, (2-hydroxyphenyl)propenone derivatives engage in two-point binding to the central metal in **L$_3$-RaPh**–Ni(Tfacac)$_2$, forming a chelate-ordered transition state that results in an intramolecular oxa-Michael addition (**Scheme 7**, Part (a)).[31] The reaction tolerated a relatively wide range of substrates to provide a series of flavanones in excellent yields (90–99%) and moderate-to-excellent enantioselectivities (40–99% ee). Significantly, the optically active flavanones can be converted into versatile building blocks such as hydrazones.[32]

Chiral **L$_3$-PiPr$_2$**-based Ni(II) and Mg(II) complexes are also efficient catalysts for the asymmetric Mannich reaction employing 1,3,5-triazinanes as electrophilic reagents and imine precursors (Scheme 7, Part (b)).[33] The in situ generated imines react smoothly with α-tetralone-derived β-keto esters or amides to give optically active 2-(β-amino)-substituted tetralones in generally good-to-excellent yields and enantioselectivities. However, the five-membered-ring β-keto amide analogue gave the corresponding product in 99% yield but with only 50% ee, while the seven-membered-ring β-keto amide counterpart gave 92% yield of the racemic product.

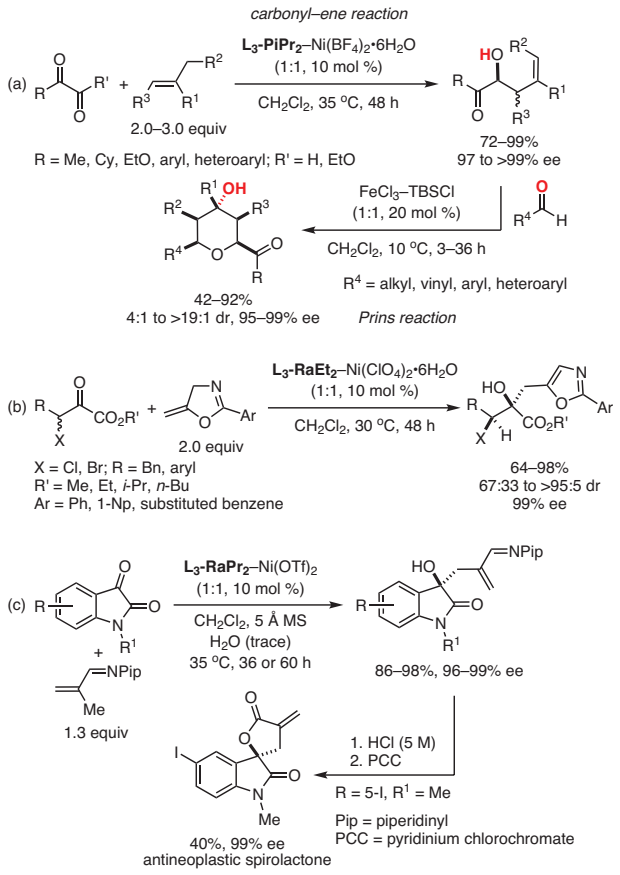

Scheme 5. Asymmetric Ene-Type Reactions Catalyzed by Ni(II)–*N,N′*-Dioxide Complexes. *(Ref. 20,21,24,25)*

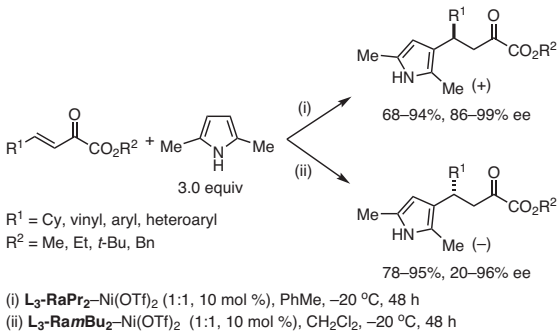

Scheme 6. Enantiodivergent Friedel–Crafts Reaction Promoted by Chiral *N,N′*-Dioxide–Ni(OTf)$_2$ Complexes. *(Ref. 30)*

4. Miscellaneous Reactions

4.1. Transformations Involving Hypervalent Iodine Salts

Hypervalent iodine salts, such as vinyl-, alkynyl-, and aryliodonium salts are attractive reagents due to their low toxicity, high reactivity, and high stability. We previously found chiral *N,N'*-dioxide–Sc(OTf)$_3$ complexes to be efficient Lewis acid catalysts for the enantioselective α-arylation of 3-substituted oxindoles with diaryliodonium salts through carbon–iodine bond formation and subsequent [1,2]-rearrangement.[34] When β-keto amides or esters were used as substrates, it was observed that chiral **L$_3$-PisEPh**–Ni(II) was a much more efficient catalyst, which gave good results in the enantioselective vinylation, alkynylation, and arylation (**Scheme 8**, Part (a)).[35] A bidentate coordination of the 1,3-dicarbonyl compound to the nickel center was proposed to rationalize the observed enantioselection.

A new strategy for the catalytic asymmetric cyclopropanation of 3-alkenyloxindoles with phenyliodonium ylide malonate has been developed (Scheme 8, Part (b)).[36] In the presence of **L$_3$-PiPr$_2$**–Ni(OTf)$_2$, a variety of spirocyclopropane-oxindoles with contiguous one tertiary and two quaternary all-carbon centers are generated with excellent yields and stereoselectivities (up to 99% yield, > 19:1 dr, and up to 99% ee). Based on EPR spectroscopic observations, a free, triplet carbene intermediate, ^{3}:C(CO$_2$Me)$_2$, was proposed as resulting from the thermal decomposition of the phenyliodonium ylide. Bidentate coordination of the 3-alkenyloxindole to the chiral nickel center through the two carbonyl groups was also proposed to precede reaction with the triplet carbene. Ring closure of the resulting singlet biradical intermediate leads to the cyclopropane product, with the observed facial selectivity being attributed to the blocking of the nearby amide unit of the ligand.

The catalytic enantioselective C$_{sp3}$–H α-alkylation of β-keto amides with phenyliodonium ylide has been achieved in the presence of the chiral **L$_3$-PiEt$_2$**–Ni(OTf)$_2$ complex.[37] Notably, the catalytic radical process is insensitive to air and moisture, and the resulting products are obtained in good yields and with excellent enantioselectivities even when the reaction is carried out on a gram scale (up to 91% yield and 97% ee).

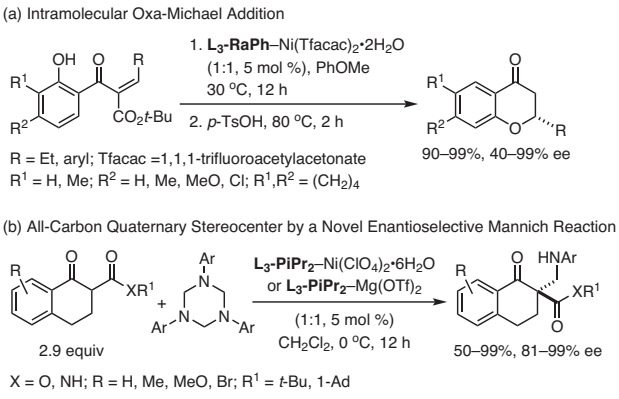

Scheme 7. Asymmetric Intramolecular Oxa-Michael Addition and Mannich Reaction. *(Ref. 31,33)*

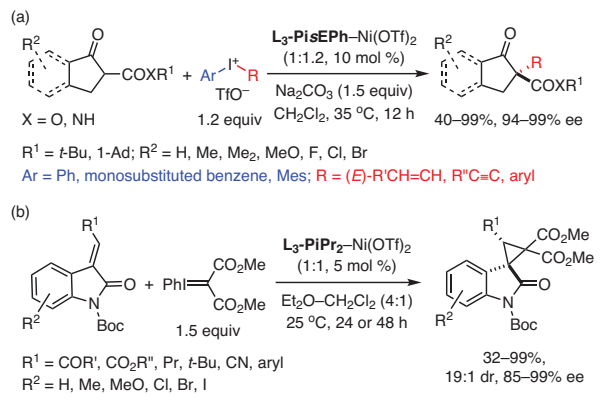

Scheme 8. Chiral *N,N'*-Dioxide–Ni(II) Catalyzed Reactions: (a) α-Vinylation, Alkynylation, and Arylation of β-keto Acid Derivatives. (b) Cyclopropanation of 3-Alkenyloxindoles. *(Ref. 35,36)*

4.2. Reduction Reaction

The asymmetric reduction of secondary and primary α-amino ketones has been achieved using *N,N'*-dioxide–Ni(II) complexes and aqueous KBH$_4$, confirming that such complexes can tolerate reducing agents and aqueous conditions. This approach provides easy access to chiral, β-amino alcohol based natural products and drug candidates, such as β$_2$-adrenoreceptor agonists. For example, chiral **L$_3$-PiEt$_2$**–Ni(OTf)$_2$ catalyzed the reduction of α-(*N*-arylamino)-ketones to chiral β-amino alcohols in good-to-excellent yields (up to 98%) and enantioselectivities (up to 97% ee) (**eq 3**).[38]

5. Application in the Synthesis of Natural Products and Drug Candidates

Hyperolactones A–C and (−)-biyouyanagin A, containing two chiral vicinal quaternary carbon centers, are a family of spirolactone natural products with significant activity against HIV. A short, catalytic, and stereodivergent synthesis of hyperolactones B and C has been achieved starting with an enantioselective dearomatization–Claisen rearrangement of allyl furyl ethers in the presence of chiral **L$_3$-PiMe$_2$**–Ni(BF$_4$)$_2$ or *ent*-**L$_3$-PiMe$_2$**–Ni(BF$_4$)$_2$ (**Scheme 9**).[39] The Ni(II)-catalyzed step was found to be generally applicable to allyl furyl ethers, and, under the optimized conditions, a number of

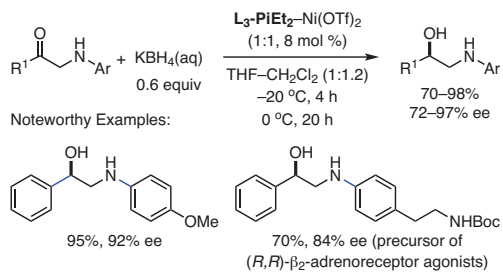

eq 3 *(Ref. 38)*

γ,δ-unsaturated carbonyl compounds were obtained in up to 99% yield, 19:1 dr, and up to 99% ee. The steric hindrance arising from the bulky amide moiety of the ligand forces the alkene unit of the substrate to preferentially approach the α position of the furan ring from one side. Thus, the stereogenic arrangement of the furanone is catalyst-controlled, while the configuration of the quaternary carbon center is determined by the *Z*/*E* configuration of the allyl substituent. As a result, four enantiomers of the products could be prepared in excellent yields and stereoselectivities by a judicious selection of the configuration of the catalyst and the alkene unit of the substrates.[39]

N,N′-Dioxide–metal complexes have been successfully applied in asymmetric cycloaddition reactions.[7c] One of the noteworthy examples is the *N,N′*-dioxide-Ni(OTf)$_2$ catalyzed regio-, diastereo-, and enantioselective aza-Diels–Alder reaction of 3-vinylindoles with isatin-derived ketimines. The reaction takes place by a concerted reaction pathway, and the regioselectivity and exo selectivity are attributed to the π–π interaction between the two indoline rings of the two reactants. The transformation affords a series of spiroindolone derivatives in good yields and with excellent enantioselectivities.[40] Furthermore, the antimalarial drug candidate NITD609 was obtained in three steps (40.6% overall yield and up to 99% ee) starting with the gram-scale, *ent*-**L$_3$-RaPr$_2$**–Ni(OTf)$_2$ catalyzed aza-Diels–Alder cycloaddition of a suitably substituted 3-vinylindole and isatin-derived ketimine (**Scheme 10**).[40]

6. Conclusion

Chiral *N,N′*-dioxide ligand–Ni(II) complexes are now practical Lewis acid catalysts in several well-known reactions. Additionally, a number of chiral nickel(II) complexes—with ligands possessing functional groups of other heteroatoms as electron-pair donors, such as amines and phosphines—have also been developed. For example, chiral nickel(II)–PyBox or nickel(II)–bis(oxazoline) complexes are efficient catalysts for enantioselective cross-couplings of nucleophiles with racemic alkyl electrophiles via radical pathways.[41] The chiral nickel(II) complexes of diamines, salen, BINAP, and TOX ligands promote various reactions as Lewis acid catalysts. Nickel and several other transition metals, with variable oxidation numbers, have considerable established organometallic chemistry, but the role of the catalyst is only beginning to be understood. Improving our understanding of the geometry, ligands, active site, and activation mode in such reactions would allow the development of more efficient, and useful catalytic asymmetric reactions.

7. Acknowledgments

We are sincerely indebted to a group of talented co-workers whose names are listed in the relevant references. We also thank the National Natural Science Foundation of China (Nos. 21625205 and 21432006) for financial support.

8. References and Notes

(1) Jacobsen, E. N., Pfaltz, A., Yamamoto H., Eds. *Comprehensive Asymmetric Catalysis* I–III; Springer-Verlag: New York, NY, 1999.

(2) Mikami, K., Lautens, M., Eds. *New Frontiers in Asymmetric Catalysis*; Wiley: Hoboken, NJ, 2007.

(3) (a) Zhou, Q.-L., Ed. *Privileged Chiral Ligands and Catalysts*; Wiley-VCH: Weinheim, Germany, 2011. (b) Stradiotto, M., Lundgren, R. J., Eds. *Ligand Design in Metal Chemistry: Reactivity and Catalysis*; Wiley: U.K., 2016.

(4) Sandoval, C. A.; Noyori, R. An Overview of Recent Developments in Metal-Catalyzed Asymmetric Transformations. In *Organic Chemistry – Breakthroughs and Perspectives*; Ding, K.-L., Dai, L.-X., Eds.; Wiley-VCH: Weinheim, Germany, 2012; Chapter 9, pp 335–363.

(5) Yoon, T. P.; Jacobsen, E. N. *Science* **2003**, *299*, 1691.

(6) Yamamoto, H., Ed. *Lewis Acids in Organic Synthesis*; Handbook of Chemoinformatics; Gasteiger, J., Ed.; Wiley-VCH: Weinheim, Germany, 2000.

(7) (a) Liu, X. H.; Lin, L. L.; Feng, X. M. *Acc. Chem. Res.* **2011**, *44*, 574. (b) Liu, X. H.; Lin, L. L.; Feng, X. M. *Org. Chem. Front.* **2014**, *1*, 298. (c) Liu, X. H.; Zheng, H. F.; Xia, Y.; Lin, L. L.; Feng, X. M. *Acc. Chem. Res.* **2017**, *50*, 2621. (d) Liu, X. H.; Dong, S. X.; Lin, L. L.; Feng, X. M. *Chin. J. Chem.* **2018**, *36*, 791.

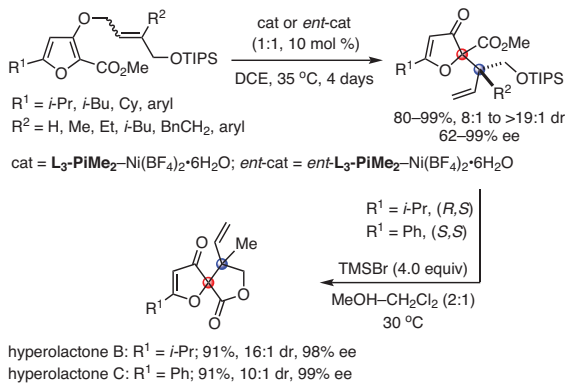

Scheme 9. Application of *N,N′*-Dioxide–Ni(II) Catalysts in a Stereodivergent Synthesis of Hyperolactones B and C. *(Ref. 39)*

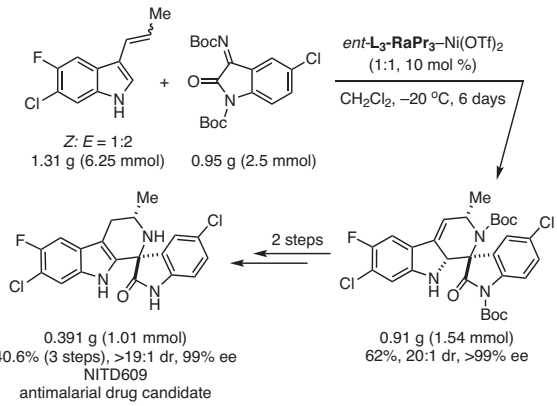

Scheme 10. Application of *N,N′*-Dioxide–Ni(II) Catalysts in a Three-Step, Gram-Scale Synthesis of the Antimalarial Drug Candidate NITD609. *(Ref. 40)*

(8) The Cambridge Crystallographic Data Centre (CCDC) numbers 1587231, 1834283, 759905, 1035849, 1035929, and 1849262 contain the supplementary crystallographic data for the *N,N'*-dioxide complexes with nickel(II).
(9) (a) Martín Castro, A. M. *Chem. Rev.* **2004**, *104*, 2939. (b) Ilardi, E. A.; Stivala, C. E.; Zakarian, A. *Chem. Soc. Rev.* **2009**, *38*, 3133.
(10) Liu, Y. B.; Hu, H. P.; Zheng, H. F.; Xia, Y.; Liu, X. H.; Lin, L. L.; Feng, X. M. *Angew. Chem., Int. Ed.* **2014**, *53*, 11579.
(11) Liu, Y. B.; Hu, H. P.; Lin, L. L.; Hao, X. Y.; Liu, X. H.; Feng, X. M. *Chem. Commun.* **2016**, *52*, 11963.
(12) Liu, Y. B.; Liu, X. H.; Hu, H. P.; Guo, J.; Xia, Y.; Lin, L. L.; Feng, X. M. *Angew. Chem., Int. Ed.* **2016**, *55*, 4054.
(13) He, X.; Zhang, Q.; Wang, W. T.; Lin, L. L.; Liu, X. H.; Feng, X. M. *Org. Lett,* **2011**, *13,* 804.
(14) Xu, X.; Zhang, J. L.; Dong, S. X.; Lin, L. L.; Lin, X. B.; Liu, X. H.; Feng, X. M. *Angew. Chem., Int. Ed.* **2018**, *57*, 8734.
(15) West, T. H.; Spoehrle, S. S. M.; Kasten, K.; Taylor, J. E.; Smith, A. D. *ACS Catal.* **2015**, *5*, 7446.
(16) Lin, X. B.; Tang, Y.; Yang, W.; Tan, F.; Lin, L. L.; Liu, X. H.; Feng, X. M. *J. Am. Chem. Soc.* **2018**, *140*, 3299.
(17) Lin, X. B.; Yang, W.; Yang, W. K.; Liu, X. H.; Feng, X. M. *Angew. Chem., Int. Ed.* **2019**, *58*, 13492.
(18) Tang, Q.; Fu, K.; Ruan, P. R.; Dong, S. X.; Su, Z. S.; Liu, X. H.; Feng, X. M. *Angew. Chem., Int. Ed.* **2019**, *58*, 11846.
(19) Liu, X. H.; Zheng, K.; Feng, X. M. *Synthesis* **2014**, *46*, 2241.
(20) Zheng, K.; Shi, J.; Liu, X. H.; Feng, X. M. *J. Am. Chem. Soc.* **2008**, *130*, 15770.
(21) Zheng, K.; Liu, X. H.; Qin, S.; Xie, M. S.; Lin, L. L.; Hu, C. W.; Feng, X. M. *J. Am. Chem. Soc.* **2012**, *134*, 17564.
(22) Zheng, K.; Liu, X. H.; Zhao, J. N.; Yang, Y.; Lin, L. L.; Feng, X. M. *Chem. Commun.* **2010**, *46*, 3771.
(23) Luo, W. W.; Zhao, J. N.; Yin, C. K.; Liu, X. H.; Lin, L. L.; Feng, X. M. *Chem. Commun.* **2014**, *50*, 7524.
(24) Liu, W.; Cao, W. D.; Hu, H. P.; Lin, L. L.; Feng, X. M. *Chem. Commun.* **2018**, *54*, 8901.
(25) Zhang, H.; Yao, Q.; Cao, W. D.; Ge, S. L.; Xu, J. X.; Liu, X. H.; Feng, X. M. *Chem. Commun.* **2018**, *54*, 12511.
(26) Janecki, T.; Błaszczyk, E.; Studzian, K.; Różalski, M.; Krajewska, U.; Janecka, A. *J. Med. Chem.* **2002**, *45*, 1142.
(27) (a) Desimoni, G.; Faita, G.; Righetti, P.; Sardone, N. *Tetrahedron* **1996**, *52*, 12019. (b) Xia, Q.; Ganem, B. *Org. Lett.* **2001**, *3*, 485.
(28) Liu, W.; Zhou, P. F.; Lang, J. W.; Dong, S. X.; Liu, X. H.; Feng, X. M. *Chem. Commun.* **2019**, *55*, 4479.
(29) Cao, W. D.; Feng, X. M.; Liu, X. H. *Org. Biomol. Chem.* **2019**, *17*, 6538.
(30) Zhang, Y. L.; Yang, N.; Liu, X. H.; Guo, J.; Zhang, X. Y.; Lin, L. L.; Hu, C. W.; Feng, X. M. *Chem. Commun.* **2015**, *51*, 8432.
(31) Wang, L. J.; Liu, X. H.; Dong, Z. H.; Fu, X.; Feng, X. M. *Angew. Chem., Int. Ed.* **2008**, *47*, 8670.
(32) Savini, L.; Chiasserini, L.; Travagli, V.; Pellerano, C.; Novellino, E.; Cosentino, S.; Pisano, M. B. *Eur. J. Med. Chem.* **2004**, *39*, 113.
(33) Lian, X. J.; Lin, L. L.; Fu, K.; Ma, B. W.; Liu, X. H.; Feng, X. M. *Chem. Sci.* **2017**, *8*, 1238.
(34) Guo, J.; Dong, S. X.; Zhang, Y. L.; Kuang, Y. L.; Liu, X. H.; Lin, L. L.; Feng, X. M. *Angew. Chem., Int. Ed.* **2013**, *52*, 10245.
(35) Guo, J.; Lin, L. L.; Liu, Y. B.; Li, X. Q.; Liu, X. H.; Feng, X. M. *Org. Lett.* **2016**, *18*, 5540.
(36) Guo, J.; Liu, Y. B.; Li, X. Q.; Liu, X. H.; Lin, L. L.; Feng, X. M. *Chem. Sci.* **2016**, *7*, 2717.
(37) Guo, J.; Liu, X. H.; He, C. Q.; Tan, F.; Dong, S. X.; Feng, X. M. *Chem. Commun.* **2018**, *54*, 12254.
(38) He, P.; Zheng, H. F.; Liu, X. H.; Lian, X. J.; Lin, L. L.; Feng, X. M. *Chem.—Eur. J.* **2014**, *20*, 13482.
(39) Zheng, H. F.; Wang, Y.; Xu, C. R.; Xu, X.; Lin, L. L.; Liu, X. H.; Feng, X. M. *Nat. Commun.* **2018**, *9*, 1968.
(40) Zheng, H. F.; Liu, X. H.; Xu, C. R.; Xia, Y.; Lin, L. L.; Feng, X. M. *Angew. Chem., Int. Ed.* **2015**, *54*, 10958.
(41) (a) Cherney, A. H.; Kadunce, N. T.; Reisman, S. E. *Chem. Rev.* **2015**, *115*, 9587. (b) Choi, J.; Fu, G. C. *Science* **2017**, *356*, eaaf7230.

About the Authors

Zhen Wang received his B.S. (2009) and Ph.D. (2014) degrees from Sichuan University. From 2014 to 2015, he was a postdoctoral fellow in Professor Yixin Lu's group at the National University of Singapore. In 2015, he joined the faculty of Chongqing University, where he is now an associate professor. His research interest is in developing new catalytic methods for asymmetric synthesis.

Xiaohua Liu received her B.S. degree in 2000 from Hubei Normal University. She then obtained her M.S. (2003) and Ph.D. (2006) degrees from Sichuan University. She is now a professor at Sichuan University. Her current research interests include asymmetric catalysis and organic synthesis.

Xiaoming Feng was born in 1964. He received his B.S. (1985) and M.S. (1988) degrees from Lanzhou University. From 1988 to 1993, he worked at Southwest Normal University, where he became an associate professor in 1991. In 1996, he received his Ph.D. degree from the Chinese Academy of Sciences (CAS) under the supervision of Professors Zhitang Huang and Yaozhong Jiang. From 1996 to 2000, he was at the Chengdu Institute of Organic Chemistry, CAS, where he was appointed Professor in 1997. He did postdoctoral research at Colorado State University from 1998 to 1999 with Professor Yian Shi. In 2000, he moved to Sichuan University as a professor, and was selected as Academician of the Chinese Academy of Sciences in 2013. He focuses on the design of chiral catalysts, development of new synthetic methods, and synthesis of bioactive compounds.

Asymmetric Allylic Substitutions Catalyzed by Iridium Complexes Derived from C(sp^2)–H Activation of Chiral Ligands


Prof. X. Zhang


Prof. S.-L. You

Xiao Zhang and Shu-Li You*

State Key Laboratory of Organometallic Chemistry
Shanghai Institute of Organic Chemistry
University of Chinese Academy of Sciences
Chinese Academy of Sciences
345 Lingling Road
Shanghai 200032, China
Email: slyou@sioc.ac.cn

Keywords. AAS; allylic substitution; asymmetric catalysis; BHPphos; branch selectivity; chiral ligand; C(sp^2)–H activation; enantioselectivity; iridium; N-heterocyclic carbene (NHC); THQphos.

Abstract. The iridium-catalyzed asymmetric allylic substitution reaction has been developed into a reliable method for the synthesis of highly enantioenriched molecules with an allylic stereocenter. The versatility of the reaction is largely attributed to the development of efficient catalysts. Some of these catalysts are iridium complexes derived from C(sp^2)–H activation of chiral ligands including THQphos (1,2,3,4-tetrahydroquinoline phosphoramidite), BHPphos (*N*-benzhydryl-*N*-phenyldinaphthophosphoramidite), and NHCs (N-heterocyclic carbenes). These catalysts exhibit exceptionally high regio-, diastereo-, and enantioselectivities as well as good tolerance of sterically hindered substrates. In this article, we briefly review the design and mechanism of action of these chiral ligands, and highlight their applications in the Ir-catalyzed allylic substitution of various nucleophiles.

Outline

1. Introduction

Transition-metal-catalyzed asymmetric allylic substitution (AAS) reactions are among the most important transformations that allow the construction of carbon–carbon or carbon–heteroatom bonds in an enantioselective fashion.[1] Early examples mainly focused on palladium catalysis, which is compatible with a wide range of nucleophiles and electrophiles and generally favors linear selectivity for mono-substituted allylic electrophiles. Catalysis by other metals has been less studied, but has shown promising control of selectivity. In particular, Ir-catalyzed asymmetric allylic substitutions have received a lot of attention in the past two decades owing to their unique reactivity profile that includes a remarkably high branch selectivity for mono-substituted allylic electrophiles and nearly perfect enantioselective control.[2]

Since the first report by Janssen and Helmchen,[3a] various chiral ligands—including oxazolinylphosphines, phosphoramidites, and dienes—have been utilized in Ir-catalyzed allylic substitution reactions.[3] Of these ligands, the phosphoramidites have contributed significantly to the development of this area, and have enabled a large number of valuable transformations with high levels of regio- and enantioselectivity. For instance, Carreira's

bidentate P,olefin coordination ligands have demonstrated the robustness of this approach by using unprotected allylic alcohols as substrates in the presence of an acidic additive.[2l,4] Under non-acidic conditions, the Feringa ligand[5a,b] and the Alexakis ligand[5c–e] are the most frequently employed ones in iridium-catalyzed allylic substitutions. Mechanistically, the active iridacycle catalyst is formed by bidentate P,C(sp³) coordination to Ir of the ligand, which is generated through C(sp³)–H activation of its methyl group.[2d,6]

Our research efforts have been focused on developing a class of ligands that undergo C(sp²)–H activation during the formation of the active catalytic iridium species. Specifically, we have developed THQphos (1,2,3,4-tetrahydroquinoline phosphoramidite),[7] BHPphos (*N*-benzhydryl-*N*-phenyldinaphthophosphoramidite),[8] and NHC (N-heterocyclic carbene)[9] ligands for the Ir-catalyzed asymmetric allylic substitution reactions (**Figure 1**). This class of chiral ligands exhibits unique performance characteristics with respect to selectivity control and substrate scope. Herein we highlight the evolution of these ligands with an emphasis on their applications in Ir-catalyzed allylic substitutions with various nucleophiles.

2. Chiral Ligand Design

The first iridium-catalyzed allylic substitution was reported by Takeuchi and Kashio in 1997.[10] The allylic substitution reactions of allylic acetates with sodium malonates proceeded with iridium complexes generated in situ from $[Ir(cod)Cl]_2$ and various phosphites. It was also observed that utilization of the better π-acceptor $P(OPh)_3$ as ligand resulted in enhanced reactivity and favored the formation of branched products. In 2002, Helmchen and co-workers investigated the possible active species and found that **K1**, generated by mixing $[Ir(cod)Cl]_2$ and $P(OPh)_3$, is unreactive.[11] Upon addition of $NaCH(CO_2Me)_2$ and $P(OPh)_3$ to **K1**, complex **K2** is formed via activation of the ortho C(sp²)–H bond of one of the phenyl groups of $P(OPh)_3$ (**Scheme 1**, Part (a)). Subsequent dissociation of $P(OPh)_3$ from **K2** delivers the catalytically active species. Based on these early findings, we developed a series of binaphthol-derived, P,C(sp²)-coordination phosphoramidite ligands, as exemplified by THQphos[7] and BHPphos,[8] which incorporate chiral elements. Later on, structurally distinct NHCs, bearing an N-aryl group at the ortho position (e.g., the D-camphor-derived NHC[9b]) were found to be suitable ligands for iridium-based catalytic systems following the same C(sp²)–H activation mode (Scheme 1, Part (b)).[9]

3. Mechanistic Studies

Among THQphos-type ligands,[7] (R,R_a)-Me-THQphos (**L1b**) outperforms in most cases. For example, its cinnamyliridium complex, **K3**,[7b] was prepared following the procedure developed by Helmchen and co-workers.[12] It is worth noting that an exclusive exo isomer was formed at the very beginning; however, after equilibration, a 4:1 mixture of exo and endo isomers was finally isolated (**Scheme 2**, Part (a)). Using **K3** in the allylic alkylation reaction of sodium dimethyl malonate with cinnamyl methyl carbonate led to comparable results with those obtained with the in situ generated catalyst, which supported the proposal that the (π-allyl)–Ir complex **K3** is the catalytically active species (Scheme 2, Part (b)). Moreover, the crystal structure of **K3** showed that: (i) The iridacycle complex is formed via a C(sp²)–H bond insertion of the phenyl group rather than C(sp³)–H bond activation of a methyl group in the ligand. (ii) Compared with the Ir-C(1) bond of **K3**, the Ir-C(3) bond is longer by 0.173 Å. The strong trans influence of the phosphorus atom, as well as the stabilizing ability of the attached phenyl ring, render C(3) more electropositive than C(1). As a result, nucleophiles prefer to attack at the C(3) position to afford highly branched allyl alkylation products. (iii) Since the *Re*-face of C(3) is well shielded by the chiral pocket of the ligand, nucleophilic substitution

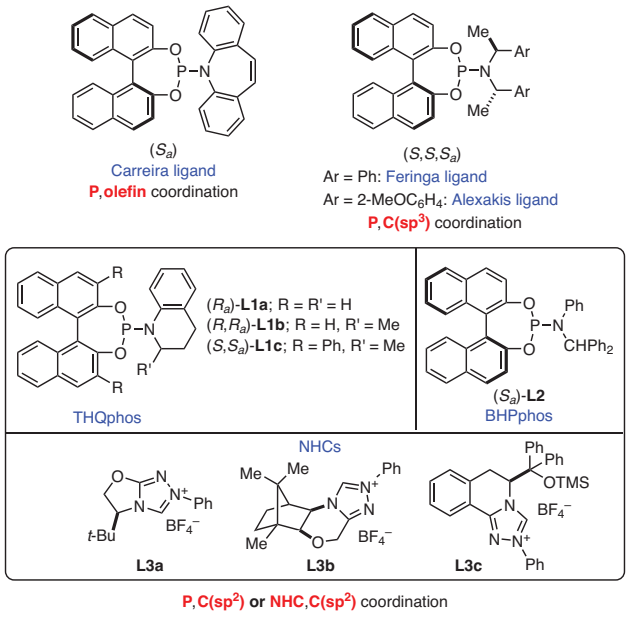

Figure 1. Representative Ligands for the Ir-Catalyzed Asymmetric Allylic Substitution Reactions. *(Ref. 7–9)*

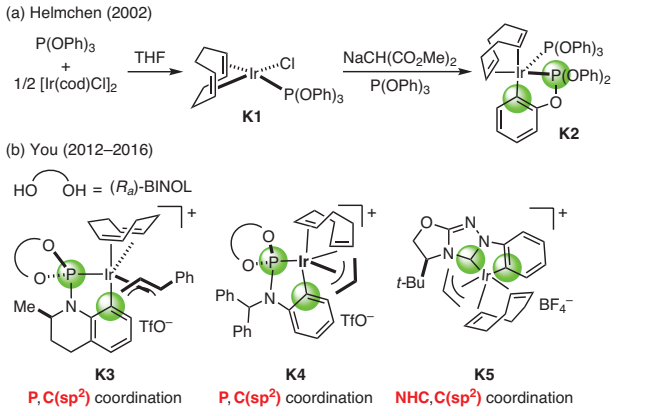

Scheme 1. Representative Iridium Complexes Formed by C(sp²)–H Activation of Ligands. *(Ref. 7b,8,9d,11)*

would occur from the *Si*-face to give the *R* configuration of the branched product. Compared with Ir complexes derived from Feringa-type ligands, **K3** has a bigger pocket for the allyl ligand, thus permitting a good tolerance of sterically bulky substrates. One possible explanation for the observed high enantioselectivity is that the kinetically favorable exo form of **K3** could be captured by nucleophiles prior to π–σ–π interconversion. The absolute configuration of the chiral products is determined by the BINOL scaffolds. Interestingly, the reactions with THQphos and the Feringa ligand derived from the same configuration of BINOL afford the products with opposite absolute configurations. Further investigations disclosed that the same C(sp^2)–H activation mode operates in the iridium complexes derived from BHPphos and the NHCs bearing an *N*-Ar group.[8,9] These three types of ligand have found wide applications in iridium-catalyzed asymmetric allylic substitution reactions.

4. Ir-Catalyzed Asymmetric Allylic Substitutions with Carbon Nucleophiles

4.1. Enolates

In 2012, our group introduced a series of *N*-aryl phosphoramidites, such as THQphos and BHPphos, as ligands for the iridium-catalyzed asymmetric allylic alkylation of sodium dimethyl malonates.[7b] (R,R_a)-Me-THQphos (**L1b**) proved to be the optimal ligand, with the corresponding reactions giving good yields and excellent regio- and enantioselectivities. It is worth noting that ortho-substituted cinnamyl carbonates, which are typically unfavored substrates in iridium catalysis with Feringa-type ligands, were well accommodated in this reaction.[7b] Recently, a chiral dihydroisoquinoline-type NHC was used as ligand for the same transformation, resulting in excellent enantioselectivity but moderate regioselectivity being achieved for a wide range of allylic substrates.[9f] Preliminary mechanistic studies have suggested that the key active species results from the same C(sp^2)–H activation mode. The modest regioselectivity is presumed to be due to electronic effects, since the phosphorus in THQphos is a stronger electron donor than an NHC (**eq 1**).[7b,9f]

An iridium-catalyzed asymmetric allylic alkylation of cyclic β-keto esters has been reported by Stoltz and co-workers.[13] The corresponding α-quaternary β-keto ester products bearing vicinal stereocenters were obtained in good yields and excellent stereoselectivities. Although diastereoselective control by a catalyst is problematic within this domain, the iridium complex derived from (R,R_a)-Me-THQphos (**L1b**) resulted in diastereoselectivities (>20:1 dr) that are much greater than those from other privileged ligands (1:1 or 1:2 dr in each case).[13,14] Stoltz's group extended the use of the Ir/**L1b** catalytic system further to address asymmetric transformations involving the more challenging acyclic β-keto esters.[15] Employing LiO*t*-Bu as base, a wide variety of nucleophiles—bearing substituents such as alkyl, allyl, propargyl, heteroaryl, and ketone functionalities at the α position—were tolerated, affording the expected products in excellent yields and selectivities. When an electron-withdrawing group was incorporated into the cinnamyl carbamate substrates, a diminished regioselectivity was observed. When the logarithm of the B/L value was plotted vs the corresponding Brown σ^+ constant, a linear relationship was revealed, which corresponded well with the experimental observations.

Stoltz's group later employed enolates derived from α,β-unsaturated malonates or α,β-unsaturated keto esters as substrates, and found that sequential α-alkylation and Cope rearrangement afforded linear γ-alkylated products in good yields and with excellent ee's.[16] (S,S_a)-diPh-THQphos (**L1c**) was identified as the optimal ligand for α-alkylation (**Scheme 3**, Part

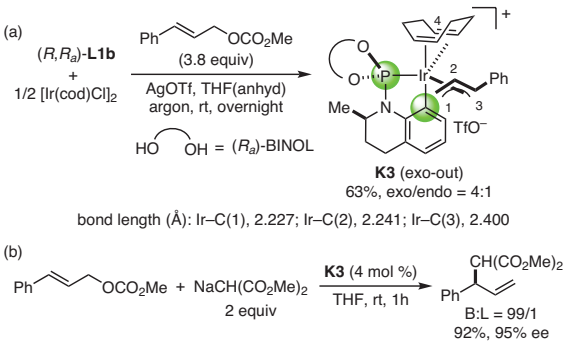

Scheme 2. Synthesis and Application of Iridium–THQphos Complex **K3**. *(Ref. 7b)*

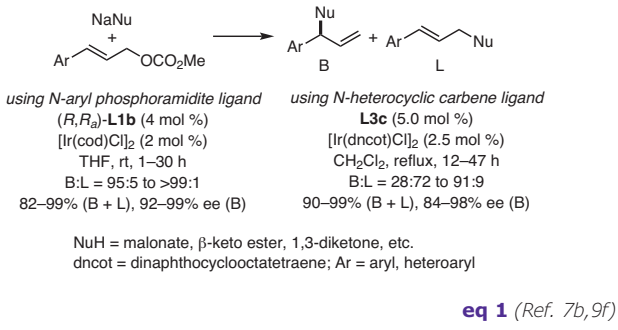

eq 1 *(Ref. 7b,9f)*

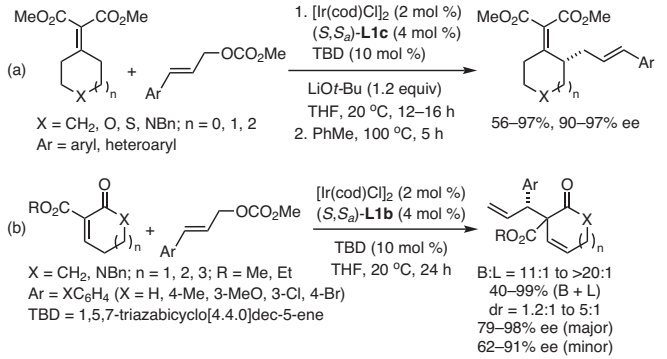

Scheme 3. Ir-Catalyzed Asymmetric Allylic γ-Alkylation of α,β-Unsaturated Malonates and Keto Esters. *(Ref. 16)*

(a)).[16] The Cope rearrangement occurred with a high degree of chirality transfer via a chair-like transition state. However, the reactions of endocyclic α,β-unsaturated β-keto esters only gave modest dr values (Scheme 3, Part (b)). Moreover, the pure diastereomers from the α-alkylation were isolated and subjected to the Cope rearrangement individually. The major isomer delivered the product in a relatively better yield through a chair-like transition state, while the minor isomer furnished a much lower yield via a boat-like transition state.

Alkyl-substituted allylic electrophiles are challenging substrates in iridium-catalyzed asymmetric allylic substitutions. Nevertheless, the Ir-catalyzed asymmetric allylic alkylation of β-keto esters with crotyl derivatives has been achieved by Stoltz and co-workers.[17] Due to the counterion effect, crotyl chloride provided better regioselective control than crotyl carbonate. With diPh-THQphos (**L1c**) as ligand, the corresponding alkylated products were furnished in good-to-excellent yields and selectivities. The same laboratory later reported that masked acyl cyanide reagents were suitable nucleophiles in the asymmetric allylic alkylation catalyzed by the iridium catalyst derived from (*S*,S_a)-**L1b**. This led to vinylated α-aryl carbonyl derivatives with high enantioselectivity (**eq 2**).[18]

Bos and Riguet reported that benzofuran-substituted γ-lactones are competent substrates in Ir-catalyzed asymmetric allylic substitutions in the presence of strong base such as LiHMDS that is required to generate the corresponding enolates. By using BHPphos (S_a)-**L2** as the optimal ligand, 1,5-hexadienes were delivered in good-to-excellent yields and selectivities (**eq 3**).[19] Interestingly, a heteroaromatic Cope rearrangement of the resultant 1,5-hexadienes followed by rearomatization permitted the efficient alkylation of the benzofuran ring at the 3 position.

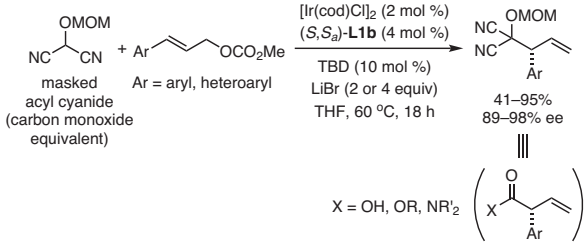

eq 2 *(Ref. 18)*

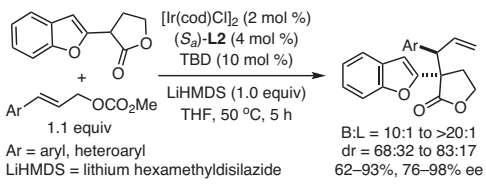

eq 3 *(Ref. 19)*

4.2. Electron-Rich Arenes

4.2.1. Indoles

Apart from soft carbon nucleophiles, aromatic compounds are also suitable substrates in iridium-catalyzed asymmetric allylic substitutions with ligands capable of undergoing C(sp²)–H activation. We reported the earliest examples back in 2009, when (*R*,R_a)-**L1b** and its analogues were synthesized and applied in the Ir-catalyzed asymmetric Friedel–Crafts reaction of indoles with allylic carbonates.[7a] High levels of regioselectivity for the branched alkylation product as well as high levels of enantioselectivity were observed. In particular, **L1b** exhibited superior performance to the Feringa-type ligands when ortho-substituted cinnamyl carbonates were used. When reacting with substrates bearing an allylic carbonate side chain at the C(3) position of indoles, an intramolecular nucleophilic attack at the more-substituted C(3) of indoles took place resulting in a spirocyclic product.[20] Systematic evaluation of various reaction parameters established that the iridium catalyst generated in situ from $[Ir(cod)Cl]_2$ and **L1b** affords the desired dearomatized products bearing all-carbon quaternary stereogenic centers in high yields and with remarkably high diastereo- and enantioselectivity (up to >99:1 dr and 97% ee) (**Scheme 4**, Part (a)).[20] The resultant spiroindolenines were amenable to further elaboration without loss of enantiomeric purity. Subsequently, an unprecedented Ir-catalyzed asymmetric allylic dearomatization–*N*-Bn iminium migration sequence was unlocked when the electronic property of the tether was tuned.[21] Synthesis of chiral tetrahydro-β-carbolines was achieved in a highly enantioselective fashion with readily accessible **L2** as the chiral ligand. An aza-spiroindolenine intermediate was proposed and detected via in situ infrared spectroscopy.

Interestingly, by employing symmetric bis(indol-3-yl)-substituted allylic carbonates as substrates, the desymmetrizing allylic dearomatization of indoles was achieved.[22] The spiroindolenines containing three contiguous stereogenic centers

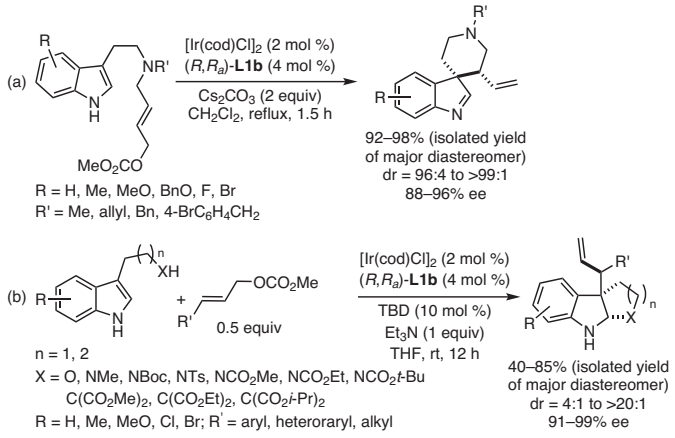

Scheme 4. Ir-Catalyzed Asymmetric Allylic Alkylation of Indole Derivatives. *(Ref. 20,24)*

were obtained as single diastereoisomers with exceptionally high enantioselectivity (up to 99% ee). The combination of $[Ir(dbcot)Cl]_2$ (dbcot = dibenzocyclooctatetraene)[23] and (S,S_a)-**L1c** exerted crucial influence on the reaction outcome. When the products were subjected to a catalytic amount of *p*-toluenesulfonic acid in refluxing THF, a ring expansion of a six- to a seven-membered-ring occurred to deliver hexahydroazepino[4,5-*b*]indoles with high diastereoselectivity. The configuration of the migrating carbon stereocenter was reversed, indicating a possible stepwise migration mechanism involving a free vinyliminium intermediate.

The intermolecular allylic dearomatization of indoles was also explored using the iridium catalyst derived from (R,R_a)-**L1b**. Allylic substitution with allylic carbonates was selective for the branched product and yielded polycyclic indolines possessing contiguous tertiary and all-carbon quaternary stereocenters in a highly chemo-, regio-, diastereo-, and enantioselective fashion.[24] Tryptophols, tryptamines, indoles with a carbon nucleophile side chain, and tryptophan derivatives were demonstrated to be suitable substrates (Scheme 4, Part (b)).

4.2.2. Pyrroles

Similarly, the $[Ir(cod)Cl]_2$–(R,R_a)-**L1b** complex catalyzed the asymmetric allylic dearomatization of pyrroles tethered with an allylic carbonate. With THF as solvent, six-membered, spiro-2*H*-pyrrole derivatives were obtained in good yields with high levels of regio-, diastereo- and enantioselectivity (**Scheme 5**, Part (a)).[25] Further transformations of the resultant products afforded diverse pharmaceutically important spirocycles. When (R_a)-**L2** was used instead of (R,R_a)-**L1b** and the tether between the pyrrole ring and the allylic carbonate moiety was shortened by one CH_2 group, a sequential dearomatization–in situ migration of the substituent from the C(2) to the C(3) position of the pyrrole ring occurred in a fashion similar to that of indoles.[21] In combination with DFT calculations, it was found that the *N*-Bn linkage enhances the migratory aptitude of the methylene group. Employing (R_a)-**L2** again and switching the substrates to the gem-diester-tethered analogues afforded stable five-membered-ring spiro-2*H*-pyrroles in good yields with excellent diastereo- and enantioselectivity.[8] Upon treatment with a catalytic amount of TsOH, stereospecific allyl migration took place smoothly, yielding the enantioenriched polycyclic pyrrole derivatives with preserved ee's. It is worth highlighting that the Ir-complex derived from $[Ir(cod)Cl]_2$ and (R_a)-**L2** is critical for excellent control of both diastereo- and enantioselectivity. As a consequence, the corresponding π-allyl iridium complex was prepared and characterized, further confirming the C(sp^2)–H activation mode of the ligand.[8]

4.2.3. Naphthols

α-Substituted β-naphthols are challenging substrates in the Ir-catalyzed asymmetric allylic dearomatization, since etherification could be a facile competing reaction. Gratifyingly, by using $[Ir(dbcot)Cl]_2$ as the iridium precursor and (S,S_a)-diPh-THQphos (**L1c**), the allylic etherification pathway was largely inhibited. The dearomatized spironaphthalenones bearing two contiguous stereogenic centers were furnished with good-to-excellent chemo-, diastereo-, and enantioselectivity (Scheme 5, Part (b)).[26] It is believed that the high C/O alkylation ratio might be caused by the restriction on ring size, as formation of six-membered rings is more facile than that of eight-membered rings. It is worth noting that superior selectivities were achieved when the nitrogen atom was protected with electron-deficient and sterically hindered groups.

5. Ir-Catalyzed Asymmetric Allylic Substitutions with Nitrogen Nucleophiles

5.1. Aliphatic Amines and Arylamines

In 2016, our research laboratory investigated the Ir-catalyzed asymmetric intermolecular allylic amination using various nitrogen nucleophiles—namely, anilines, indolines, benzylamines, and 2-vinylanilines—in the presence of (S,S_a)-**L1c**.[7c] To our delight, we observed a significant advantage over the Feringa ligand with respect to regio- and enantioselective control when challenging ortho-substituted cinnamyl carbonates were employed as substrates. Remarkably, the utilization of either (S,S_a)-**L1c**, its diastereomer (R,S_a)-**L1c**, or a mixture of equal amounts of the two resulted in the same reaction outcome, indicating that the stereocenter of 2-methyl-THQ was not essential in this case. X-ray crystallographic analysis of the catalyst complex further supported the proposal that the active iridacycle was generated via C(sp^2)–H bond activation of the THQ moiety of the ligand.[7c]

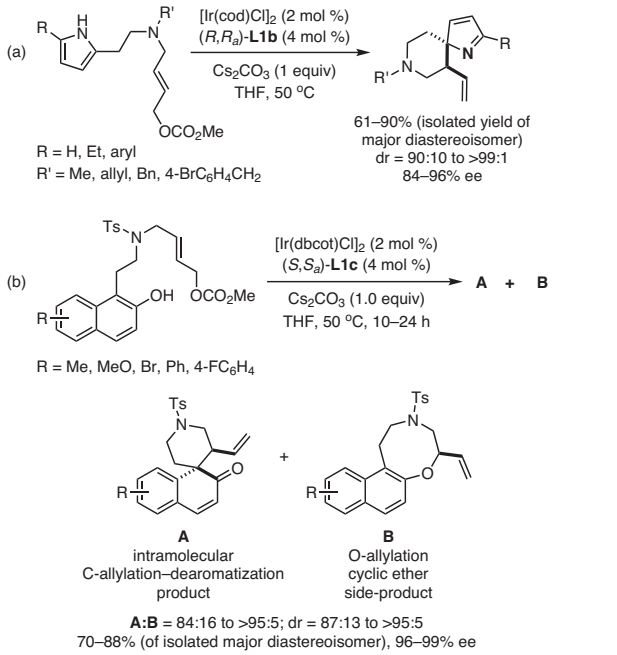

Scheme 5. Ir-Catalyzed Asymmetric Allylic Alkylation of (a) Pyrrole and (b) Naphthol Derivatives. *(Ref. 25,26)*

5.2. Nitrogen-Containing Heterocycles

Our research efforts had demonstrated that indoles and pyrroles with electron-donating or electron-neutral groups attached to the core would undergo a dearomatization–migration reaction sequence. However, when an electron-withdrawing group is installed at the C(2) position, a highly enantioselective intramolecular allylic amination of indoles and pyrroles is enabled by an iridium complex generated in situ from $[Ir(cod)Cl]_2$ and L-*tert*-butylalaninol-derived triazolium salt (**L3a**), first introduced by the research group of Enders.[9a] For the first time, chiral NHC carbenes were demonstrated as suitable ligands for Ir-catalyzed asymmetric allylic substitutions.[9d] Preliminary mechanistic studies suggested that C(sp²)–H activation takes place at the ortho C(sp²)–H bond of the N-aryl group of the ligand. Later, Ir–**L3b** prepared from $[Ir(cod)Cl]_2$ and D-camphor-derived **L3b**, was successfully applied in the same transformation. In both cases, the corresponding indolopiperazinones and piperazinones were furnished in good yields and high enantioselectivities (**eq 4**).[9e] To further broaden the substrate scope for pyrroles, the iridium catalysts derived from chiral phosphoramidites were exploited. Particularly, the utilization of THQphos (**L1b** or **L1c**) significantly improved the enantioselectivity of the reactions involving bromo-substituted pyrroles.[27]

C(sp²)–H activation ligands are also capable of promoting asymmetric allylic dearomatization reactions with nitrogen-containing, electron-deficient heteroarenes.[28–30] With (R,R_a)-**L1b** as the optimal ligand, a variety of heterocycles including pyrazines, quinolines, isoquinolines, benzoxazoles, benzothiazoles, and benzimidazoles underwent asymmetric allylic dearomatization reactions smoothly, affording highly functionalized products in good-to-excellent yields with excellent enantioselectivity (**Scheme 6**, Part (a)).[28,29] In accordance with well-established Ir-catalysis pathways, the allylic carbonate reacts first with the chiral iridium catalyst. The liberated methoxide anion abstracts the α proton in the substrate, rendering the N-attack feasible due to delocalization of the negative charge. Alternatively, N-alkylation occurs prior to deprotonation. As supporting evidence, and under certain conditions, the intermediate resulting from direct N-attack has been captured in situ and isolated. The synthetic utility of this method has been demonstrated by a facile synthesis of compound **2**,[29] which can be easily converted into (+)-gephyrotoxin[31] through known reaction steps[32] (Scheme 6, Part (b)).

The reaction was then extended to the more challenging hydroxyquinoline derivatives.[33] However, the frequently used phosphoramidites—including the Feringa and the Alexakis ligands, Me-THQphos, and BHPphos—failed to give satisfactory results. However, to our great delight, the anticipated intramolecular allylic alkylation reactions of 5- and 7-hydroxyquinolines were achieved with good-to-excellent yields and enantioselectivities with the iridium catalyst generated in situ from $[Ir(dbcot)Cl]_2$ and the Enders NHC (**L3a**) (**eq 5**).[33] Theoretical calculations supported the hypothesis that the aromatic character of the two consecutive rings of the hydroxyquinoline was weakened. Remarkably, performing the reaction directly in air and using undistilled THF as solvent led to comparable results, further highlighting the robustness of Ir–NHC catalysis. Based on this method, a key intermediate (a phenol variant of *ent*-**2**) for the synthesis of (+)-gephyrotoxin was delivered in only two steps from the product of the reaction. This method is also a rare example of allylic chlorides being viable precursors in the Ir-catalyzed asymmetric allylic substitution reaction.

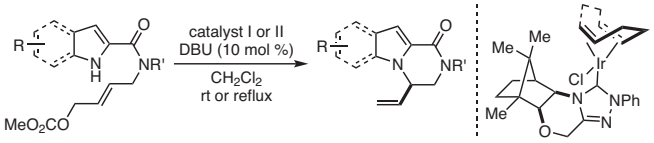

eq 4 *(Ref. 9d,9e)*

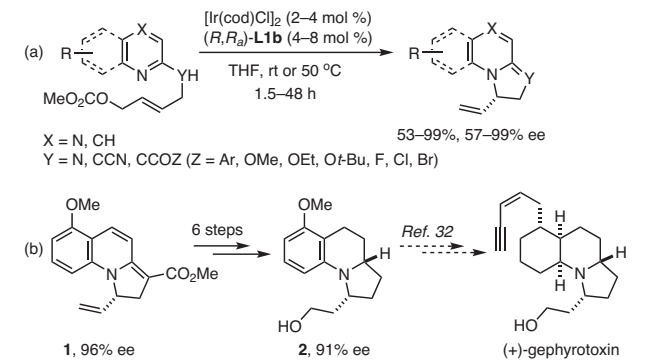

Scheme 6. (a) The Iridium-Catalyzed Asymmetric Allylic Dearomatization of Nitrogen-Containing Heterocycles and (b) Its Application to a Formal Synthesis of (+)-Gephyrotoxin, a Naturally Occurring Histrionicotoxin. *(Ref. 28,29)*

6. Ir-Catalyzed Asymmetric Allylic Substitutions with Oxygen Nucleophiles

The catalytic, enantioselective construction of chiral N,O-heterocycles remains a challenging task in organic synthesis.

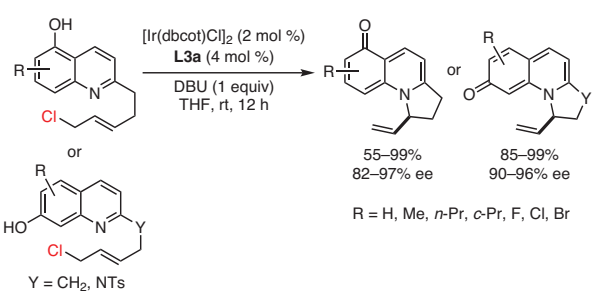

eq 5 *(Ref. 33)*

In 2014, Feringa and co-workers reported an unprecedented synthesis of such scaffolds through a highly efficient iridium-catalyzed intramolecular allylic substitution with the amide group providing the oxygen nucleophile.[34] By employing the catalyst generated from $[Ir(cod)Cl]_2$ and (S_a)-**L1a**, Feringa's team was able to prepare differentially substituted oxazolines, oxazines, and benzoxazines in good-to-excellent yields and with high enantiomeric purity (**Scheme 7**).[34]

7. Conclusion and Outlook

Chiral phosphoramidite and NHC ligands capable of undergoing C(sp^2)–H activation have been widely employed in Ir-catalyzed asymmetric allylic substitution (AAS) reactions. Among them, THQphos and BHPphos participate in P,C(sp^2) coordination with the Ir center. As a result of both electronic and steric influences, high levels of branched regioselectivity and asymmetric induction are generally observed. Intriguingly, the newly developed catalysts tolerate well ortho-substituted cinnamyl carbonates, which were challenging substrates in prior similar studies. The catalysts also display remarkable diastereoselective control when prochiral nucleophiles are employed. Furthermore, the C(sp^2)–H activation mode has been extended to structurally distinct N-heterocyclic carbene ligands, whereby the active iridium catalyst results from a bidentate NHC,C(sp^2) coordination. With NHC as the chiral ligand, Ir-catalyzed asymmetric allylic substitution reactions can occur in a highly enantioselective fashion. However, regioselective control is still problematic for the intermolecular variants. Nevertheless, NHCs show significant advantages in some instances, as exemplified by the asymmetric allylic alkylation of challenging hydroxyquinolines.

Despite considerable progress, the substrate scope for currently available methods is still limited to commonly used nucleophiles, such as enolates or aromatic compounds, and activated allylic electrophiles. In this regard, expanding the substrate scope is an important goal in our current investigations. On the other hand, efforts will also be directed to exploring structurally distinct ligands capable of C(sp^2)–H activation, as well as exploring new types of asymmetric reactions beyond the Ir-catalyzed AAS.[35]

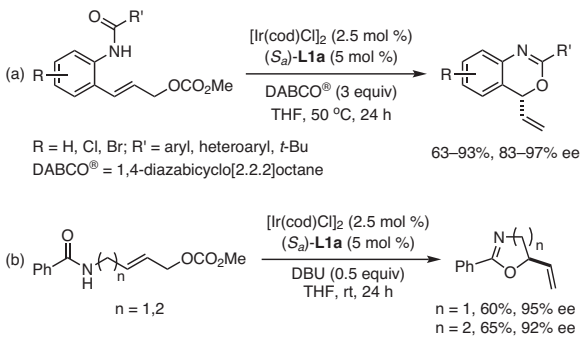

Scheme 7. Feringa's Ir-Catalyzed Intramolecular Asymmetric Allylic Substitution Reaction with Amide Oxygen Nucleophiles. *(Ref. 34)*

8. Acknowledgments

We thank the National Key R&D Program of China (2016YFA0202900), National Natural Science Foundation of China (91856201, 21572252, 21821002), Strategic Priority Research Program (XDB20000000) and Key Research Program of Frontier Sciences (QYZDY-SSW-SLH012) of the Chinese Academy of Sciences, and the Science and Technology Commission of Shanghai Municipality (16XD1404300) for their generous financial support.

9. References

(1) For selected reviews, see: (a) Trost, B. M.; van Vranken, D. L. *Chem. Rev.* **1996**, *96*, 395. (b) Trost, B. M. *Chem. Pharm. Bull.* **2002**, *50*, 1. (c) Trost, B. M.; Crawley, M. L. *Chem. Rev.* **2003**, *103*, 2921. (d) Milhau, L.; Guiry, P. J. *Top. Organomet. Chem.* **2012**, *38*, 95.

(2) For selected reviews, see: (a) Helmchen, G.; Dahnz, A.; Dübon, P.; Schelwies, M.; Weihofen, R. *Chem. Commun.* **2007**, 675. (b) Helmchen, G. In *Iridium Complexes in Organic Synthesis*; Oro, L. A., Claver, C., Eds.; Wiley-VCH: Weinheim, Germany, 2009; pp 211–250. (c) Wu, Y.; Yang, D.; Long, Y. *Chin. J. Org. Chem.* **2009**, *29*, 1522. (d) Hartwig, J. F.; Stanley, L. M. *Acc. Chem. Res.* **2010**, *43*, 1461. (e) Hartwig, J. F.; Pouy, M. J. *Top. Organomet. Chem.* **2011**, *34*, 169. (f) Liu, W.-B.; Xia, J.-B.; You, S.-L. *Top. Organomet. Chem.* **2012**, *38*, 155. (g) Tosatti, P.; Nelson, A.; Marsden, S. P. *Org. Biomol. Chem.* **2012**, *10*, 3147. (h) Hethcox, J. C.; Shockley, S. E.; Stoltz, B. M. *ACS Catal.* **2016**, *6*, 6207. (i) Qu, J.; Helmchen, G. *Acc. Chem. Res.* **2017**, *50*, 2539. (j) Zhang, X.; You, S.-L. *Chimia* **2018**, *72*, 589. (k) Cheng, Q.; Tu, H.-F.; Zheng, C.; Qu, J.-P.; Helmchen, G.; You, S.-L. *Chem. Rev.* **2019**, *119*, 1855. (l) Rössler, S. L.; Petrone, D. A.; Carreira, E. M. *Acc. Chem. Res.* **2019**, *52*, 2657. (m) Qu, J.-P.; Helmchen, G.; Yang, Z.-P.; Zhang, W.; You, S.-L. *Org. React.* **2019**, *99*, 423.

(3) (a) Janssen, J. P.; Helmchen, G. *Tetrahedron Lett.* **1997**, *38*, 8025. (b) Defieber, C.; Grützmacher, H.; Carreira, E. M. *Angew. Chem., Int. Ed.* **2008**, *47*, 4482.

(4) For selected early examples, see: (a) Lafrance, M.; Roggen, M.; Carreira, E. M. *Angew. Chem., Int. Ed.* **2012**, *51*, 3470. (b) Rössler, S. L.; Krautwald, S.; Carreira, E. M. *J. Am. Chem. Soc.* **2017**, *139*, 3603.

(5) (a) De Vries, A. H. M.; Meetsma, A.; Feringa, B. L. *Angew. Chem., Int. Ed. Engl.* **1996**, *35*, 2374. (b) Teichert, J. F.; Feringa, B. L. *Angew. Chem., Int. Ed.* **2010**, *49*, 2486. (c) Langlois, J. B.; Alexakis, A. *Top. Organomet. Chem.* **2012**, *38*, 235 (DOI: https://doi.org/10.1007/3418-2011-12). (d) Tissot-Croset, K.; Polet, D.; Alexakis, A. *Angew. Chem., Int. Ed.* **2004**, *43*, 2426. (e) Alexakis, A.; Polet, D. *Org. Lett.* **2004**, *6*, 3529.

(6) For selected early examples, see: (a) Ohmura, T.; Hartwig, J. F. *J. Am. Chem. Soc.* **2002**, *124*, 15164. (b) Kiener, C. A.; Shu, C.; Incarvito, C.; Hartwig, J. F. *J. Am. Chem. Soc.* **2003**, *125*, 14272. (c) Madrahimov, S. T.; Hartwig, J. F. *J. Am. Chem. Soc.* **2012**, *134*, 8136. (d) Madrahimov, S. T.; Li, Q.; Sharma, A.; Hartwig, J. F. *J. Am. Chem. Soc.* **2015**, *137*, 14968.

(7) (a) Liu, W.-B.; He, H.; Dai, L.-X.; You, S.-L. *Synthesis* **2009**, 2076. (b) Liu, W.-B.; Zheng, C.; Zhuo, C.-X.; Dai, L.-X.; You,

S.-L. *J. Am. Chem. Soc.* **2012**, *134*, 4812. (c) Zhang, X.; Liu, W.-B.; Cheng, Q.; You, S.-L. *Organometallics* **2016**, *35*, 2467.
(8) Zhuo, C.-X.; Cheng, Q.; Liu, W.-B.; Zhao, Q.; You, S.-L. *Angew. Chem., Int. Ed.* **2015**, *54*, 8475.
(9) (a) Enders, D.; Kallfass, U. *Angew. Chem., Int. Ed*. **2002**, *41*, 1743. (b) Li, Y.; Feng, Z.; You, S.-L. *Chem. Commun.* **2008**, 2263. (c) Li, G.-T.; Gu, Q.; You, S.-L. *Chem. Sci.* **2015**, *6*, 4273. (d) Ye, K.-Y.; Cheng, Q.; Zhuo, C.-X.; Dai, L.-X.; You, S.-L. *Angew. Chem., Int. Ed*. **2016**, *55*, 8113. (e) Ye, K.-Y.; Wu, K.-J.; Li, G.-T.; Dai, L.-X.; You, S.-L. *Heterocycles* **2017**, *95*, 304 (DOI: 10.3987/COM-16-S(S)19; https://www.heterocycles.jp/newlibrary/libraries/journal/95/1). (f) Bao, C.-C.; Zheng, D.-S.; Zhang, X.; You, S.-L. *Organometallics* **2018**, *37*, 4763.
(10) Takeuchi, R.; Kashio, M. *Angew. Chem., Int. Ed. Engl.* **1997**, *36*, 263.
(11) Bartels, B.; García-Yebra, C.; Rominger, F.; Helmchen, G. *Eur. J. Inorg. Chem.* **2002**, 2569.
(12) (a) Spiess, S.; Raskatov, J. A.; Gnamm, C.; Brödner, K.; Helmchen, G. *Chem.—Eur. J.* **2009**, *15*, 11087. (b) Raskatov, J. A.; Spiess, S.; Gnamm, C.; Brödner, K.; Rominger, F.; Helmchen, G. *Chem.—Eur. J.* **2010**, *16*, 6601.
(13) Liu, W.-B.; Reeves, C. M.; Virgil, S. C.; Stoltz, B. M. *J. Am. Chem. Soc.* **2013**, *135*, 10626.
(14) The iridium complex was generated in situ by treatment of $[Ir(cod)Cl]_2$ and ligand with 1,5,7-triazabicyclo[4.4.0]undec-5-ene (TBD): (a) Lipowsky, G.; Miller, N.; Helmchen, G. *Angew. Chem., Int. Ed.* **2004,** *43*, 4595. (b) Shu, C.; Leitner, A.; Hartwig, J. F. *Angew. Chem., Int. Ed*. **2004**, *43*, 4797.
(15) Liu, W.-B.; Reeves, C. M.; Stoltz, B. M. *J. Am. Chem. Soc.* **2013**, *135*, 17298.
(16) Liu, W.-B.; Okamoto, N.; Alexy, E. J.; Hong, A. Y.; Tran, K.; Stoltz, B. M. *J. Am. Chem. Soc.* **2016**, *138*, 5234.
(17) Hethcox, J. C.; Shockley, S. E.; Stoltz, B. M. *Angew. Chem., Int. Ed.* **2016**, *55*, 16092.
(18) Hethcox, J. C.; Shockley, S. E.; Stoltz, B. M. *Org. Lett.* **2017**, *19*, 1527.
(19) Bos, M.; Riguet, E. *Chem. Commun.* **2017**, *53*, 4997.
(20) Wu, Q.-F.; He, H.; Liu, W.-B.; You, S.-L. *J. Am. Chem. Soc.* **2010**, *132*, 11418.
(21) Zhuo, C.-X.; Wu, Q.-F; Zhao, Q.; Xu, Q.-L.; You, S.-L. *J. Am. Chem. Soc.* **2013**, *135*, 8169.
(22) Wang, Y.; Zheng, C.; You, S.-L. *Angew. Chem., Int. Ed.* **2017**, *56*, 15093.
(23) Spiess, S.; Welter, C.; Franck, G.; Taquet, J.-P.; Helmchen, G. *Angew. Chem., Int. Ed.* **2008**, *47*, 7652.
(24) Zhang, X.; Liu, W.-B.; Tu, H.-F.; You, S.-L. *Chem. Sci.* **2015**, *6*, 4525.
(25) Zhuo, C.-X.; Liu, W.-B.; Wu, Q.-F.; You, S.-L. *Chem. Sci.* **2012**, *3*, 205.
(26) Cheng, Q.; Wang, Y.; You, S.-L. *Angew. Chem., Int. Ed.* **2016**, *55*, 3496.
(27) Zhuo, C.-X.; Zhang, X.; You, S.-L. *ACS Catal.* **2016**, *6*, 5307.
(28) Yang, Z.-P.; Wu, Q.-F.; You, S.-L. *Angew. Chem., Int. Ed.* **2014**, *53*, 6986.
(29) Yang, Z.-P.; Wu, Q.-F.; Shao, W.; You, S.-L. *J. Am. Chem. Soc.* **2015**, *137*, 15899.
(30) Yang, Z.-P.; Zheng, C.; Huang, L.; Qian, C.; You, S.-L. *Angew. Chem., Int. Ed.* **2017**, *56*, 1530.
(31) Daly, J. W.; Witkop, B.; Tokuyama, T.; Nishikawa, T.; Karle, I. L. *Helv. Chim. Acta* **1977**, *60*, 1128.
(32) Ito, Y.; Nakajo, E.; Nakatsuka, M.; Saegusa, T. *Tetrahedron Lett*. **1983**, *24*, 2881.
(33) Yang, Z.-P.; Jiang, R.; Zheng, C.; You, S.-L. *J. Am. Chem. Soc.* **2018**, *140*, 3114.
(34) Zhao, D.; Fañanás-Mastral, M.; Chang, M.-C.; Otten, E.; Feringa, B. L. *Chem. Sci.* **2014**, *5*, 4216.
(35) For an application of BHPphos in a Pd-catalyzed decarboxylation–cycloaddition sequence, see: Li, T.-R.; Tan, F.; Lu, L.-Q.; Wei, Y.; Wang, Y.-N.; Liu, Y.-Y.; Yang, Q.-Q.; Chen, J.-R.; Shi, D.-Q.; Xiao, W.-J. *Nat. Commun.* **2014**, *5*, Article No. 5500 (DOI: https://doi.org/10.1038/ncomms6500).

About the Authors

Xiao Zhang received her B.Sc. degree in chemistry in 2010 from Anhui Normal University, and completed her Ph.D. degree in 2015 under the direction of Professor Shu-Li You at the Shanghai Institute of Organic Chemistry (SIOC). She then spent two years as a Humboldt postdoctoral fellow with Professor Eric Meggers at Philipps-Universität Marburg. In 2017, she joined SIOC as Assistant Professor, and was promoted to Associate Professor in June of 2018. Her research interests are in the areas of transition-metal catalysis and photochemistry.

Shu-Li You received his B.Sc. degree in chemistry in 1996 from Nankai University. He obtained his Ph.D. degree in 2001 from the Shanghai Institute of Organic Chemistry (SIOC) under the supervision of Professor Li-Xin Dai, and then carried out postdoctoral studies with Professor Jeffery Kelly at The Scripps Research Institute. From 2004 to 2006, he worked at the Genomics Institute of the Novartis Research Foundation as a PI before joining SIOC as Professor in 2006. He is currently the director of the State Key Laboratory of Organometallic Chemistry. His research interests focus mainly on asymmetric C–H functionalization and catalytic asymmetric dearomatization (CADA) reactions.

Recent Advances in Sulfuration Chemistry Enabled by Bunte Salts


Prof. M. Wang


Ms. Y. Li

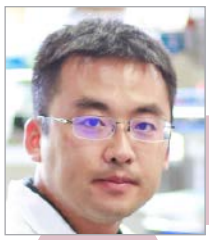
Prof. X. Jiang

Ming Wang, Yaping Li, and Xuefeng Jiang*

a State Key Laboratory of Estuarine and Coastal Research
East China Normal University
3663 North Zhongshan Road
Shanghai 200062, China
b Shanghai Key Laboratory of Green Chemistry and Chemical Process
East China Normal University
3663 North Zhongshan Road
Shanghai 200062, China
Email: xfjiang@chem.ecnu.edu.cn

Keywords. Bunte salt; *S*-aryl(alkyl) thiosulfate sodium salts; sodium thiosulfate; sulfuration reagent; sulfide; sulfur-containing heterocycles; dithiocarbamates; thiophosphates; metal nanoparticles; glycosyl.

Abstract. Bunte salts are easy-to-handle crystalline solids, even when incorporating highly lipophilic organic moieties, and generally have little-to-no odor. Due to the unique properties of Bunte salts, they have been frequently utilized in the synthesis of sulfides, sulfur-containing heterocycles, thiophosphates, other compound classes, and metal nanoparticles. This short review focuses on recent applications of Bunte salts in the synthesis of sulfur-containing compounds with particular emphasis on the synthesis of sulfides.

Outline

1. Introduction

Alkyl and aryl thiosulfate sodium salts are known as Bunte salts, after Hans Bunte who first reported them in 1874.[1] He prepared the first such salt by reactiing ethyl bromide with sodium thiosulfate ($Na_2S_2O_3$) to yield *S*-ethyl thiosulfate sodium salt as a crystalline solid. Bunte salts, as the easy-to-handle crystalline solids, generally have little-to-no odor.[2–3] The sulfur trioxide group in Bunte salts could be viewed as an electron-withdrawing group preventing strong coordination of the sulfur atom to metals. Moreover, we obtained the crystal structure of a Bunte salt in 2015 and found that its sulfur–sulfur bond is longer than the traditional S–S bond, which may be activated easily.[4] Over the past few years, enormous efforts have been devoted to developing synthetic methodologies for the application of Bunte salts. The present article concisely reviews recently reported methodologies for the application of Bunte salts, with particular emphasis on the synthesis of sulfides. The presentation is organized according to the structures of the reaction partners of Bunte salts.

2. Preparation of Bunte Salts

2.1. Alkyl Bunte Salts

Alkyl Bunte salts have traditionally and conveniently been prepared by reaction of the inexpensive and odorless sodium thiosulfate ($Na_2S_2O_3$) with alkyl halides.[5–8] More recently, various modifications of the reaction conditions have been developed for

a diversity of alkyl halides. Both primary and secondary halides are compatible with the transformation, and the desired Bunte salt products are obtained in generally excellent yields.

2.2. Aryl Bunte Salts

Janeba and co-workers reported a novel and facile route to polysubstituted aryl and heteroaryl Bunte salts by reaction of aromatic thiocyanates with sodium sulfite.[9] Their synthesis could be conducted under catalyst-free and room temperature conditions to generate the desired Bunte salts in good yields. Monosubstituted thiocyanatobenzothiazole and polysubstituted thiocyanatopyrimidines, which contain labile hydrogens such as NH_2 and OH, were compatible with the reaction conditions.

A year later, Reeves's group disclosed the first direct and general method for the synthesis of a variety of aryl, heteroaryl, and vinyl Bunte salts in 66–89% yields.[8] The approach involves a Cu(I)-catalyzed reaction of the widely available halide precursors with sodium thiosulfate (1.5 equiv) in DMSO at 80 °C for 2–6 h. It is worth noting that, in the case of vinyl halides, the geometry of the carbon–carbon double bond was preserved in the reaction. This synthetic method is currently one of the most efficient routes to such Bunte salts because of the wide availability and broad compatibility of the halide starting materials.

In addition to the above strategies, several other original methods have been developed for the synthesis of aryl Bunte salts. For example, aryl Bunte salts were obtained by sulfonylation of aryl thiols with *N*-pyridinium sulfonic acid ($C_5H_5NSO_3H$)[10] or with chlorosulfonic acid ($ClSO_3H$),[11] and by reaction of sodium sulfite with aryl disulfides (or aryl sulfenyl chlorides).[12]

2.3. Glycosyl Bunte Salts

Very recently, glycosyl Bunte salts (*S*-glycosyl thiosulfates) have been developed by Shoda and co-workers as a new class of synthetic intermediates in carbohydrate chemistry[13] The one-pot reaction is carried out in H_2O–CH_3CN, and it involves the direct condensation of unprotected mono-, di-, and polysaccharides with $Na_2S_2O_3$ in the presence of 2-chloro-1,3-dimethylimidazolinium chloride (DMC) as dehydrating agent. Glucose, allose, xylose, mannose, rhamnose, and galactose all underwent this mild reaction efficiently, giving rise to the corresponding glycosyl Bunte salts in up to 94% yields. The utility of these *S*-glycosyl thiosulfates was then demonstrated by converting β-D-glucosyl Bunte salt into 1-thio-β-D-glucose, glucosyl disulfide, 1,6-anhydroglucose, and ethyl α-D-glucopyranoside.

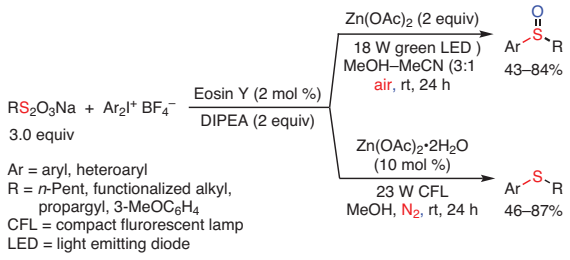

Scheme 1. Photocatalytic Sulfoxide and Sulfide Formation through Controlled Sulfoxidation and Sulfenylation of Diaryliodonium Salts. *(Ref. 14)*

3. Bunte Salts for the Synthesis of Sulfides

The main application of Bunte salts is in the synthesis of sulfides, since these salts are stable, odorless, and green when compared with thiols as substrates.

3.1. Coupling through C–X Bond Cleavage

In 2017, we developed a controlled sulfoxidation of diaryliodonium salts with Bunte salts in air and under photocatalytic conditions in which dual electron- and energy-transfer as well as single-electron-transfer processes were involved (**Scheme 1**).[14] When the reaction was carried out under a nitrogen atmosphere, sulfenylation products were conveniently obtained. This approach could be used in the late-stage modification of pharmaceuticals and sugar derivatives, which were highly compatibile with the reaction conditions.

In the proposed mechanism, the excited-state catalyst Eosin Y* (EY*) reacts with the diaryliodonium salt via a single-electron transfer process to generate an aryl radical. The aryl radical then couples with the Bunte salt to afford a sulfide radical. The electron-transfer process between the sulfide radical (ArS•R) and $EY^{+\bullet}$ provides the sulfide product (ArSR) and regenerates the photosensitizer EY. In the presence of air, an energy-transfer process takes place between $^3O_2$ and EY* to generate $^1O_2$, the key active oxygen species, which was confirmed by fluorescent quenching experiments. Reaction of the in situ generated sulfide (ArSR) with $^1O_2$ forms a persulfoxide intermediate (R(Ar)-S^+–O–O^-), which is stabilized by $Zn(OAc)_2$. Reaction of the persulfoxide with a second in situ generated sulfide leads to two molecules of the observed sulfoxide product (ArS(=O)R).

In 2014, our group developed a Pd-catalyzed double C–S bond forming reaction for the synthesis of aryl alkyl sulfides. Aryl and heteroaryl iodides efficiently reacted with alkyl chlorides to provide the desired sulfides in excellent yields. In this transformation, $Na_2S_2O_3·5H_2O$ was employed as an environmentally friendly and odorless sulfur atom source to generate the Bunte salt in situ.[15] Late-stage modification of pharmaceutical molecules was also achieved to demonstrate the synthetic potential of this protocol.

3.2. Coupling through C–N Bond Cleavage

An analogous Cu-catalyzed double C–S bond forming reaction has been developed for the synthesis of aryl alkyl sulfides from aromatic amines and alkyl halides via in situ generated Bunte salts.[16] Heterocyclic substrates and active-hydrogen-containing substrates were tolerated in this transformation, which permitted the late-stage sulfuration of functionalized aryl amines, including such interesting amines as sulfamethoxazole, sulfadiazine, and the antitumor drug lenalidomide. Axially chiral (*R*)-(+)-2,2′-diamino-1,1′-binaphthalene could also be

transformed into the corresponding bis(benzyl sulfide) product without racemation (38% yield, 99% ee), which offers a facile strategy for the synthesis of chiral, sulfur-containing ligands. Moreover, amine derivatives of glucose and amino acids were tolerated in the reaction, hinting at its potential usefulness in bioorthogonal reactions.

Subsequently, we successfully extended this protocol to the Cu-catalyzed reaction of substituted 1-aryltriazenes and alkyl chlorides in water at room temperature and in the absence of any surfactant with the aim of developing an environmentally friendly variant.[17] We were also delighted to discover that the outcome of the reaction was not significantly affected by the addition of such biomolecules as amino acids, nucleosides, oligosaccharides, proteins, and HeLa cell lysates, highlighting again the promise of its potential applications in bioorthogonal studies.

A photocatalytic variant involved reacting diazonium salts with alkyl or aryl Bunte salts in the presence of $Ru(bpy)_3Cl_2$ (**Scheme 2**).[18] The reaction did not proceed when the Bunte salt was replaced with BnSH or BnSSBn, demonstrating the unique behavior of the Bunte salt in this system. Both alkyl and aryl Bunte salts were well-tolerated in this transformation. Both an oxidative and a reductive quenching process were possible in the transformation. At first, the Ru(II) catalyst is activated by visible light to generate $^{3*}[Ru(bpy)_2(bpy^{\bullet-})Cl_2]$, which undergoes an oxidative quenching process with the diazonium salt to form Ru^{3+} and an aryl diazonium radical ($Ar–N^{\bullet}\equiv N\ BF_4^-$). Bunte salt $R'SSO_3Na$ releases an electron to the solvent and affords a thiosulfate radical cationic species, which couples with the aryl diazonium radical to provide the sulfide products. The solvent shuttles an electron to Ru^{3+} and regenerates the Ru(II) catalyst. A similar catalytic cycle is proposed to operate in the reductive quenching process.

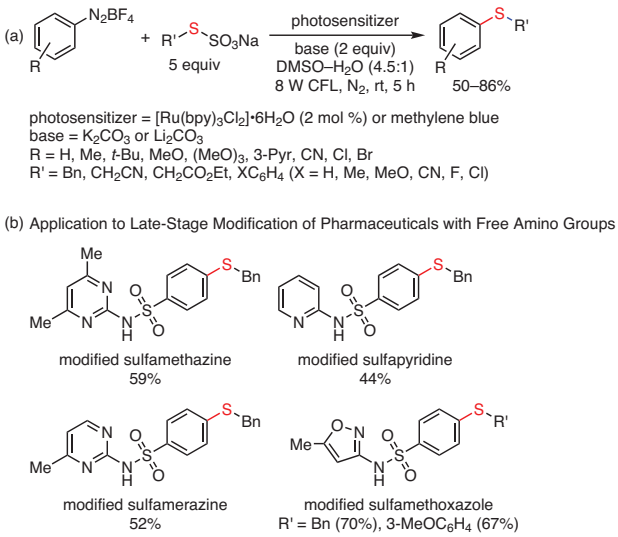

Scheme 2. Photocatalytic Sulfide Formation from Diazonium Salts and Alkyl and Aryl Thiosulfates and Its Application to the Late-Stage Modification of Pharmaceuticals. *(Ref. 18)*

An interesting extension of this approach has been disclosed by Jiang, Yi, and co-workers.[19] In this instance, aromatic primary amines were subjected to an efficient, Cu-catalyzed Sandmeyer-type monofluoromethylthiolation by employing the Bunte salt sodium *S*-(fluoromethyl)sulfurothioate ($FH_2CS–SO_2–ONa$). The intermediate aryldiazonium salts were generated in situ using *tert*-butyl nitrite (*t*-BuONO) and a variety of aryl and heteroaryl primary amines, leading to the desired sulfides in moderate-to-good yields (43–77%). The late-stage monofluoromethylthiolation of biologically relevant sulfonamides and the gastroprokinetic agent mosapride were also achieved in acceptable isolated yields (41–73%). Interestingly, Bunte salt $FH_2CS–SO_2–ONa$ was also utilized in the monofluoromethylthiolation of substituted aryl thiols under similar conditions to provide the corresponding aryl monofluoromethyl disulfides in 58–78% isolated yields.

3.3. Coupling through C–O Bond Cleavage

An efficient, catalytic, and metal-free sulfide synthesis from allyl or propargyl alcohols and organic halides was reported by Chu et al.[20] The reaction takes place at 80 °C in air and in aqueous medium in the presence of two equivalents of tetra-*n*-butylammonium iodide (TBAI), leading to the formation of the two C–S bonds of the sulfide. TBAI plays the dual role of phase-transfer agent and a hydrolysis promoter of the Bunte salt initially formed from the halide. The hydrolysis gives rise to a key intermediate mercaptan species, which then combines with the carbocation derived from the allylic or propargylic alcohol to provide the final sulfide product. A wide variety of functionalized terminal and internal allylic alcohols as well as propargylic alcohols and organic halides proved compatible with the eco-friendly reaction conditions. These authors also demonstrated the value of their novel protocol by sulfurating important molecules (**eq 1**),[20] including sulfur-modified epiandrosterone.

A year later, the same laboratory described the efficient reaction of a wide variety of benzyl alcohols—including diarylmethanol, triphenylmethanol, propynols, and allylic alcohols—and alkyl halide derived Bunte salts in water at 100 °C.[21] Both in situ generated Bunte salts and pre-prepared ones reacted smoothly to provide unsymmetrical sulfides in moderate-to-excellent yields.

Very recently, Ma, Xu, and collaborators developed a scalable, one-pot reaction between alcohols, $Na_2S_2O_3·5H_2O$, and heteroaryl chlorides under catalyst-, additive-, and solvent-free

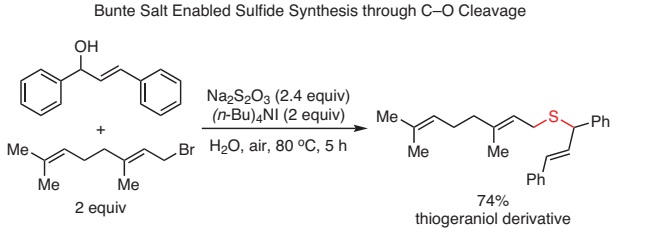

eq 1 *(Ref. 20)*

conditions at 140 °C.[22] Primary and secondary benzylic alcohols, heteroarylmethanols, and primary aliphatic alcohols were competent substrates, giving rise to 31 desired unsymmetrical heteroaryl sulfides in 16–86% yields.

3.4. Coupling through C–C Bond Cleavage

An interesting, copper-catalyzed decarboxylative cross-coupling of alkynyl carboxylic acids with Bunte salts for the synthesis of alkynyl chalcogenides has been disclosed by Liu and Yi.[23] A wide range of Bunte salts including benzyl, aryl, and alkyl ones, worked well to furnish the products in moderate-to-good yields. Alkyl Bunte salts provided only moderate yields due to the formation of the disulfide as byproduct. Both (hetero)aryl- and alkylpropiolic acids were suitable partners, affording the desired alkynyl sulfides in good-to-excellent yields. Interestingly, seleno Bunte salts also proved applicable in the reaction, leading to the construction of unsymmetrical alkynyl selenosulfides (**eq 2**).[23]

3.5. Coupling through C–H Bond Cleavage

Two efficient and C(3)-selective protocols for the sulfenylation of 1*H*-indoles[24,25] and 1*H*-pyrrolo[2,3-*b*]pyridine[25] with Bunte salts has been achieved under eco-friendly and metal-free conditions, leading to the corresponding 3-alkyl- and 3-arylthioindoles in moderate-to-high yields. In the first protocol, a stoichiometric amount of tetra-*n*-butylammonium iodide is used, while in the second 20 mol % of elemental iodine is utllized. In the proposed mechanisms of both protocols, the catalytic cycle is initiated by reaction of adventitious water with the Bunte salt (RS–SO_3Na) to form bisulfate (HSO_4^-) and an intermediate thiol species, which is then oxidized by I_2 to the actual thiolating species, RSI. The latter then attacks the 3 position of the indole, giving rise to the observed 3-thioindole products. The usefulness of the second protocol was demonstrated by a facile synthesis (**eq 3**) of methyl 5-methoxy-3-((3,4,5-trimethoxyphenyl)thio)-1*H*-indole-2-carboxylate,[25] a potent tubulin polymerization inhibitor, in 67% isolated yield (after chromatography), in stark contrast to a prior method in which the carboxylate was obtained in only 4% yield. More recently, a very similar mechanism has been proposed for the transition-metal-free and regioselective sulfenylation of 4-anilinocoumarins catalyzed by potassium iodide (20 mol %).[26] This method provides access to 3-alkylthio-4-anilinocoumarins with potential biological activities in moderate-to-excellent yields.

3.6. Reactions with Grignard Reagents and Boronic Acids

Reeves and co-workers developed the reaction of Bunte salts with Grignard reagents as a mild (THF, 0 °C to rt) and general route to sulfides that avoids using air-sensitive and malodorous thiols as starting materials.[8] The reaction is compatible with a broad range of alkyl, aryl, and vinyl Bunte salts and alkyl, (hetero)aryl, vinyl, and alkynyl Grignard reagents and provides the sulfides in 68–99% isolated yields. The authors demonstrated the usefulness of their approach by a straightforward and high yield (82%) synthesis of a combretastatin analogue. It is also worth noting that an alkynyllithium, instead of the corresponding Grignard Reagent, was also effective in the transformation. In 2015, the Cu-catalyzed direct oxidative cross-coupling between boronic acids and Bunte salts for the synthesis of unsymmetrical sulfides was developed by our group (**eq 4**).[27] Silver carbonate and di-*tert*-butyl peroxide (DTBP) were used as the oxidants, and a CO_2 atmosphere was required to suppress formation of the disulfide byproduct. This strategy was readily applied to the late-stage diversification of biologically active molecules. Moreover, the unsymmetrical diaryl sulfide products can undergo an oxidative dehydrogenative cyclization process to provide unsymmetrical dibenzothiophenes (DBTs), which form the core of photoactive compounds and conducting polymers.

3.7. Reaction with Organosilicon Reagents

A novel and tunable Pd-catalyzed oxidative cross-coupling of Bunte salts with aryl- or heteroaryl(triethoxy)silanes was recently disclosed by our group (**Scheme 3**).[28] The selectivity

Decarboxylative Cross-Coupling of Seleno Bunte Salts with Propiolic Acids

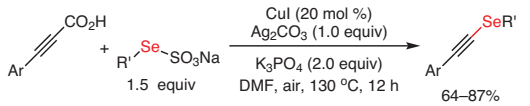

Ar = 4-XC_6H_4 (X = Me, MeO, CF_3, Cl, Br)
R' = Cy, *c*-Hep, $YC_6H_4CH_2$ (Y = H, Me, Cl, Br, CN, NO_2), 2-Me-5-FC_6H_3

eq 2 *(Ref. 23)*

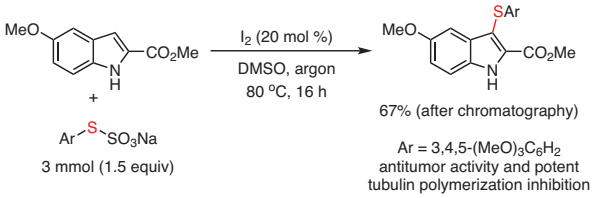

eq 3 *(Ref. 25)*

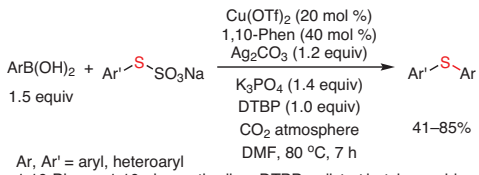

Ar, Ar' = aryl, heteroaryl
1,10-Phen = 1,10-phenanthroline; DTBP = di-*tert*-butyl peroxide

Noteworthy Application Products:

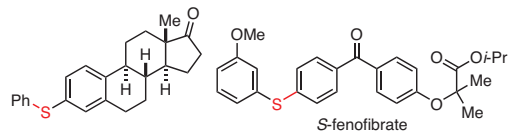

S-estratrien
(67% from estratrien Bunte salt)

S-fenofibrate
(73% from bis(pinacolato)boron
fenofibrate)

eq 4 *(Ref. 27)*

for Hiyama-type coupling or one-carbon (C1) insertion was controlled by the absence or presence of palladium ligand: Sulfides were afforded under ligand-free conditions, whereas thiol esters were formed with bidentate phosphine ligands under a carbon monoxide atmosphere. Aryl and alkyl Bunte salts were competent reactants in both protocols, providing the corresponding products in moderate-to-excellent yields. PhS-modified estratrien was also obtained by the Hiyama-type coupling reaction. Mechanistic studies of the C1-insertion reaction led to proposing a plausible pathway for thiol ester formation. In this pathway, a chelated $PdCl_2$ species is generated with the bis(diphenylphosphino)alkane ligand. Transmetalation through Cl^- displacement by the Bunte salt is followed by CO insertion. Loss of SO_3, organosilicon transmetalation, and reductive elimination lead to the observed thiol ester product.

3.8. Sulfuration of Isoxazoles

An interesting, atom- and step-economical, one-pot, three-component reaction cascade employing acetylenic oximes, $Na_2S_2O_3$, and aryl iodides has been reported by Li et al (**eq 5**).[29] The reaction sequence is carried out in air and in 1-(3-cyanopropyl)-3-methylimidazolium chloride ([Cpmim]Cl) ionic liquid under Pd-NHC catalysis. A variety of substituted aryl iodides and acetylenic oximes reacted smoothly with $Na_2S_2O_3$ to afford highly substituted 4-arylthio-1,2-oxazoles in moderate-to-high isolated yields. In contrast, alkyl iodides did not react and, in the case of 1-iodobutane, the starting material was recovered completely. In the proposed mechanism for the reaction cascade, the isoxazole ring is formed first in a trans oxypalladation of the oxime. The resulting palladium–isoxazole intermediate undergoes a chloride–$ArSSO_3^-$ exchange with the Bunte salt generated in situ from the aryl iodide. The final two steps consist of loss of SO_3 and reductive elimination to form the observed isoxazole products.

4. Synthesis of Dithiocarbamates and Thiophosphates

Recently, we developed a novel, efficient, and one-pot method for the construction of dithiocarbamates from Bunte salts, secondary amines, and a thiocarbonyl surrogate (K_2S + $CHCl_3$).[30] A wide range of amines—including 5- and 6-membered cyclic amines, dialkylamines, and methylaniline—reacted with alkyl and aryl Bunte salts in the presence of potassium sulfide and chloroform, furnishing the dithiocarbamates in moderate-to-high isolated yields (**eq 6**).[30] Interestingly, some of the dithiocarbamates exhibited promising selective bioactivity against human histone deacetylase 8 (HDAC8), highlighting the potential of this method for the development of novel HDAC8 inhibitors with a dithiocarbamate core. This stoichiometric process is believed to occur via initial dichlorocarbene (generated from $Ba(OH)_2$ and $CHCl_3$) insertion into the N–H bond of the amine to give a dichloromethylamine intermediate that is readily converted into the corresponding monochloromethylimine cation. Addition of the alkyl or aryl thiol derived from the Bunte salt to this imine cation generates an α-alkyl/arylthioimine cation. Trisulfur radical anion ($S_3^{\bullet-}$)—formed from K_2S in NMP—addition, intramolecular hydrogen atom transfer (HAT), and homolytic S–S bond cleavage (with loss of S_2^-) affords the dithiocarbamate in the presence of base.

Lin, Yan, and co-workers have reported an efficient and eco-friendly NaBr-catalyzed coupling reaction of Bunte salts with phosphonates ($R_2P(O)H$, where R = alkoxy or aryl) in the presence of two equivalents of H_2O_2 as the oxidant and AcOH as additive.[31] The corresponding thiophosphates were obtained in 40–92% yields by a pathway that is initiated by the generation of the active alkyl/arylthiol species through hydrolysis of the Bunte salt with water at 80 °C.

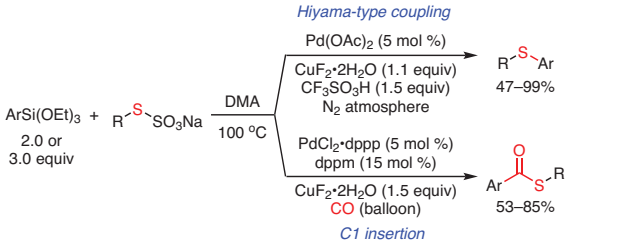

Ar = XC_6H_4 (X = H, Me, F, Cl, MeO), thien-3-yl, 9*H*-fluoren-2-yl, estratrien-3-yl
R = XC_6H_4 (X = H, Me, MeO, Me_2, CF_3, Cl), Me, *n*-Bu, *n*-$C_{12}H_{25}$, Bn, 1-Np, 2-Np
dppp = 1,3-bis(diphenylphosphino)propane; dppm = bis(diphenylphosphino)methane

Scheme 3. Divergent Cross-Coupling of Organosilicon Reagents with Bunte Salts. *(Ref. 28)*

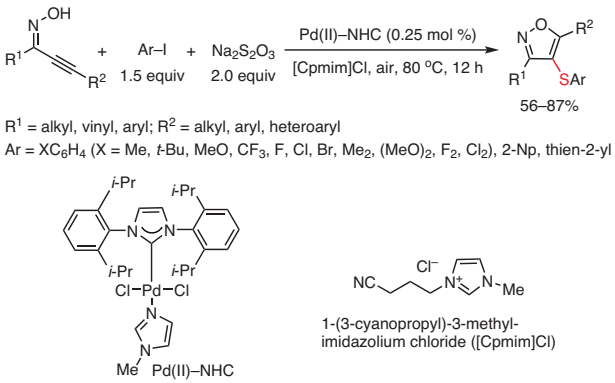

R^1 = alkyl, vinyl, aryl; R^2 = alkyl, aryl, heteroaryl
Ar = XC_6H_4 (X = Me, *t*-Bu, MeO, CF_3, F, Cl, Br, Me_2, $(MeO)_2$, F_2, Cl_2), 2-Np, thien-2-yl

eq 5 *(Ref. 29)*

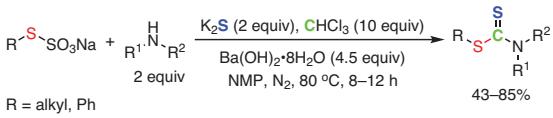

R = alkyl, Ph
R^1,R^2 = Me,Ph; Me,Bn; Bn_2; Et_2; heterocycle
NMP = 1-methyl-2-pyrrolidinone

eq 6 *(Ref. 30)*

5. Application in Metal Nanoparticles

Metal nanoparticles (MNPs) are used in biomedical assays and treatments and for the construction of microscale optical devices. A number of chemical strategies have been devised for synthesizing functionalized metal nanoparticles of various sizes.[32] Since Bunte salts have no odor and lower reactivity than thiols, they are generally utilized for the synthesis of metal nanoparticles with a sulfur-containing headgroup. Lukkari and co-workers found that Bunte salts can generate self-assembled monolayers (SAMs) on gold under anaerobic conditions, and chemisorb forming an Au–S bond.[33] The S–SO_3^- bond in Bunte salts (RS–SO_3^-) is cleaved during adsorption of the RS moiety onto the gold surface, releasing the SO_3^- group. The following year, Murray's group reported the first example of metal nanoparticles, in which alkanethiolate-protected AuNPs were prepared by Bunte salts as ligand precursors (**Scheme 4**, Part (a)).[34] Employing the same protocol, they later explored the preparation of water-soluble, monolayer-protected nanoparticles (SO_3–AuNP) by using the strong-acid-functionalized Bunte salt of 2-acrylamido-2-methyl-1-propanesulfonic acid as precursor (Scheme 4, Part (b)).[35]

A thiosulfate approach was also utilized by Shon and Cutler for the one-pot preparation of alkanethiolate-capped silver nanoparticles (AgNPs) in aqueous media.[36] The AgNPs, produced by borohydride ($NaBH_4$) reduction of silver nitrate, were stabilized by adsorption of *S*-dodecylthiosulfate (*n*-$C_{12}H_{25}S$–SO_3^-) onto the particle surface followed by elimination of the SO_3^- fragment. Later, Shon and other co-workers reported a two-phase synthesis of water-soluble, carboxylate-functionalized, and alkanethiolate-capped palladium nanoparticles (PdNPs) from Bunte salts (ω-carboxyl-*S*-alkanethiosulfate sodium salt).[37,38] These PdNPs were then investigated as catalysts for the hydrogenation of allyl alcohol to 1-propanol versus its isomerization to propanal. Their results showed that the sulfur ligand structure, its conformation, and its degree of surface coverage were crucial in determining the activity and selectivity of the PdNP catalysts.

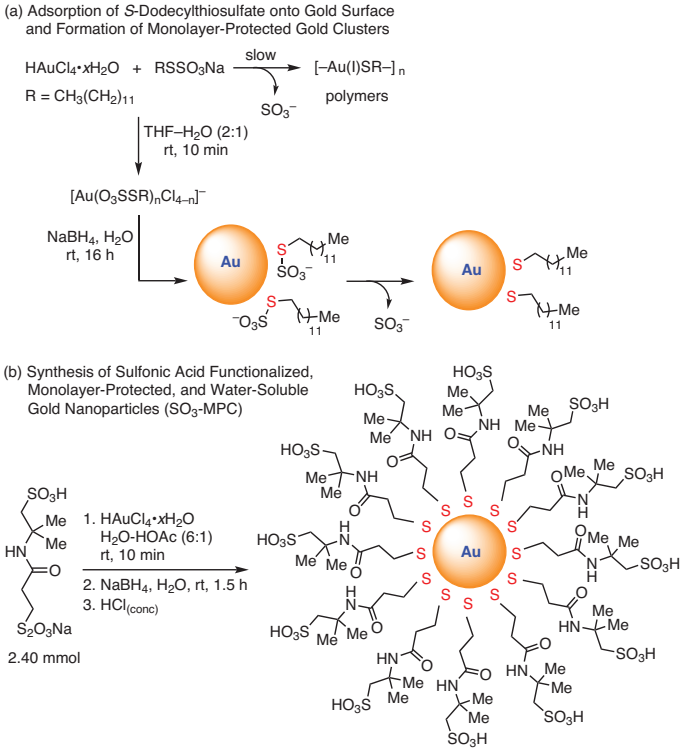

Scheme 4. The Synthesis of Gold Nanoparticles from Bunte Salts. *(Ref. 34,35)*

6. Conclusion

The fact that Bunte salts are stable, easy-to-handle crystalline solids with generally little-to-no odor and unique chemical properties has made them attractive thiol sources and desirable substrates for a wide variety of chemical reactions. Not only have Bunte salts served as an important component of new protocols for shorter and more efficient syntheses of known sulfur-containing compounds, but also as key precursors in the synthesis of novel and bioactive sulfur-containing molecules and sulfur-modified drugs. Although quite a few effective strategies have so far been devised for the application of Bunte salts in many types of reaction, there is still a need for even more efficient and practical methods for their use in facilitating the synthesis of structuraly diverse sulfur-containing compounds. Drug discovery is one area that we believe Bunte salts, as optimal sulfurating agents, are poised to play an increasingly important role in.

7. Acknowledgments

The authors are grateful for the financial support provided by The National Key Research and Development Program of China (2017YFD0200500), NSFC (21971065, 21722202, 21672069, and 21871089 for M. W.), S&TCSM of Shanghai (Grant 18JC1415600), the Professor of Special Appointment (Eastern Scholar) Program at Shanghai Institutions of Higher Learning, and the National Program for Support of Top-Notch Young Professionals.

8. References

(1) Bunte, H. *Chem. Ber.* **1874**, 7, 646.
(2) Kunath, D. *Chem. Ber.* **1963**, *96*, 157.
(3) Distler, H. *Angew. Chem., Int. Ed.* **1967**, *6*, 544.
(4) Qiao, Z.; Jiang, X. *Org. Biomol. Chem.* **2017**, *15*, 1942, and references therein.
(5) Westlake, H. E., Jr.; Dougherty, G. *J. Am. Chem. Soc.* **1942**, *64*, 149.
(6) Gattow, G.; Hanewald, B. *Z. Anorg. Allg. Chem.* **1978**, *444*, 112.
(7) Baker, R. H.; Barkenbaus, C. *J. Am. Chem. Soc.* **1936**, *58*, 262.
(8) Reeves, J. T.; Camara, K.; Han, Z. S.; Xu, Y.; Lee, H.; Busacca, C. A.; Senanayake, C. H. *Org. Lett.* **2014**, *16*, 1196.
(9) Jansa, P.; Čechová, L.; Dračínský, M.; Janeba, Z. *RSC Adv.* **2013**, *3*, 2650.
(10) Baumgarten, P. *Chem. Ber.* (presently *Eur. J. Inorg. Chem.*) **1930**, *63*, 1330 (https://onlinelibrary.wiley.com/doi/epdf/10.1002/cber.19300630606).

(11) Tanaka, T.; Nakamura, H.; Tamura, Z. *Chem. Pharm. Bull.* **1974**, *22*, 2725.
(12) Lecher, H. Z.; Hardy, E. M. *J. Org. Chem.* **1955**, *20*, 475.
(13) Meguro, Y.; Noguchi, M.; Li, G.; Shoda, S. *Org. Lett.* **2018**, *20*, 76.
(14) Li, Y.; Wang, M.; Jiang, X. *ACS Catal.* **2017**, *7*, 7587.
(15) Qiao, Z.; Wei, J.; Jiang, X. *Org. Lett.* **2014**, *16*, 1212.
(16) Li, Y.; Pu, J.; Jiang, X. *Org. Lett.* **2014**, *16*, 2692.
(17) Zhang, Y.; Li, Y.; Zhang, X.; Jiang, X. *Chem. Commun.* **2015**, *51*, 941.
(18) Li, Y.; Xie, W.; Jiang, X. *Chem.—Eur. J.* **2015**, *21*, 16059.
(19) Liu, F.; Jiang, L.; Qiu, H.; Yi, W. *Org. Lett.* **2018**, *20*, 6270.
(20) Chu, X.-Q.; Xu, X.-P.; Ji, S.-J. *Chem.—Eur. J.* **2016**, *22*, 14181.
(21) Liu, B.-B.; Chu, X.-Q.; Liu, H.; Yin, L.; Wang, S.-Y.; Ji, S.-J. *J. Org. Chem.* **2017**, *82*, 10174.
(22) Ma, X.; Yu, J.; Yan, R.; Yan, M.; Xu, Q. *J. Org. Chem.* **2019**, *84*, 11294.
(23) Liu, F.; Yi, W. *Org. Chem. Front.* **2018**, *5*, 428.
(24) Li, J.; Cai, Z.-J.; Wang, S.-Y.; Ji, S.-J. *Org. Biomol. Chem.* **2016**, *14*, 9384.
(25) Qi, H.; Zhang, T.; Wan, K.; Luo, M. *J. Org. Chem.* **2016**, *81*, 4262.
(26) Li, G.; Zhang, G.; Deng, X.; Qu, K.; Wang, H.; Wei, W.; Yang, D. *Org. Biomol. Chem.* **2018**, *16*, 8015.
(27) Qiao, Z.; Ge, N.; Jiang, X. *Chem. Commun.* **2015**, *51*, 10295.
(28) Qiao, Z.; Jiang, X. *Org. Lett.* **2016**, *18*, 1550.
(29) Li, J.; Wu, Y.; Hu, M.; Li, C.; Li, M.; He, D.; Jiang, H. *Green Chem.* **2019**, *21*, 4084.
(30) Tan, W.; Jänsch, N.; Öhlmann, T.; Meyer-Almes, F.-J.; Jiang, X. *Org. Lett.* **2019**, *21*, 7484.
(31) Min, C.; Zhang, R.; Liu, Q.; Lin, S.; Yan, Z. *Synlett* **2018**, *29*, 2027.
(32) San, K. A.; Shon, Y.-S. *Nanomaterials* **2018**, *8*, 346.
(33) Lukkari, J.; Meretoja, M.; Kartio, I.; Laajalehto, K.; Rajamäki, M.; Lindström, M.; Kankare, J. *Langmuir* **1999**, *15*, 3529.
(34) Shon, Y.-S.; Gross, S. M.; Dawson, B.; Porter, M.; Murray, R. W. *Langmuir* **2000**, *16*, 6555.
(35) Shon, Y.-S.; Wuelfing, W. P.; Murray, R. W. *Langmuir* **2001**, *17*, 1255.
(36) Shon, Y.-S.; Cutler, E. *Langmuir* **2004**, *20*, 6626.
(37) Gavia, D. J.; Shon, Y.-S. *Langmuir* **2012**, *28*, 14502.
(38) Gavia, D. J.; Maung, M. S.; Shon, Y.-S. *ACS Appl. Mater. Interfaces* **2013**, *5*, 12432.

About the Authors

Ming Wang received his Ph.D. degree in 2011 from East China University of Science and Technology. From 2011 to 2014, he was a postdoctoral researcher under the guidance of Professor Yonggui Robin Chi at Nanyang Technological University, Singapore. In 2014, he joined East China Normal University as a lecturer, and is currently an associate professor at East China Normal University.

Yaping Li received her B.S. degree in 2018 from Jiangxi Normal University. She is now working with Professor Xuefeng Jiang toward her master's degree at East China Normal University.

Xuefeng Jiang is a professor at East China Normal University. He received his B.S. degree in 2003 from Northwest University (Xi'an, Shaanxi, China). He then joined Professor Shengming Ma's research group at the Shanghai Institute of Organic Chemistry, Chinese Academy of Sciences, where he received his Ph.D. degree in 2008. From 2008 to 2011, Xuefeng worked as a postdoctoral researcher on the total synthesis of natural products in the research group of Professor K. C. Nicolaou at The Scripps Research Institute. His independent research interests have focused on green sulfur chemistry and methodology-oriented total synthesis.

MilliporeSigma

Illuminated synthesis

From discovery to scale-up:

Photoreactors and catalysts to deliver consistency and reproducibility to your research.

Chemists have long struggled with reproducibility in photoredox catalysis. Both varied reaction setups and individual reactions performed with the same setup can be tricky. Our new labware seeks to alleviate these issues by providing photoreactors for each stage of reaction development while ensuring high levels of consistency across reactions and between runs.

When combined with our broad portfolio of iridium and ruthenium catalysts and acridinium-based photocatalysts, these tools free synthetic chemists to focus on their next breakthrough.

To view our complete portfolio offering, visit **SigmaAldrich.com/photocatalysis**

Sigma-Aldrich®

Lab & Production Materials

P-Chiral Phosphorus Ligands for Cross-Coupling and Asymmetric Hydrogenation Reactions


Ms. T. Wu


Prof. G. Xu


Prof. W. Tang

Ting Wu, Guangqing Xu, and Wenjun Tang*[a,b]

[a] State Key Laboratory of Bio-Organic and Natural Products Chemistry
Center for Excellence in Molecular Synthesis
Shanghai Institute of Organic Chemistry
Chinese Academy of Sciences
345 Lingling Road
Shanghai 200032, China

[b] School of Chemistry and Materials Science
Hangzhou Institute for Advanced Study
University of Chinese Academy of Sciences
1 Sub-lane Xiangshan
Hangzhou 310024, China
Email: tangwenjun@sioc.ac.cn

Keywords. P-chiral; phosphorus ligands; asymmetric cross-coupling; Suzuki–Miyaura coupling; axial chirality; asymmetric dearomative coupling; α-arylation; asymmetric hydrogenation; all-carbon quaternary stereocenters.

Abstract. The asymmetric cross-coupling and asymmetric hydrogenation reactions are highly relevant to synthetic organic chemists in both academia and industry. Chiral phosphorus ligands have played a central role in improving the efficiency, selectivity, and scope of these transition-metal-catalyzed asymmetric transformations. Nevertheless, the invention of new phosphorus ligands and their applications in these two types of reaction are still urgently needed to further expand their scope and improve their efficiency and enantioselectivity. This mini-review summarizes our recent efforts in developing P-chiral, mono- and bisphosphorus ligands that possess unique structural motifs. It also highlights their powerful applications in promoting the asymmetric Suzuki–Miyaura coupling, asymmetric dearomative cross-coupling, asymmetric α-arylation, and various asymmetric hydrogenations, with particular emphasis on practicality and efficiency of the transformations (low catalyst loading, good atom economy, and high enantioselectivity).

Outline

1. Introduction

P-Chiral phosphorus ligands have played a significant role in the advancement and industrialization of asymmetric catalysis.[1,2] For example, Knowles developed CAMP and DiPAMP ligands in the early 1970s, which not only set the bar high for highly enantioselective rhodium-catalyzed asymmetric hydrogenation, but also ushered in the era of asymmetric catalytic transformations for industrial applications[3,4] Imamoto later developed a series of P-chiral bisphosphorus ligands—BisP*,[5] MiniPhos, and QuinoxP*®[6]—which are highly effective for various Rh- or Pd-catalyzed carbon–carbon and carbon–hydrogen bond-forming reactions. In the meantime, Zhang developed a series of 1,2-bisphospholane ligands, TangPhos,[7] DuanPhos,[8] and ZhangPhos,[9] which were successfully applied in asymmetric hydrogenation, hydroformylation, and other reactions. Despite these advances, the development of chiral phosphorus ligands with new structural motifs to address numerous unsolved challenges in asymmetric catalysis remains a necessary and

worthy pursuit. This mini-review highlights our group's recent efforts to design and synthesize novel P-chiral mono- and bisphosphorus ligands based on the 2,3-dihydrobenzo[*d*][1,3]-oxaphosphole (DHBOP) motif and to apply them in asymmetric cross-coupling and hydrogenation reactions.[2,10,11]

2. Design and Development of P-Chiral Phosphorus Ligands Based on the 2,3-Dihydrobenzo[*d*][1,3]-oxaphosphole Motif

The inspiration for employing this structural motif originated with TangPhos, a highly efficient but air-sensitive chiral bisphospholane ligand.[7] Preparation of both enantiomers of TangPhos has remained a challenge owing to the use of sparteine as the chiral reagent in the synthesis. Not only is the natural (+)-sparteine expensive and in limited supply, but an effective surrogate of its antipode, (–)-sparteine, is also scarce. To overcome the synthetic challenge and air-sensitivity of TangPhos, we sought an air-stable, operationally simple, and modular version of TangPhos. Introducing two aryl rings into the oxaphosphole structure thus led to the DHBOP motif, which could be prepared from readily available starting materials in only three steps and could be resolved easily to provide both enantiomers on a kilogram scale. Additionally, most ligands derived from this structure are air-stable solids and thus operationally simple to handle. Furthermore, the excellent modularity and tunability of this unique structure have allowed us to develop a series of chiral mono- and bisphosphorus ligands that have shown excellent reactivities and enantioselectivities in various asymmetric catalytic reactions.

Chiral monophosphorus ligands have played increasingly important roles in developing new and efficient asymmetric catalytic reactions.[12] However, designing efficient chiral monophosphorus ligands is much more difficult than designing bisphosphorus ligands due to the lack of a conformationally defined and systematically tunable ligand framework. We have been fortunate to have developed a library of conformationally well-defined and electron-rich P-chiral biaryl monophosphorus ligands based on the DHBOP motif (**Figure 1**). Structurally, these are more stable and electron-rich ligands than chiral monophosphoramide ligands, and most are also air-stable crystalline solids, which are relatively easy to handle. Additionally, the high tunability of the steric and electronic properties of the P-chiral biaryl monophosphorus ligand structure enables the broad application of such ligands in various catalytic systems.

The chiral, BIBOP-type bisphosphorus ligands also have unique structural features when compared to the well-known bisphosphorus ligands such as BINAP and DuPhos. Variation of the R' groups at the 4,4′ positions led to a series of chiral bisphosphorus ligands (Type I)—e.g., BIBOP, MeO-BIBOP, WingPhos, and ArcPhos—with various depths, shapes, and electronic properties of the chiral pocket. Another group of chiral bisphosphorus ligands (Type II)—e.g., BABIBOP, Me-BABIBOP, and *i*Pr-BABIBOP—are formally constructed by dimerization at the 4 position of DHBOP (Figure 1). One interesting non-C_2-symmetric bisphosphorus ligand is MeO-POP, which has proven a highly efficient ligand in rhodium-catalyzed asymmetric hydrogenations. In addition to these mono- and bisphosphorus ligands, a series of P,P=O ligands

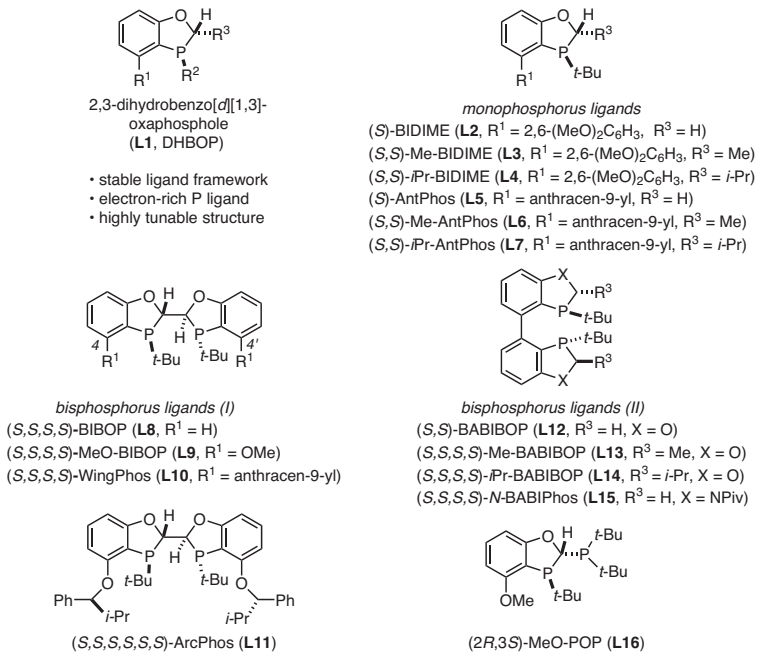

Figure 1. The Highly Tunable and Stable 2,3-dihydrobenzo[*d*][1,3]oxaphosphole (DHBOP) Motif and Novel, Air-Stable, Crystalline, and Highly Efficient Mono- and Bisphosphorus Ligands Derived from It.

have been developed. The P=O moiety is designed to provide a hemilabile coordination to the metal center, thus inhibiting a β-hydride elimination or a second transmetalation, and promoting an effective aryl–alkyl cross-coupling.

3. Chiral Monophosphorus Ligands for Cross-Coupling

Cross-coupling is one of the most important carbon–carbon bond-forming reactions, and has been widely applied in the electronics, materials, and pharmaceutical industries. Thanks to the recent development of phosphorus ligands, the scope of the cross-coupling reaction has been significantly expanded. Nevertheless, significant challenges remain such as tolerance of steric hindrance, compatibility of various functional groups, and excellent stereocontrol in forming axial chirality or all-carbon quaternary centers. To overcome these challenges, we developed a series of sterically hindered and electron-rich P-chiral monophosphorus ligands for the purpose of investigating the sterically hindered aryl–aryl and aryl–alkyl cross-couplings.[13] Moreover, an efficient, sterically hindered aryl–isopropyl coupling has also been developed for the first time by employing a sterically hindered P,P=O ligand.[14] In the rest of this article, we will concisely highlight our recent results for the asymmetric Suzuki–Miyaura coupling,[15–20] asymmetric dearomative cross-coupling,[21–23] and α-arylation.[24–25]

3.1. Asymmetric Suzuki–Miyaura Coupling

Axially chiral biaryl structural motifs are found in a large number of biologically important natural products as well as in thousands of ligands for asymmetric catalysis. Although there have been quite a few reported methods for the construction of chiral biaryl units,[26] the asymmetric Suzuki–Miyaura coupling remains of significant interest in this regard owing to its mild reaction conditions, broad functional group compatibility, and nontoxic nature of the starting materials.[11] To that end, we have demonstrated the advantages of utilizing monophosphorus ligands such as (*S*)-BIDIME (**L2**) and (*S*)-AntPhos (**L5**) in the Pd-catalyzed, sterically demanding Suzuki–Miyaura coupling leading to tetra-ortho-substituted biaryls among others.[15]

We initially pursued the asymmetric construction of chiral tri-ortho-substituted biaryls[16] for which, and despite considerable research efforts prior to our work, an efficient and practical synthetic protocol utilizing the asymmetric Suzuki–Miyaura coupling remained elusive. Our approach involved incorporating a noncovalent π–π interaction between the two aryl partners at the reductive elimination stage. Employing this approach and monophosphorus ligand (*S*,*S*)-Me-BIDIME (**L3**), an efficient, mild, and enantioselective Suzuki–Miyaura coupling between naphthyl bromide **1** and 1-naphthylboronic acid (**2**) was achieved, providing the biaryl coupling product **3** in 95% yield and 96% ee (**Scheme 1**, Part (a)).[16]

Since a large number of natural products feature chiral *ortho*-hydroxy- or *ortho*-methoxybiaryl structures, we then developed an efficient asymmetric Suzuki–Miyaura coupling between arylboronic acids and aryl bromides bearing an ortho oxygen-protecting group (OPG).[17] To achieve high enantioselectivity, an effective noncovalent second interaction needed to be introduced. After screening a series of OPG's, we found that excellent enantioselectivity was achieved when the bis(2-oxo-3-oxazolidinyl)phosphinyl (BOP) protecting group was employed. The significant increase in enantioselectivity in going from O–P(O)Ph_2 to O–BOP pointed to an important noncovalent interaction with the O–BOP group. The substrate scope further revealed the importance of the extended π system of the arylboronic acid for high enantioselectivity. All these observations suggested the presence of a significant polar–π interaction between the highly polarized BOP group and the extended π system of the arylboronic acid during the reductive elimination step. The chiral *ortho*-*O*–BOP biaryl products were subsequently applied to concise and stereoselective total syntheses of the biologically active natural products korupensamine A and B, and michellamine B (Scheme 1, Part (b)).[17]

The trifluoromethanesulfonyl group can also be an effective ortho OPG group in the asymmetric Suzuki–Miyaura coupling that uses Pd-(*S*,*S*)-Me-BIDIME (**L3**) as the catalyst system (Scheme 1, Part (c)).[18] Utilizing this protocol, a series of chiral biaryl triflates were synthesized in excellent ee's and yields.

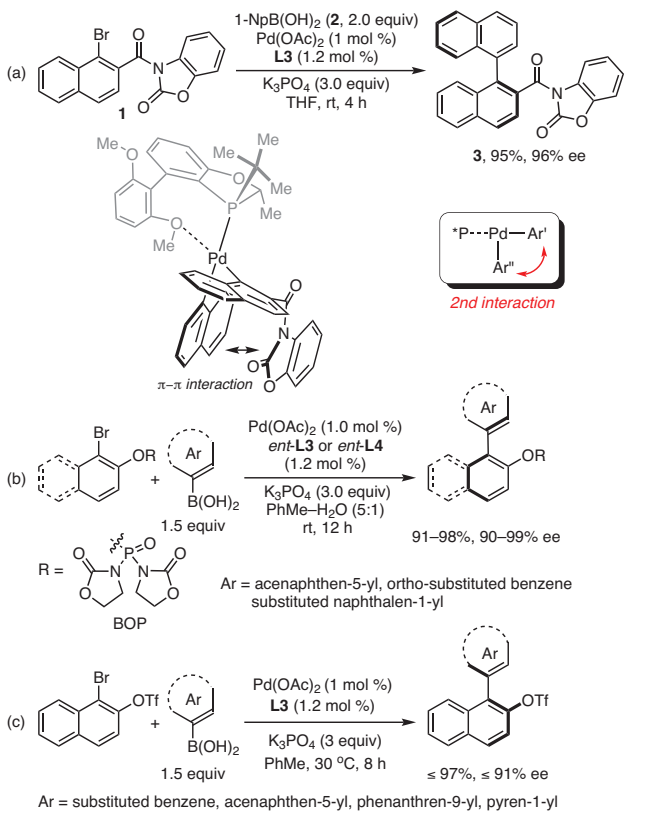

Scheme 1. Construction of Highly Sterically Hindered Biaryls by a Mild, Efficient, and Highly Enantioselective Suzuki–Miyaura Coupling Enabled by Chiral, Monophosphorus Ligands. *(Ref. 16–18)*

The biaryl triflate products underwent further elaborations such as carbonylation, Suzuki–Miyaura coupling, Miyaura borylation, and Sonogashira coupling to forge a variety of chiral biaryl derivatives.

Tetra-ortho-substituted biaryls can also be accessed by the asymmetric Suzuki–Miyaura or Negishi coupling by employing a chiral monophosphorus ligand.[19] Although high enantioselectivities were obtained for a few substrates with the employment of sterically hindered ligands, the asymmetric Suzuki–Miyaura cross-coupling did not prove to be general. Low or no yield was obtained with slight variation of substrate structure. The corresponding Negishi cross-coupling provided only slightly better yields of the tetra-ortho-substituted biaryls, but with lower enantioselectivities.[19]

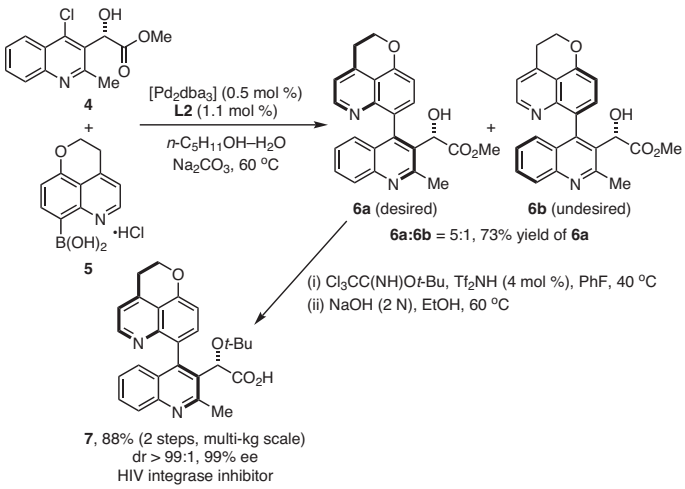

Scheme 2. Ligand (*S*)-BIDIME (**L2**) Enabled Suzuki Cross-Coupling as a Key Step in a Concise, Robust, Safe, Economical, and Asymmetric Synthesis of an HIV Integrase Inhibitor. *(Ref. 20)*

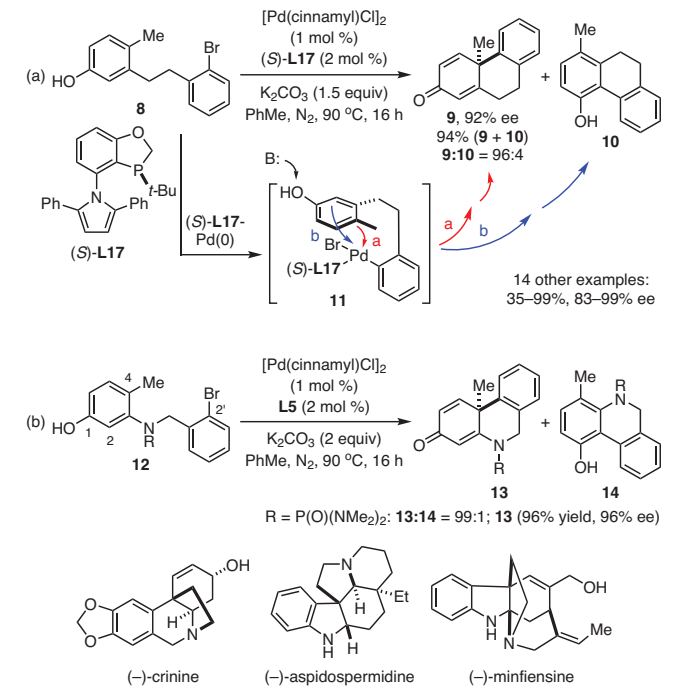

Scheme 3. P-Chiral Biaryl Monophosphorus Ligands Enabling the Efficient and Stereoselective Intramolecular Dearomative Cross-Coupling, a Key Step in the Synthesis of Fused Tricyclic Cores of Biologically Active Natural Products. *(Ref. 21–24)*

Compound **7** is a quinoline-based allosteric integrase inhibitor, whose structure features an axially chiral biaryl backbone with an attached *ortho*-(α-(*tert*-butoxy)acetic acid) side chain. A robust and practical synthesis was needed to support its advancement through the drug development process. Thus, a diastereoselective Suzuki–Miyaura coupling of aryl chloride **4** and arylboronic acid **5** was exploited to install the chiral biaryl backbone, with the best result being obtained with ligand (*S*)-BIDIME (**L2**) (**Scheme 2**).[20] Under the optimized reaction conditions (1-pentanol–water and 60 °C) a 5:1 diastereomeric ratio of **6a** to **6b** was achieved, and the desired precursor (**6a**) to **7** was isolated in 73% yield, which is significantly better than the 40% yield and 2:1 ratio of **6a** to **6b** obtained with SPhos.[20]

3.2. Asymmetric Dearomative Cross-Coupling

Fused tricyclic skeletons containing chiral, all-carbon quaternary centers, such as chiral phenanthrenones, are found in numerous complex terpenes and steroids that exhibit interesting biological activities.[21,22] Complementing the asymmetric Heck reaction, the enantioselective intramolecular dearomative cross-coupling has become an important strategy to assemble these chiral skeletons. Over the past several years, our research group has undertaken the total synthesis of terpenoids, steroids, alkaloids, and polyketide natural products by taking advantage of the powerful, intramolecular, and enantioselective dearomative cross-coupling reaction.

The program originated with the study of the asymmetric palladium-catalyzed cyclization of bromine-substituted phenol **8**, which can lead to the formation of the desired coupling product **9**—containing a chiral, all-carbon quaternary center—as well as the achiral molecule **10** (**Scheme 3**, Part (a)).[22] Products **9** and **10** arise from a common intermediate, **11**, and, although **9** is thermodynamically less stable than **10**, its formation could be kinetically more favorable in the presence of a suitable catalyst. Among all the ligands screened, P-chiral biaryl monophosphorus ligand (*S*)-**L17** was found to promote the formation of the desired product, **9**, smoothly in high yield and with the highest enantioselectivity (92% ee). In the proposed stereochemical model for the cyclization, the high stereoselectivity observed with (*S*)-**L17** is rationalized by stipulating that the 2,5-diphenylpyrrole moiety of (*S*)-**L17** and its bulky *tert*-butyl group dictate the orientation of substrate coordination. Substrate **8**, after oxidative addition to palladium to form **11** and nucleophilic substitution, could adopt two major conformations, with the less strained one being more favored and leading to the observed *R* configuration of **9**.[22] By using this methodology, a series of biologically important

terpenes, such as triptoquinone H,[21] and (–)-totaradiol[22] were efficiently synthesized. In addition, this approach proved crucial in a nine-step, enantioselective synthesis of the strong immunosuppressant (+)-dalesconol A that relied on the use of chiral (*R*)-AntPhos (*ent*-**L5**) as the chiral ligand.[23] A steroid skeleton was also constructed efficiently by using this method.[21]

The success we achieved in the all-carbon, fused tricyclic systems prompted us to explore nitrogen-containing polycyclic frameworks also incorporating a chiral, all-carbon quaternary center (Scheme 3, Part (b)).[24] While the anticipated structural difference was simply the formation of a dihydrophenanthridinone unit instead of a phenanthrenone one, it turned out that such a minor structural variation had a dramatic effect on the chemoselectivity of the reaction. Substrate **12a** (R = H) did not undergo the cyclization, while substrate **12b** (R = Piv) provided the undesired nonchiral compound **14b**. We reasoned that the chemoselectivity could be altered by changing the *N*-R protecting group. Interestingly, after screening Piv, Ms, Ts, Tris, Nos, Tf, SO_2NMe_2, and $P(O)(NMe_2)_2$ as the nitrogen protecting group, we discovered that the bulky phosphoramide group $P(O)(NMe_2)_2$ led to the desired coupling product, **13**, in excellent yield. When (*S*)-AntPhos (**L5**) was employed as ligand, the desired chiral dehydrophenanthridin-3(5*H*)-one product **13** [R = $P(O)(NMe_2)_2$] was isolated in 96% yield and 96% ee.

DFT calculations helped rationalize the dramatic effect of the *N*-R protecting group on the chemoselectivity. In substrate **12** [R = $P(O)(NMe_2)_2$], the C-2′ position (CBr) is in closer proximity to the C-4 position than is the case with substrate **12** (R = Piv). NBO analysis also showed that the charge on C-4 in **12** [R = $P(O)(NMe_2)_2$] was –0.071, more negative than that on C-2 (–0.017). Thus the higher nucleophilicity of the C-4 position in substrate **12** [R = $P(O)(NMe_2)_2$] leads preferentially to the desired intramolecular dearomative cyclization forming compound **13**.[24]

Finally, the asymmetric dearomative cross-coupling enabled the enantioselective synthesis of three distinct and challenging biologically important polycyclic alkaloids:[24] concise and gram-scale total synthesis of (–)-crinine, an efficient total synthesis of indole alkaloid (–)-aspidospermidine, and a formal total synthesis of (–)-minfiensine.

3.3. Asymmetric α-Arylation of Carbonyl Compounds

The search for efficient asymmetric catalytic methods to construct all-carbon quaternary stereocenters is gaining significant momentum. The palladium-catalyzed, asymmetric α-arylation of carbonyl compounds remains one of most efficient and powerful methods to assemble chiral all-carbon quaternary stereocenters, and the type of chiral ligand on palladium is key to achieving the desired reactivity and enantioselectivity. Our group has found that (*R*)-BIDIME (*ent*-**L2**) is an exceptional ligand for the asymmetric α-coupling of indanones **15** with ortho-substituted 2-bromoarenes **16.** The ketone products, **17**, incorporating a chiral quaternary carbon center, are generated in up to 98% yield and 99% ee (**Scheme 4**, Part (a)).[25] Taking advantage of this methodology, we achieved the efficient and enantioselective synthesis of the antidepressant (*S*)-nafenodone (3 steps), the sceletium alkaloid (+)-sceletium A-4 (4 steps), (–)-corynoline (5 steps), and (–)-deN-corynoline (3 steps).[25]

Carrying out an efficient cross-coupling between α-bromo carbonyl compounds and arylboron reagents under palladium catalysis remains a tough challenge.[26] Although such a transformation has been realized with chiral Ni[27] or Fe[28] catalysts, palladium catalysis often features much lower catalyst loading and is amenable to industrial applications. Nevertheless, the palladium-catalyzed coupling of benzyl 2-bromopropionate with phenylboronic acid in the presence of known ligands afforded the undesired des-bromo ester and biphenyl in all cases without forming the desired cross-coupling product.[29] Since monophosphorus ligands based on the DHBOP motif have been successfully applied in the coupling between aryl halides and aryl- or alkylboronic acids, we surmised that the enantioselective palladium-catalyzed coupling of α-bromo carbonyl compounds with arylboronic acids could be accomplished by a judicious choice of ligand. The key to success would be the effective inhibition of the homocoupling of the arylboronic acids, which results from a second transmetalation.[30] Thus, we postulated that a bulky P,P=O ligand could offer a secondary hemilabile interaction besides the Pd–P coordination, which would make the second transmetalation difficult due to steric hindrance.[30]

Careful ligand engineering and screening identified a bulky P,P=O ligand, **L18**, as optimal.[30] Using **L18**, the desired aryl–alkyl cross-coupling product was isolated in moderate yield and a decent ee. Because, in this case, the racemic α-bromo carboxamide was employed as substrate, the cross-coupling

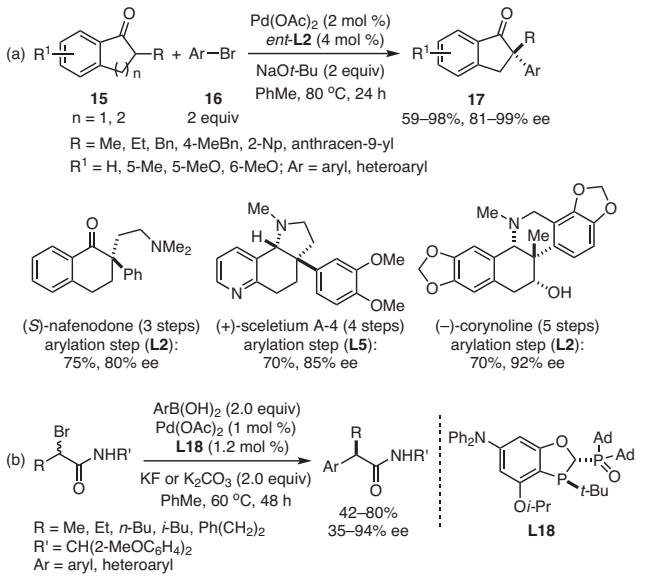

Scheme 4. Chiral Quaternary Carbon Formation by the Catalytic, Asymmetric α-Arylation Employing P-Chiral Biaryl Monophosphorus Ligands. *(Ref. 25,30)*

was essentially a dynamic kinetic resolution (DKR) process. The base and the acidity of the substrates were important parameters for both yield and enantioselectivity. Optimization of the reaction parameters revealed that KF as the base and $CH(2\text{-}MeOC_6H_4)_2$ as the nitrogen protecting group were optimal for both yield and enantioselectivity (Scheme 4, Part (b)).[30]

4. Chiral Bisphosphorus Ligands for Asymmetric Hydrogenation

The past few decades have seen significant advances in the asymmetric hydrogenation, and a number of important industrial processes have been implemented based on this reaction.[1] Since cost is a significant factor in judging whether a chemical reaction is viable or not on an industrial scale, turnover numbers (TONs) must be considered for it and should be as high as possible. Our belief that bisphosphorus ligands based on the DHBOP motif could address these issues and other unmet challenges led us to develop three ligand frameworks for the catalytic asymmetric hydrogenation. Our efforts led to BIBOP (**L8**), which could be prepared in two stereoisomeric forms and tuned both sterically and electronically by changing the substituents at the 4 and 4′ positions.[31] Some of the novel bisphosphorus ligands that were developed in this way—e.g., BIBOP, MeO-BIBOP, and others—have proved to be excellent ligands for the enantioselective catalytic hydrogenation reaction.

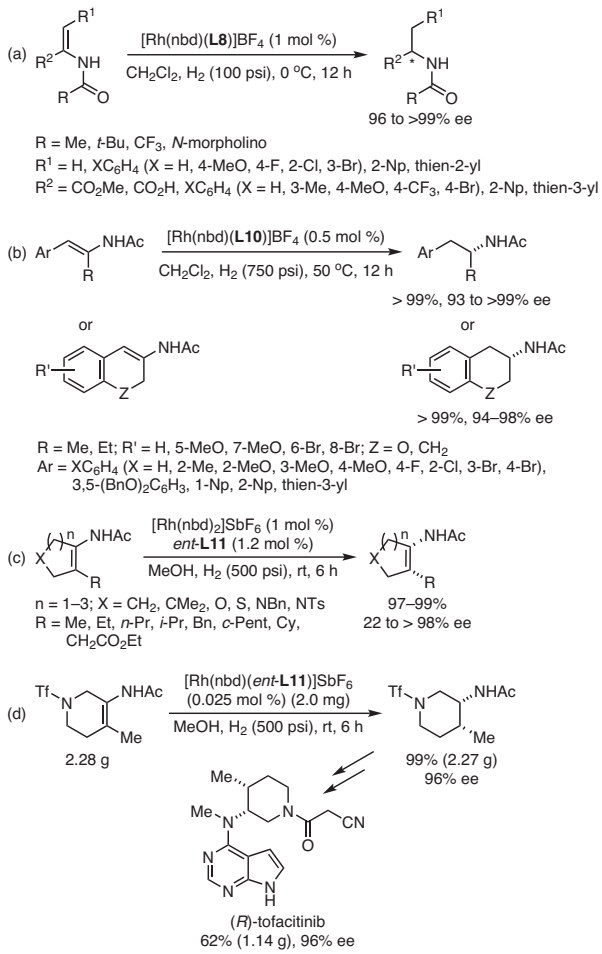

Scheme 5. Efficient Enantioselective Olefin Hydrogenations Enabled by Chiral Bisphosphorus Ligands. *(Ref. 31,33,34)*

Rh–BIBOP (Rh–**L8**) exhibited excellent catalytic efficiency in the asymmetric hydrogenation of various functionalized olefins such as α-(acylamino)acrylic acid derivatives, α-aryl enamides, β-(acylamino)acrylic acid derivatives, and dimethyl itaconate (**Scheme 5**, Part (a)).[31] Various functionalities were tolerated, and excellent enantioselectivities (up to 99% ee) and TONs (up to 2,000) were achieved in the synthesis of chiral α- and β-amino acids, chiral amines, and chiral carboxylic acid derivatives.

MeO-BIBOP (**L9**) is another air-stable but more electron-donating ligand. With Rh-**L9** as the catalyst, a 200,000 TON was achieved in the rhodium-catalyzed hydrogenation of *N*-(1-(4-bromophenyl)vinyl)acetamide, which was the highest TON reported then for the hydrogenation of α-aryl enamides. Similarly, a pyridine-substituted enamide was also hydrogenated with a Rh–MeO-BIBOP catalyst to provide the hydrogenation product in quantitative yield and 97% ee.[32] By installing two 9-anthryl groups at the 4 and 4′ positions, a structurally interesting chiral bisphosphorus ligand—WingPhos (**L10**) was designed and synthesized. The salient feature of WingPhos is the position of the two 9-anthryl groups that protrude directly toward the coordinated substrate, forming a deep chiral pocket capable of long-range stereochemical control. Notably, the two diagonal quadrants bearing two *tert*-butyl groups no longer provided a direct influence on substrate coordination, and the anthryl groups in the other two quadrants presumably influence substrate coordination, leading to high enantioselectivities. The Rh–WingPhos complex was a highly efficient catalyst for the rhodium-catalyzed hydrogenation of (*E*)-β-aryl enamides, forming a variety of chiral cyclic and acyclic β-arylamines with different functionalities in excellent enantioselectivities at low catalyst loadings (TONs up to 10,000) (Scheme 5, Part (b)).[33] Because (*E*)-β-aryl enamides could be conveniently synthesized, this method provided a practical synthesis of various chiral β-arylamine derivatives.

ArcPhos (**L11**) is a conformationally defined, electron-rich, C_2-symmetric, P-chiral bisphosphorus ligand. It is highly efficient in the rhodium-catalyzed asymmetric hydrogenation of carbocyclic and heterocyclic tetra-substituted enamides. Excellent enantioselectivities (up to 98% ee) and up to 10,000 TON were achieved, which was the highest reported up until then (Scheme 5, Part (c)).[34] NMR experiments and X-ray diffraction studies revealed that *ent*-**L11** had a conformational preference whereby the flexible isopropyl groups are directed toward the rhodium center due to both stereoelectronic and steric effects. Moreover, the asymmetric hydrogenation of a heterocyclic starting material with [Rh(nbd)(*ent*-**L11**)]SbF_6 as catalyst led to *N*-trifluoromethanesulfonyl *cis*-3-acylamino-4-methylpiperidine (99% yield, 96% ee), and enabled an efficient and practical synthesis of the Janus kinase inhibitor (*R*)-tofacitinib (Scheme 5, Part (d)).[34]

Our group has also developed a series of novel bisphosphorus ligands, **L12**–**L14**.[35] This type of ligand possesses the following characteristics: (i) The chirality of the ligand arises from the central P-chirality instead of from the biaryl axial chirality. (ii) The ligand adopts coordination modes with the metal similar to those of BINAP- or BIPHEP-type ligands. (iii) Its steric and electronic properties can be highly modulated by varying the R^3 group at the 2 and 2′ positions. By employing Pd–*i*Pr-BABIBOP (Pd–*ent*-**L14**) as catalyst, the hydrogenation of ethyl 3-oxo-3-phenylpropanoate proceeded in pentafluoropropanol–TFA under 514 psi of H_2 to form the chiral alcohol product in 93% ee and 99% yield with a TON of up to 10,000 (**Scheme 6**, Part (a)).[35] Besides applications in palladium-catalyzed asymmetric hydrogenation, other BABIBOPs have also been successfully used in the rhodium-catalyzed asymmetric hydrogenation of di- and tri-substituted enamides (Scheme 6, Part (b))[36] and the copper-catalyzed hydrogenation of 2-substituted 1-tetralones via dynamic kinetic resolution (Scheme 6, Part (c)).[37] The novel, C_1-symmetric bisphosphorus ligand, MeO-POP, is an operationally convenient solid. It has proven equally effective or even superior to the preceding C_2-symmetric bisphosphorus ligands in the rhodium-catalyzed asymmetric hydrogenation of α-(acylamino)acrylates and β-(acylamino)acrylates, providing excellent enantioselectivities (up to >99% ee) and high TONs (up to 10,000).[38] For example, in the presence of 0.01 mol % [Rh(nbd)(**L16**)]BF_4, methyl 2-acetamido-3-(2-chlorophenyl)-acrylate was hydrogenated in methanol to provide the corresponding chiral α-amino acid derivative in 98% ee.

5. Miscellaneous Asymmetric Transformations

In addition to applications in the asymmetric cross-coupling and asymmetric hydrogenation, chiral phosphorus ligands incorporating a DHBOP moiety have been extensively utilized in a variety of other asymmetric transformations (**Scheme 7**). BIBOP-type ligands have been successfully used in nucleophilic additions of boron reagents to aldehydes, ketones, and imines, to generate chiral homopropargylic alcohols,[39] tertiary alcohols,[40] and α-tertiary amines[41] in excellent enantioselectivities. The Rh–(*R*)-BIDIME catalyst, Rh–*ent*-**L2**, enabled the asymmetric hydroboration of α-aryl enamides with $B_2(pin)_2$, providing a series of chiral α-amino tertiary boronic esters in excellent ee's and satisfactory yields.[42] In the Pd-catalyzed diboration of 1,1-disubstituted allenes, (*S*)-BIDIME (**L2**) performed the best among several chiral mono- and bisphosphorus ligands tested, and led to the formation of a series of chiral tertiary diboronic esters in excellent yields and ee's.[43] Using (*S*)-AntPhos (**L5**) or (*S*)-BIDIME (**L2**), our group effected the first Ni-catalyzed reductive coupling to generate, in high yields and high ee's, chiral tertiary allylic alcohols attached to a tetrahydrofuran[44] or to a pyrrolidine ring.[45] The reaction had a broad scope and permitted the efficient asymmetric synthesis of the lignan dehydroxycubebin as well

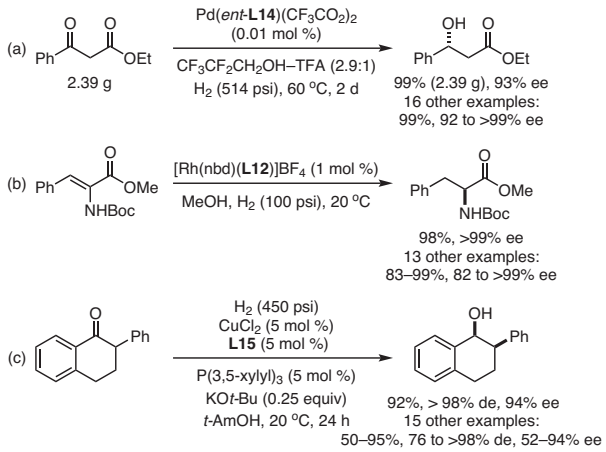

Scheme 6. Asymmetric Hydrogenations Catalyzed by Biaryl Bisphosphorus Ligands. *(Ref. 35–37)*

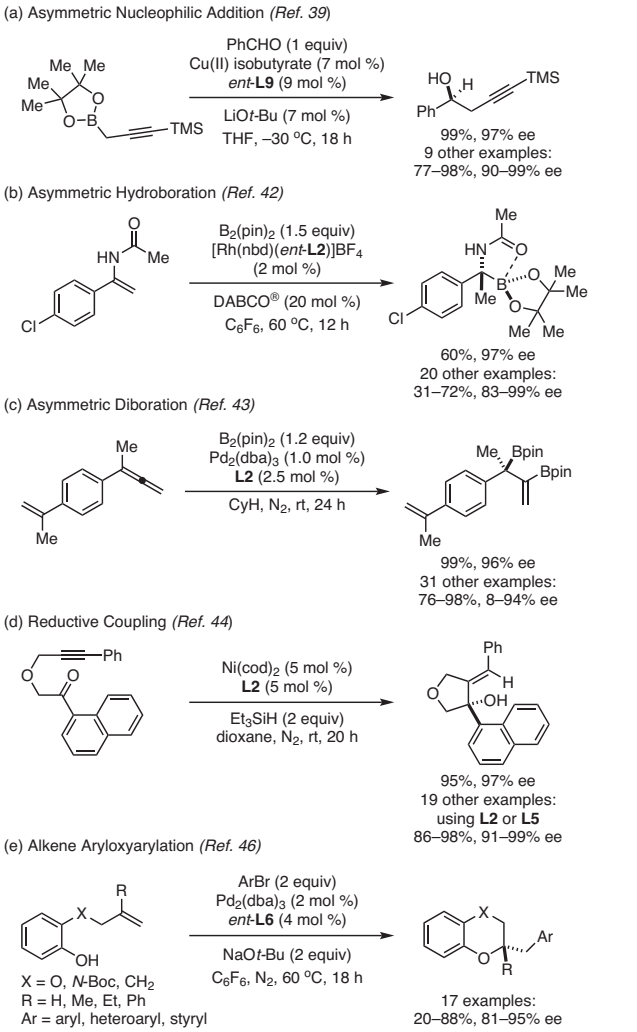

Scheme 7. Miscellaneous Efficient Asymmetric Transformations Enabled by P-Chiral Phosphorus Ligands Based on the DHBOP Motif.

as chiral dibenzocyclooctadiene skeletons. Finally, chiral biaryl monophosphorus ligand (*R,R*)-Me-AntPhos (*ent*-**L6**) led to good yields and excellent enantioselectivities in the asymmetric alkene aryloxyarylation.[46]

6. Conclusion and Outlook

Over the last ten years, our research group has designed and developed chiral phosphorus ligands based on the 2,3-dihydrobenzo[*d*][1,3]oxaphosphole (DHBOP) motif in order to address unmet challenges in asymmetric organic synthesis. High enantioselectivities and turnover numbers, low catalyst loadings, and generally mild conditions have been achieved in a number of reactions by the judicious use of one of these ligands and the metal catalyst. In this way, efficient asymmetric cross-coupling, hydrogenation, hydroboration, cyclization, and nucleophilic addition, among others, have been readily carried out on a very wide range of substrates. Our continued efforts to design and develop novel and efficient phosphorus ligands for new applications in synthetic organic chemistry will help transform the fields of catalysis and synthesis and make useful contributions to the agrochemical and pharmaceutical industries.

7. Acknowledgments

We thank our co-workers from the Tang research group at SIOC, our previous colleagues at Boehringer Ingelheim Pharmaceuticals, and collaborators involved in this research topic. We are grateful for financial support from the Strategic Priority Research Program of the Chinese Academy of Sciences (XDB20000000), CAS (QYZDY-SSW-SLH029), NSFC (21725205, 21432007, 21572246, and 21702223), and the K. C. Wong Education Foundation.

8. References

(1) Tang, W.; Zhang, X. *Chem. Rev.* **2003**, *103*, 3029.
(2) Xu, G.; Senanayake, C. H.; Tang, W. *Acc. Chem. Res.* **2019**, *52*, 1101.
(3) Knowles, W. S. *Acc. Chem. Res*. **1983**, *16*, 106.
(4) Vineyard, B. D.; Knowles, W. S.; Sabacky, M. J.; Bachman, G. L.; Weinkauff, D. J. *J. Am. Chem. Soc.* **1977**, *99*, 5946.
(5) Imamoto, T.; Watanabe, J.; Wada, Y.; Masuda, H.; Yamada, H.; Tsuruta, H.; Matsukawa, S.; Yamaguchi, K. *J. Am. Chem. Soc.* **1998**, *120*, 1635.
(6) Imamoto, T.; Sugita, K.; Yoshida, K. *J. Am. Chem. Soc.* **2005**, *127*, 11934, and references therein.
(7) Tang, W.; Zhang, X. *Angew. Chem., Int. Ed.* **2002**, *41*, 1612.
(8) Liu, D.; Zhang, X. *Eur. J. Org. Chem*. **2005**, *2005*, 646.
(9) Zhang, X.; Huang, K.; Hou, G.; Cao, B.; Zhang, X. *Angew. Chem., Int Ed.* **2010**, *49,* 6421.
(10) Li, C.; Chen, D.; Tang, W. *Synlett* **2016**, *27*, 2183.
(11) Yang, H.; Tang, W. *Chem. Rec.* **2019**, *19, 1* (DOI:10.1002/tcr.201900003).
(12) Fu, W.; Tang, W. *ACS Catal.* **2016**, *6*, 4814.
(13) Tang, W.; Capacci, A. G.; Wei, X.; Li, W.; White, A.; Patel, N. D.; Savoie, J.; Gao, J. J.; Rodriguez, S.; Qu, B.; Haddad, N.; Lu, B. Z.; Krishnamurthy, D.; Yee, N. K.; Senanayake, C. H. *Angew. Chem., Int. Ed.* **2010**, *49*, 5879.
(14) Li, C.; Chen, T.; Li, B.; Xiao, G.; Tang, W. *Angew. Chem., Int. Ed.* **2015**, *54*, 3792.
(15) Zhao, Q.; Li, C.; Senanayake, C. H.; Tang, W. *Chem.—Eur. J.* **2013**, *19*, 2261.
(16) Tang, W.; Patel, N. D.; Xu, G.; Xu, X.; Savoie, J.; Ma, S.; Hao, M.-H.; Keshipeddy, S.; Capacci, A. G.; Wei, X.; Zhang, Y.; Gao, J. J.; Li, W.; Rodriguez, S.; Lu, B. Z.; Yee, N. K.; Senanayake, C. H. *Org. Lett.* **2012**, *14*, 2258.
(17) Xu, G.; Fu, W.; Liu, G.; Senanayake, C. H.; Tang, W. *J. Am. Chem. Soc.* **2014**, *136*, 570.
(18) Yang, X.; Xu, G.; Tang, W. *Tetrahedron* **2016**, *72*, 5178.
(19) Patel, N. D.; Sieber, J. D.; Tcyrulnikov, S.; Simmons, B. J.; Rivalti, D.; Duvvuri, K.; Zhang, Y.; Gao, D. A.; Fandrick, K. R.; Haddad, N.; Lao, K. S.; Mangunuru, H. P. R.; Biswas, S.; Qu, B.; Grinberg, N.; Pennino, S.; Lee, H.; Song, J. J.; Gupton, B. F.; Garg, N. K.; Kozlowski, M. C.; Senanayake, C. H. *ACS Catal.* **2018**, *8*, 10190.
(20) Fandrick, K. R.; Li, W.; Zhang, Y.; Tang, W.; Gao, J.; Rodriguez, S.; Patel, N. D.; Reeves, D. C.; Wu, J.-P.; Sanyal, S.; Gonnella, N.; Qu, B.; Haddad, N.; Lorenz, J. C.; Sidhu, K.; Wang, J.; Ma, S.; Grinberg, N.; Lee, H.; Tsantrizos, Y.; Poupart, M.-A.; Busacca, C. A.; Yee, N. K.; Lu, B. Z.; Senanayake, C. H. *Angew. Chem., Int. Ed.* **2015**, *54*, 7144.
(21) Cao, Z.; Du, K.; Liu, J.; Tang, W. *Tetrahedron* **2016**, *72*, 1782.
(22) Du, K.; Guo, P.; Chen, Y.; Cao, Z.; Wang, Z.; Tang, W. *Angew. Chem., Int. Ed.* **2015**, *54*, 3033.
(23) Zhao, G.; Xu, G.; Qian, C.; Tang, W. *J. Am. Chem. Soc.* **2017**, *139*, 3360.
(24) Du, K.; Yang, H.; Guo, P.; Feng, L.; Xu, G.; Zhou, Q.; Chung, L. W.; Tang, W. *Chem. Sci.* **2017**, *8*, 6247.
(25) Rao, X.; Li, N.; Bai, H.; Dai, C.; Wang, Z.; Tang, W. *Angew. Chem., Int. Ed.* **2018**, *57*, 12328.
(26) Wencel-Delord, J.; Panossian, A.; Leroux, F. R.; Colobert, F. *Chem. Soc. Rev.* **2015**, *44*, 3418.
(27) Lundin, P. M.; Fu, G. C. *J. Am. Chem. Soc.* **2010**, *132,* 11027.
(28) Iwamoto, T.; Okuzono, C.; Adak, L.; Jin, M.; Nakamura, M. *Chem. Commun.* **2019**, *55*, 1128.
(29) Liu, C.; He, C.; Shi, W.; Chen, M.; Lei, A. *Org. Lett.* **2007**, *9*, 5601.
(30) Li, B.; Li, T.; Aliyu, M. A.; Li, Z. H.; Tang, W. *Angew. Chem., Int. Ed.* **2019**, *58,* 11355.
(31) Tang, W.; Qu, B.; Capacci, A. G.; Rodriguez, S.; Wei, X.; Haddad, N.; Narayanan, B.; Ma, S.; Grinberg, N.; Yee, N. K.; Krishnamurthy, D.; Senanayake, C. H. *Org. Lett.* **2010**, *12*, 176.
(32) Reeves, J. T.; Tan, Z.; Reeves, D. C.; Song, J. J.; Han, Z. S.; Xu, Y.; Tang, W.; Yang, B.-S.; Razavi, H.; Harcken, C.; Kuzmich, D.; Mahaney, P. E.; Lee, H.; Busacca, C. A.; Senanayake, C. H. *Org. Process Res. Dev.* **2014**, *18*, 904.
(33) Liu, G.; Liu, X.; Cai, Z.; Jiao, G.; Xu, G.; Tang, W. *Angew. Chem., Int. Ed.* **2013**, *52*, 4235.
(34) Li, C.; Wan, F.; Chen, Y.; Peng, H.; Tang, W.; Yu, S.; McWilliams, J. C.; Mustakis, J.; Samp, L.; Maguire, R. J. *Angew. Chem., Int. Ed.* **2019**, *58*, 13573.
(35) Jiang, W.; Zhao, Q.; Tang, W. *Chin. J. Chem.* **2018**, *36*, 153.
(36) Li, G.; Zatolochnaya, O. V.; Wang, X.-J.; Rodriguez, S.; Qu, B.;

Desrosiers, J.-N.; Mangunuru, H. P. R.; Biswas, S.; Rivalti, D.; Karyakarte, S. D.; Sieber, J. D.; Grinberg, N.; Wu, L.; Lee, H.; Haddad, N.; Fandrick, D. R.; Yee, N. K.; Song, J. J.; Senanayake C. H. *Org. Lett.* **2018**, *20*, 1725.

(37) Zatolochnaya, O. V.; Rodriguez, S.; Zhang, Y.; Lao, K. S.; Tcyrulnikov, S.; Li, G.; Wang, X.-J.; Qu, B.; Biswas, S.; Mangunuru, H. P. R.; Rivalti, D.; Sieber, J. D.; Desrosiers, J.-N.; Leung, J. C.; Grinberg, N.; Lee, H.; Haddad, N.; Yee, N. K.; Song, J. J.; Kozlowski, M. C.; Senanayake, C. H. *Chem. Sci.* **2018**, *9*, 4505.

(38) Tang, W.; Capacci, A. G.; White, A.; Ma, S.; Rodriguez, S.; Qu, B.; Savoie, J.; Patel, N. D.; Wei, X.; Haddad, N.; Grinberg, N.; Yee, N. K.; Krishnamurthy, D.; Senanayake, C. H. *Org. Lett.* **2010**, *12*, 1104.

(39) Fandrick, D. R.; Fandrick, K. R.; Reeves, J. T.; Tan, Z.; Tang, W.; Capacci, A. G.; Rodriguez, S.; Song, J. J.; Lee, H.; Yee, N. K.; Senanayake, C. H. *J. Am. Chem. Soc.* **2010**, *132*, 7600.

(40) Huang, L.; Zhu, J.; Jiao, G.; Wang, Z.; Yu, X.; Deng, W.-P.; Tang, W. *Angew. Chem., Int. Ed.* **2016**, *55*, 4527.

(41) Zhu, J.; Huang, L.; Dong, W.; Li, N.; Yu, X.; Deng, W.-P.; Tang, W. *Angew. Chem., Int. Ed.* **2019**, *58*, 16119.

(42) Hu, N.; Zhao, G.; Zhang, Y.; Liu, X.; Li, G.; Tang, W. *J. Am. Chem. Soc.* **2015**, *137*, 6746.

(43) Liu, J.; Nie, M.; Zhou, Q.; Gao, S.; Jiang, W.; Chung, L. W.; Tang, W.; Ding, K. *Chem. Sci.* **2017**, *8*, 5161.

(44) Fu, W.; Nie, M.; Wang, A.; Cao, Z.; Tang, W. *Angew. Chem., Int. Ed.* **2015**, *54*, 2520.

(45) Liu, G.; Fu, W.; Mu, X.; Wu, T.; Nie, M.; Li, K.; Xu, X.; Tang, W. *Commun. Chem.* **2018**, *1*, Article No. 90 (DOI: 10.1038/s42004-018-0092).

(46) Hu, N.; Li, K.; Wang, Z.; Tang, W. *Angew. Chem., Int. Ed.* **2016**, *55*, 5044.

Trademarks. DABCO® (Evonik Degussa GmbH); QuinoxP*® (Nippon Chemical Industrial Co., Ltd.).

About the Authors

Ting Wu received her B.S. degree in 2016 from Soochow University in Suzhou, Jiangsu (China). In the fall of 2016, she moved to the Shanghai Institute of Organic Chemistry to pursue a doctoral degree under the direction of Professor Wenjun Tang. She is currently conducting research in the area of asymmetric catalysis.

Guangqing Xu obtained his Ph.D. degree in 2015 from the Shanghai Institute of Organic Chemistry, Chinese Academy of Sciences. He became a researcher in Professor Wenjun Tang's group after graduation, and is currently an associate professor at the Shanghai Institute of Organic Chemistry. His research interests are in the areas of asymmetric catalysis and process chemistry.

Wenjun Tang received his Ph.D. degree in 2003 from The Pennsylvania State University (University Park, PA). After a two-year postdoctoral research appointment at the Scripps Research Institute (La Jolla, CA), he worked for six years as a process chemist at Boehringer Ingelheim Pharmaceuticals (Ridgefield, CT). In 2011, he accepted his current position as a research professor at the Shanghai Institute of Organic Chemistry, Chinese Academy of Sciences. His research interests are in the areas of asymmetric catalysis, total synthesis of natural products, and development of efficient chemical processes.

MilliporeSigma

get connected

Get ChemNews

Get current news and information about chemistry with our free monthly *ChemNews* email newsletter. Learn new techniques, find out about late-breaking innovations from our collaborators, access useful technology spotlights, and share practical tips to keep your lab at the fore.

For more information, visit
SigmaAldrich.com/ChemNews

Sigma-Aldrich®
Lab & Production Materials

MilliporeSigma
P.O. Box 14508
St. Louis, MO 63178
USA

VOLUME 53, NO. 2 | **2020**
SPECIAL ISSUE: FOCUS ON SUSTAINABILITY

MilliporeSigma

ALDRICHIMICA ACTA

Carbon Dioxide Capture and Recycling to Methanol: Building a Carbon-Neutral Methanol Economy

Designing Renewable, High-Performance Solvents with Improved Toxicity Profiles

sustainability

An Essential Part of Our Corporate Strategy

Presently, global businesses must operate and thrive in an interconnected world fraught with global risks and uncertainties. These have become increasingly complex and are often determined by external factors, such as geopolitics and societal or technological dynamics, as well as internal ones. Corporate strategic decision making, inevitably, must deal with an ever-changing environment where the risks and opportunities for business have become harder to identify and even more difficult to quantify.

Sustainable development has become not only a necessary element of such strategic decision making, but an essential prerequisite for meeting challenges and being successful as a company in the long run. The 17 Sustainable Development Goals (SDGs) put forth by the United Nations provide a blueprint for peace and prosperity for people and the planet now and into the future. Science and technology are important elements of strategies for reaching these goals.

At Merck KGaA, Darmstadt, Germany, we have taken on the challenge of incorporating these goals in the way we conduct our business. Our core belief is that, with our broad and diversified setup, we combine a unique bandwidth of expertise in many fields of science and technology that enables us to deliver the solutions to many of the sustainability problems the world is facing today. At the same time, this approach allows us to remain successful and adapt to a wide range of future scenarios. Sustainability goals included in our group strategy as well as our business strategies lead to positive contributions to society. Take for example our Sustainable Business Value tool, which we developed to quantify the overall environmental, social, and economic sustainability impact of our technologies and products on the societies we are operating in. Other examples are our DOZN™ platform, which helps developers evaluate the relative greenness of a process, and our Greener Alternatives Platform, which now counts close to one thousand greener alternatives to conventional products.

The common thread that runs through all our efforts with regard to sustainability is that we are curious minds dedicated to human progress.

Sincerely yours,

Herwig A. Buchholz, Prof. Dr.
Head of Group Corporate Sustainability
Merck KGaA, Darmstadt, Germany

ALDRICHIMICA ACTA
VOL. 53, NO. 2 • 2020

Merck KGaA, Darmstadt, Germany
Frankfurter Strasse 250
64293 Darmstadt, Germany
Phone +49 6151 72 0

To Place Orders / Customer Service
Contact your local office or visit
SigmaAldrich.com/order

Technical Service
Contact your local office or visit
SigmaAldrich.com/techinfo

General Correspondence
Editor: Sharbil J. Firsan, Ph.D.
Sharbil.Firsan@milliporesigma.com

Subscriptions
Request your FREE subscription to the *Aldrichimica Acta* at **SigmaAldrich.com/Acta**

The entire *Aldrichimica Acta* archive is available at **SigmaAldrich.com/Acta**

Aldrichimica Acta (ISSN 0002-5100) is a publication of Merck KGaA, Darmstadt, Germany.

"PLEASE BOTHER US."

Dear Fellow Chemists,

Professor Amir H. Hoveyda of the Department of Chemistry at Boston College and the Institute for Supramolecular Science and Engineering at the University of Strasbourg kindly suggested we offer bis(2,4,6-triisopropylphenyl)borane [HB(trip)$_2$, **907847**], a traceless protecting group for alkenes with functional groups such as hydroxyl and carboxyl that are incompatible with olefin metathesis conditions. HB(trip)$_2$ was found to be superior to HB(pin) in this regard and to allow for the direct synthesis of geometrically well-defined di- and trisubstituted alkenes incorporating carboxyl groups under mild metathesis conditions. The approach significantly expands the scope of the kinetically controlled Mo-catalyzed *Z*- and *E*-selective olefin metathesis.

Mu, Y.; Nguyen, T. T.; van der Mei, F. W.; Schrock, R. R.; Hoveyda, A. H. *Angew. Chem., Int. Ed.* **2019**, *58*, 5365.

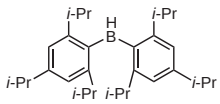

HB(trip)$_2$, **907847**

907847	Bis(2,4,6-triisopropylphenyl)borane (HB(trip)$_2$), ≥95%	1 g 5 g

We welcome your product ideas. Do you need a product that is not featured on our website? Ask us! For more than 60 years, your research needs and suggestions have shaped our product offering. Email your suggestion to **techserv@sial.com**.

Daniel Boesch, VP
Head of Lab and Specialty Chemicals

TABLE OF CONTENTS

ABOUT OUR COVER

What better to exemplify the ideals of Sustainability (renewable resources, benign processes, recycling, etc.) than a depiction of a windmill and a grainfield at harvest time! Both use renewable natural resources: the mill is powered by the wind, and the plants consume water and sunlight. Perhaps the rainbow framing part of the scene is an apt symbol of humanity's hope for a sustainable and sunnier future.

The Great Windmill and the Rainbow (oil on canvas, 88.9 x 116.8 cm) was painted in 1888 by the famed landscape artist Jean-Charles Cazin (1841–1901). A good friend of Auguste Rodin,* Cazin received his artistic training at the Free School of Drawing in Paris and is best known for his depiction of charming and serene French countryside scenes with very few if any human or animal figures. Save for a trip to England, Cazin lived and worked all his life in France, mainly in his native region, the Pas-de-Calais.

Detail from ***The Great Windmill and the Rainbow***. Photo courtesy The National Gallery of Art, Washington, DC.

This painting is in the Corcoran Collection (William A. Clark Collection) at the National Gallery of Art, Washington, DC.

* *One of Rodin's masterpieces is* The Burghers of Calais *group sculpture. To find out about the link of this sculpture to Cazin, visit* ***SigmaAldrich.com/Acta***

Is your cure in our library?

Open Global Health Library for infectious disease research* from Merck KGaA, Darmstadt, Germany

We want to support researchers worldwide – especially in low and middle income countries – to find new cures for life-threatening infectious diseases. That's why we created the Open Global Health Library: a collection of compounds you can use to develop life-changing drugs.

Discover the next Praziquantel

One of the best successes of our library is Praziquantel. It was initially developed by Merck KGaA, Darmstadt, Germany as a potential antipsychotic, and then provided to Bayer for testing worm parasite treatments. The library compound was eventually repurposed by the two companies to develop Praziquantel, an anthelmintic drug, approved in 1980. Today, it is on the WHO list of essential medicines. Your drug could be next.

Look inside the library

Our library contains pre-selected compounds that cover a wide range of molecular targets for infectious disease research. All compounds are small molecules (not bio-logicals), supplied as 10 mM solutions in 30 µL DMSO.

Is the library for you?

If you're researcher at a university, research institute or private company, then yes it is! The Open Global Health Library is open to applications for research and development purposes.

Your benefits

After you send us a brief outline of your intended research, we'll send you an agreement to sign. Once that's settled, we'll send you the compound library. It's that simple, clear and sincere. You'll have no fees, are free to publish your results, and will retain all rights to your intellectual property.

Use our compounds free of charge

Retain intellectual property rights

Feel free to publish your results

Request follow-up discussions

Ready to create the next cure?

Learn more about the **Open Global Health Library:**
EMDgroup.com/OpenGlobalHealthLibrary

*Given the limited number of plates available, plates will be prioritized for non-COVID19 infectious disease research.

The businesses of Merck KGaA, Darmstadt, Germany operate as EMD Serono, MilliporeSigma and EMD Performance Materials in the U.S. and Canada.

34257 11/2020

Carbon Dioxide Capture and Recycling to Methanol: Building a Carbon–Neutral Methanol Economy


Mr. Raktim Sen


Dr. Alain Goeppert


Prof. G. K. Surya Prakash

Raktim Sen, Alain Goeppert, and G. K. Surya Prakash*

Loker Hydrocarbon Research Institute and Department of Chemistry
University of Southern California, University Park
Los Angeles, CA 90089-1661, USA
Email: gprakash@usc.edu

Keywords. CO_2 capture; CO_2 utilization; homogeneous hydrogenation; direct air capture; formamides; formate esters; carbon neutral cycle; methanol economy; renewable methanol; pincer catalysts.

Abstract. Increasing atmospheric CO_2 concentration and associated global warming can be linked directly to rising anthropogenic CO_2 emissions. These emissions, outpacing the natural carbon cycle, originate predominantly from the burning of finite fossil fuel resources. As a unified solution to the challenges of global warming and energy-needs issues, a sustainable and renewable "methanol economy" concept has been proposed. Methanol, the simplest alcohol, is already utilized on a large scale as a carbon feedstock for synthesizing a plethora of organic compounds. Furthermore, methanol is a convenient liquid fuel and an attractive energy carrier. Chemical recycling of CO_2, a greenhouse gas, to produce methanol, a green fuel, is of paramount importance for a carbon-neutral methanol economy. Recent advances in this research area are discussed with a focus on low-temperature homogeneous catalysis. In addition, this review provides a detailed discussion of integrated CO_2 capture, including direct air capture (DAC), and recycling into methanol—a research field that has gained significant attention over the past five years.

Outline

1. Introduction

Over the past two centuries, the world's population growth and rapid industrial development have been accompanied by an exponential surge in energy demand. To meet this demand, we have relied primarily on nature's reserves of fossil fuels (stored carbon). These were formed over millions of years and are now

used for a multitude of applications ranging from electricity generation, heating, transportation, and cooking to feedstock for manufacturing most carbon-based chemicals and materials. Presently, around 80% of our energy demand is still covered by the combustion of fossil fuels such as coal, petroleum, and natural gas,[1,2] resulting in the inevitable emission of one of their unwanted combustion products: carbon dioxide.[3] This emission has led to a dramatic increase in the atmospheric CO_2 concentration to about 420 ppm presently (as of July 2020).[4] This marks a 70% rise from the pre-industrial 18th century levels of around 250 ppm. As a direct consequence, a substantial rise in average global temperatures has been observed. Already up by ~0.8 °C in the past century, a further rise of up to 5 °C is being predicted over the 21st century.[5,6] Associated problems such as rising sea levels, ocean acidification, increasing wildfires, and more extreme and unpredictable weather patterns have already emerged as early signs of this trend,[7] not to mention an ongoing loss of biodiversity.[8] As a result, a worldwide effort to address global warming and related issues culminated in the Kyoto Protocol and the subsequent Paris Agreement, which adopted a more sustainable framework for development with minimal carbon emissions.[9]

In order to address the increasing accumulation of CO_2 in the atmosphere (>17 Gt in 2018),[3] various technologies are being developed to capture CO_2 either directly at its emission source or from diffused sources such as ambient air.[10–16] Processes based on solutions of amines and amino alcohols as well as alkali hydroxides are already being used on a large scale to scrub the CO_2 found in industrial exhausts.[15] Following capture, CO_2 can be desorbed, pressurized, and sequestered underground in geological formations (carbon capture and sequestration (CCS)).[17,18] Alternatively, carbon capture and recycling (CCR) is a value-added process,[19] wherein the concentrated CO_2 can be utilized as a carbon feedstock to manufacture a multitude of chemicals and materials such as methanol, formic acid, dimethyl ether, urea, and polyurethanes (**Figure 1**).[20–25]

Among the products accessible through hydrogenation of CO_2,[22,26] methanol is an attractive derivative that has numerous key applications as an alternative fuel, fuel additive, hydrogen storage medium, and a valuable C1 feedstock for producing a variety of hydrocarbon-based chemicals and polymers.[2,27–29] Lately, there has been an increasing demand for methanol in a number of countries as a fuel substitute (M100) and gasoline additive (M15, M85) in cars, buses, and ships as well as a fuel for boilers and for cooking.[2] Presently, methanol is derived predominantly from fossil fuels, mostly natural gas and coal, through syngas.

As part of the *Methanol Economy*—a concept that we have championed with Professor George A. Olah, our late colleague, mentor and Nobel Laureate—a more sustainable production of methanol through hydrogenative recycling of CO_2 is proposed.[2] In this CCR scheme, CO_2 from any, but preferably renewable, source is combined with hydrogen obtained from renewable sources to produce renewable methanol in a carbon-neutral and sustainable energy model.[30] In such a process, the CO_2 emitted when the renewable methanol is combusted as a fuel can be captured back and utilized again for methanol synthesis, thus closing the carbon loop and establishing a carbon-neutral cycle. Production

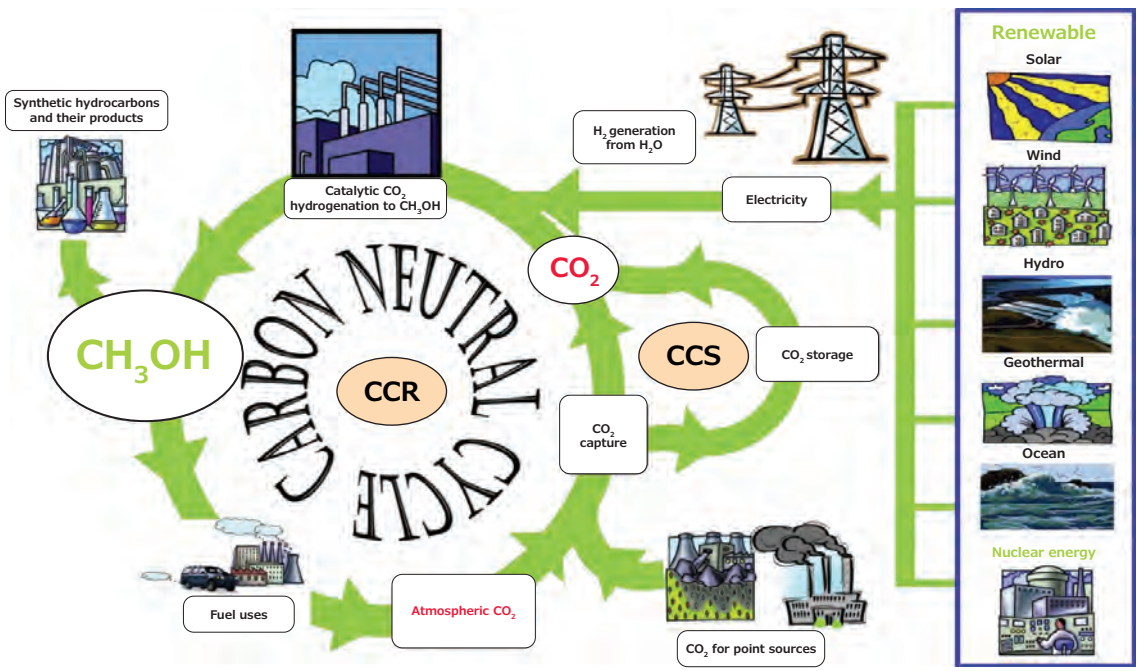

Figure 1. Anthropogenic Carbon Cycle in the Context of the Methanol Economy. *(Reproduced with Permission from Reference 42. © 2018, Springer Nature.)*

of renewable methanol from CO_2 has already been realized in the George Olah Renewable Methanol Plant operated by Carbon Recycling International (CRI) in Iceland.[31] Annually, around 5,500 tonnes of CO_2 emitted from geothermal vents are captured and recycled to synthesize 5 million liters of renewable methanol, trademarked as Vulcanol® (**Figure 2**).[2,31] The required hydrogen is produced locally through water electrolysis using electricity generated from hydro and geothermal sources in Iceland.

2. Methanol: A Versatile Fuel and Carbon Feedstock

Methanol (CH_3OH), known as wood alcohol, is the simplest alcohol, a convenient one-carbon liquid at room temperature that is easy to store, transport, and dispense. It is a prominent building block to synthesize various chemicals and materials such as formaldehyde, methyl *tert*-butyl ether (MTBE), acetic acid, and various polymers, paints, adhesives, construction materials, pharmaceuticals, and many others (**Figure 3**).[2,29] Industrially, methanol can also be catalytically converted into a variety of olefins and hydrocarbons through the methanol-to-olefin (MTO) and methanol-to-gasoline (MTG) processes.[32] In essence, most of the carbon-based chemicals and fuels presently obtained from petroleum and natural gas can be derived from methanol.[29] When this is coupled with methanol synthesis through CO_2 recycling, the methanol economy has the potential to liberate us in the long run from our dependence on finite reserves of fossil fuels and pave the way for a sustainable future.[33,34]

Besides its applications as a feedstock, methanol is an excellent fuel that is very clean-burning. It is a direct drop-in fuel in internal combustion engines (ICE), gas turbines, cooking stoves, boilers, and direct methanol fuel cells (DMFC).[35–37] Furthermore, because of its high octane number, methanol is widely used as an additive to gasoline.[38] Methanol also has a considerable hydrogen storage capacity (H_2 content = 12.6 wt %), and the stored hydrogen can be easily extracted through methanol reforming and utilized in hydrogen fuel cells (reformed methanol fuel cell, RMFC).[39–41] Hence, methanol is a suitable liquid organic hydrogen carrier (LOHC).[42] Our group and others have made significant contributions in this field by using both homogeneous and heterogeneous catalysts in the presence of water or amines (**Scheme 1**).[33,39,40,42–58] However, this is not the focus of this review.

2.1. Methanol Synthesis from Syngas

Methanol is currently produced at a scale of more than 100 billion liters annually, predominantly from fossil sources like coal and natural gas.[4,21] In the relevant industrial processes, these carbon sources are first converted into a mixture of CO and H_2, referred to as synthesis gas or syngas. Syngas generally comprises CO and H_2 as well as a minor fraction of CH_4 and CO_2.

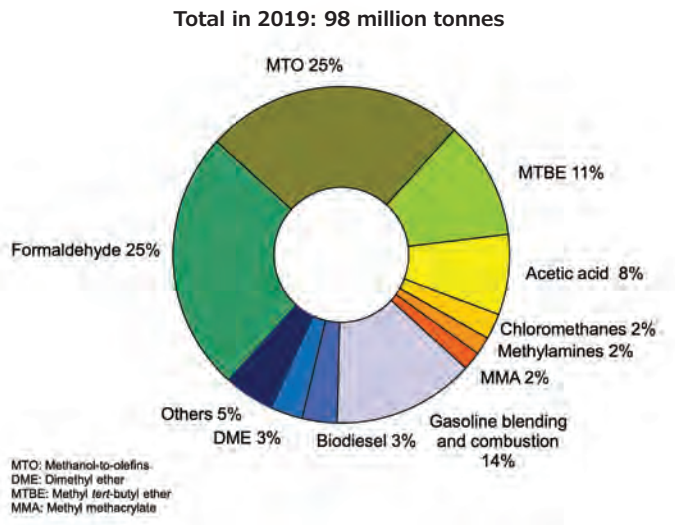

Figure 3. The Worldwide Demand for Methanol in 2019. *(Data from the Methanol Institute/Methanol Market Services Asia (MMSA), 2019)*

Figure 2. The George Olah Renewable Methanol Plant Operated by Carbon Recycling International (CRI) in Iceland (Left); the Methanol Economy Book, 3rd Edition (Right). *(Reproduced with permission from reference 2. © 2018, John Wiley and Sons)*

After adjustment and purification, this gas mixture is converted into methanol in the presence of a commercial heterogeneous catalyst ($Cu/ZnO/Al_2O_3$ based) at temperatures of about 250 °C and pressures of 50 bar and higher. The process produces methanol with a maximum conversion of about 30% per cycle due to the thermodynamic equilibrium at that temperature. Complete conversion of the syngas to methanol is obtained by continuously recycling the unreacted gases through the catalyst.[2,4,59,60]

In the field of homogeneous catalysis, only limited progress has been achieved in the study of CO hydrogenation to CH_3OH.[61–65] The advantage of these processes is that they operate at much lower temperatures, pushing the equilibrium of the exothermic CO hydrogenation further towards the production of methanol. Hence, the conversion to methanol is significantly enhanced compared to the thermodynamic limit of about 30% observed in the industrial processes using heterogeneous catalysts. Jens and Mahajan independently reported the reduction of CO to CH_3OH using homogeneous nickel carbonyl and copper acetate catalysts, respectively.[66–68] In CH_3OH as a solvent, the conversion proceeded through the formation of methyl formate followed by further reduction to methanol. While these systems demonstrated the feasibility of obtaining methanol from syngas at low temperatures (80–140 °C) with moderate-to-high conversions, both systems required highly caustic media (NaOMe or NaH) and led to the formation of the flammable and highly toxic $Ni(CO)_4$. In 2019, our group reported a novel amine-assisted route to access CH_3OH from syngas. Using high-boiling amines, the reaction proceeded at 140 °C through two steps: (i) K_3PO_4 catalyzed anchoring of CO onto the amine as formamide, and (ii) hydrogenation of formamides to CH_3OH in the presence of H_2 and ruthenium PNP catalysts.[69] This efficient conversion was demonstrated both as a two-step sequential process as well as a one-pot direct process. Following our report, Checinski, Beller, and co-workers showed that manganese-based PNP catalysts are also active for the conversion, albeit with lower TONs.[70]

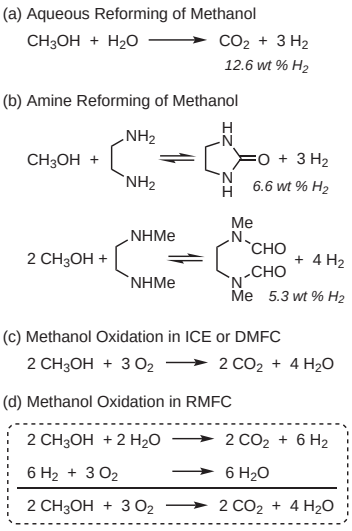

Scheme 1. Methanol Reforming (a and b) and Oxidation of Methanol in ICE, DMFC, and RMFC (c and d). *(Ref. 33,39,40,42–58)*

3. CO_2 Hydrogenation to Methanol

3.1. Heterogeneous Catalysis

Similar to the conventional process of obtaining methanol from syngas ($CO + 2\ H_2 \rightleftharpoons CH_3OH$ $\Delta H_{298K} = -21.7$ kcal mol^{-1}), CO_2 can be activated by the same class of catalysts to undergo hydrogenation to methanol ($CO_2 + 3\ H_2 \rightleftharpoons CH_3OH + H_2O$ $\Delta H_{298K} = -11.9$ kcal mol^{-1}). This correlates to the widely accepted mechanism of the CO-to-methanol process that is understood to proceed in large part through the transformation of CO to CO_2 via the water–gas shift (WGS) reaction. $Cu/ZnO/Al_2O_3$ and similar heterogeneous catalysts have been shown to catalyze the reaction at high temperatures (230–300 °C) and pressures (50–75 bar).[71–76] The catalysis is known to suffer from the parallel side reaction of reverse water–gas shift (RWGS) ($CO_2 + H_2 \rightleftharpoons CO + H_2O$ $\Delta H_{298K} = 9.8$ kcal mol^{-1}). Unfortunately, the water produced during this process slowly deactivates the catalyst traditionally used for the methanol synthesis. While the route has a high selectivity of >99% for methanol, high reaction temperatures limit the conversion of CO_2 to a thermodynamic value of around 30% in a single pass. To enhance the overall conversion, the unreacted gas mixture is recycled multiple times. Over the past few years, significant advances have taken place in the development of other heterogeneous catalytic systems capable of improved conversions, better resistance to the water-induced deactivation, and of minimizing the RWGS reaction. One approach has been to modify the $Cu/ZnO/Al_2O_3$ catalyst system. Other approaches include entirely new types of catalyst such as Ni–Ga, Pd, Pt, and In_2O_3 based catalysts, among others.[21,74,77–81] Very recently, Heldebrant and co-workers studied the condensed-phase CO_2 hydrogenation to CH_3OH using heterogeneous Cu- and Pd-based catalysts in a tertiary amine–alcohol solvent, at somewhat lower temperatures of 120–170 °C.[82,83]

3.2. Homogeneous Catalysis: A Low-Temperature Alternative

While heterogeneous catalysts for the hydrogenation of CO_2 to methanol are robust, relatively inexpensive, and can be recycled with ease, there has been an ongoing search for new catalytic systems that offer alternate routes to methanol at lower temperatures and with higher CO_2 conversions. In this context, homogeneous metal complexes are an attractive class of catalysts, which can catalyze the hydrogenation under relatively mild conditions. Additionally, homogeneous systems allow for a better and easier understanding of the reaction mechanism at a molecular level. Based on experimental and mechanistic insights, the catalytic framework can be rationally tuned to improve the efficiency and selectivity of the process. Moreover, desirable homogeneous catalysts should exhibit high turnovers and considerable stability over the long run at temperatures required for the transformation.[84]

3.2.1. Routes for Accessing Methanol

Hydrogenation of CO_2 to methanol with H_2 can proceed through various intermediates and derivatives of CO_2. These include organic carbonates (acyclic and cyclic), urea derivatives, carbamates, formate esters, formamides, formic acid, and carbon monoxide (**Scheme 2**). Derivatives such as carbonates, carbamates, and urea can be obtained from CO_2 without any reduction step, and these species can be hydrogenated with three equivalents of H_2 to obtain methanol. On the other hand, pathways through intermediates such as CO, formic acid, formamides, and formate esters require two consecutive hydrogenation steps: first, reduction of CO_2 to these intermediates with one equivalent of H_2, followed by further hydrogenation of these species to CH_3OH using two equivalents of H_2.

3.2.2. The Beginning

The first example of a homogeneous catalytic system for CO_2 hydrogenation to methanol was reported by Tominaga et al. in 1993 and 1995.[85,86] The hydrogenation was catalyzed by a $Ru_3(CO)_{12}$ complex with KI as an additive in *N*-methyl-2-pyrrolidone as solvent. The reaction operated at high temperatures (160–240 °C) and a net pressure of 80 bar (CO_2:$3H_2$), proceeding through CO as an intermediate, which was also observed as a side product along with CH_4 (by further reduction of CH_3OH). While these reports documented a novel homogenous system for CO_2 hydrogenation to CH_3OH, the process suffered from several drawbacks including low yields, poor selectivity, and high operating temperatures that are comparable to those in the existing heterogeneous systems.

3.2.3. Hydrogenation of CO_2 Derivatives to Methanol

Almost two decades later, a pivotal report by Milstein and co-workers revealed that methanol can be accessed from various CO_2 derivatives, such as dimethyl carbonate, methyl carbamates and methyl formates under mild, homogeneous, and catalytic hydrogenation conditions (110 °C, 10 atm H_2) (see Scheme 2).[87] While direct CO_2 hydrogenation was not achieved, an indirect sequential route to CH_3OH from CO_2 was established, since these species can be readily obtained from CO_2 through known processes. This work also demonstrated the use of ruthenium pincer catalysts for such transformations, a superior class of homogenous catalysts that exhibit high stability and structural rigidity at high temperatures. Since this initial report by Milstein, similar metal pincer complexes have been widely used with impressive performance, and hence, are often preferred for CO_2 hydrogenation and similar transformations.[88,89] Milstein's group also reported in 2011 the hydrogenation of urea derivatives, as CO_2 surrogates, to CH_3OH and amines using a Ru–PNN catalyst.[90] The following year, Ding and co-workers reported the hydrogenation of a cyclic carbonate, namely ethylene carbonate, to CH_3OH and ethylene glycol using Ru–PNP catalysts.[91] Later, other examples of urea and ethylene carbonate hydrogenation to methanol were reported using ruthenium-, manganese-, and cobalt-based complexes.[92–96]

3.2.4. Direct CO_2 Hydrogenation to Methanol

In 2011, Huff and Sanford disclosed a catalytic cascade process in which three different homogeneous catalysts, $(PMe_3)_4Ru(Cl)(OAc)$, $Sc(OTf)_3$, and (PNN)Ru(CO)(H), operate sequentially to effect the synthesis of CH_3OH from $CO_2/3H_2$ (40 bar) at 75–135 °C (**Figure 4**).[97] In CD_3OH solvent, the reaction proceeded through the sequence: (i) CO_2 hydrogenation to formic acid catalyzed by $Ru(PMe)_3(Cl)(OAc)$, (ii) esterification of formic acid with CD_3OH to methyl formate catalyzed by $Sc(OTf)_3$, and (iii) hydrogenation of methyl formate to methanol, catalyzed by (PNN)Ru(CO)(H). The sequential process was also demonstrated in a one-pot setup. Inspired by this work, a similar cascade system was reported by Goldberg and co-workers who employed Ru and Ir pincer complexes in conjunction with $Sc(OTf)_3$.[98] Very recently, Byers, Tsung, and co-workers prepared a highly recyclable catalyst system by encapsulation of the Ru pincer catalysts in a Zr-based MOF (UiO-66), obtaining remarkably high TONs.[99] In 2012, Klankermayer, Leitner, and co-workers reported the CO_2 hydrogenation to CH_3OH through a formate ester route in the presence of EtOH[100] and, later, through a direct hydrogenation route in the absence of alcohol additive[101] by using single-ruthenium phosphine complexes with triphos and similar ligands.[102] Subsequently, Beller and co-workers reported a similar route that utilizes homogeneous catalysts based on cobalt complexes with triphos and similar ligands.[103,104] Further, in the context of additive-free direct CO_2 hydrogenation, the groups of Himeda and Laurenczy reported the reduction of CO_2 to methanol through formic acid disproportionation catalyzed by iridium-based molecular complexes.[105] Notably, the reactions were performed in an aqueous solution (with and without H_2SO_4) at a relatively low temperature of 70 °C.

The catalytic systems discussed up to this point for CO_2 hydrogenation to methanol operate under neutral or slightly acidic conditions. In contrast to such systems, CO_2 hydrogenation in

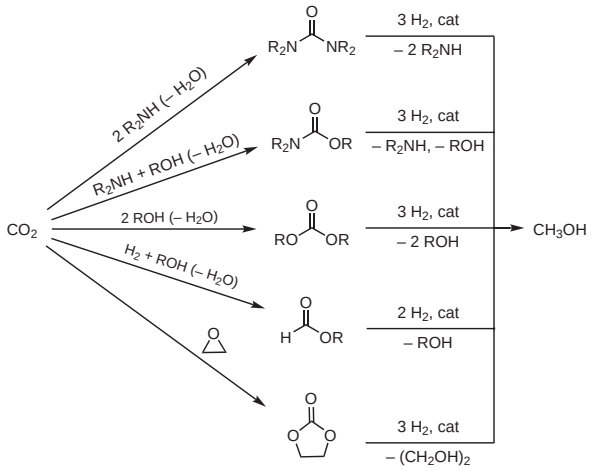

Scheme 2. Accessing Methanol through the Indirect Hydrogenation of CO_2.

the presence of amines can operate under basic conditions. At the same time, most state of the art CO_2 capture technologies usually function under basic conditions (CO_2 being a weak acid) using amines and amino alcohols as sorbents.[10,106] Hence, the amine-assisted CO_2 hydrogenation route is of significant interest, as it allows for the integration of two key processes: CO_2 capture and CO_2 utilization as a one-pot system.[81] Advances in this area are discussed in detail in Section 4.

The first example of an amine-assisted process for converting CO_2 to methanol was disclosed by Sanford and co-workers in 2015 (**Figure 5**).[107] Employing dimethylamine as a model amine, the hydrogenation of CO_2 to methanol proceeded through key intermediates with the amine: ammonium carbamate, ammonium formate, and formamide. The reaction was performed using a temperature ramp (95–155 °C), and was catalyzed by a Ru-PNP catalyst, Ru-MACHO®-BH. The same year, Ding's research group reported a morpholine-mediated sequential route for hydrogenating CO_2 to methanol through formamide intermediates by utilizing the same class of ruthenium pincer catalysts.[108] During this period, our group also studied methanol synthesis from CO_2 using Ru-MACHO® catalysts in the presence of commercially available and high-boiling polyamines such as pentaethylenehexamine (PEHA).[109] In that study, the recyclability of the catalyst was also successfully demonstrated. Later, the groups of Wass and Kayaki independently reported significant advances in the amine-assisted CO_2-to-methanol field using ruthenium catalysts.[110,111] In the emerging area of homogeneous base-metal-catalyzed hydrogenation of CO_2 to methanol, our group revealed in 2017 the first such system that utilizes a manganese(I)–PNP complex and which proceeds through formamide intermediates in a sequential one-pot process.[112] In 2019, Hazari, Bernskötter, and co-workers published a similar route using iron–PNP catalysts.[113] Two years earlier, Martins and co-workers had described an iron(II) scorpionate, $[FeCl_2\{\kappa^3\text{-}HC(pz)_3\}]$ (pz = pyrazol-1-yl), based catalytic system for the one-pot conversion of CO_2 to CH_3OH at a relatively mild temperature of 80 °C.[114]

In addition to the routes of CO_2-to-methanol conversion described in this section, there have been significant advances in achieving this transformation through various additional approaches involving photocatalysis, electrocatalysis, enzymatic catalysis, hydride-based reagents such as boranes and silanes as well as others.[115–127] These methodologies are beyond the scope of this review.

4. Integrated CO_2 Capture and Recycling to Methanol

The production of methanol by chemical recycling of CO_2 captured from various sources provides a sustainable path to the carbon-neutral methanol economy.[20,21,60,128–130] In this regard, integration of the two steps, (i) CO_2 capture and (ii) CO_2 hydrogenation to methanol, has been realized recently.[128,131] In such combined processes, CO_2 can be captured using amines or alkali hydroxides under ambient conditions (room temperature and atmospheric pressure) from concentrated as well as

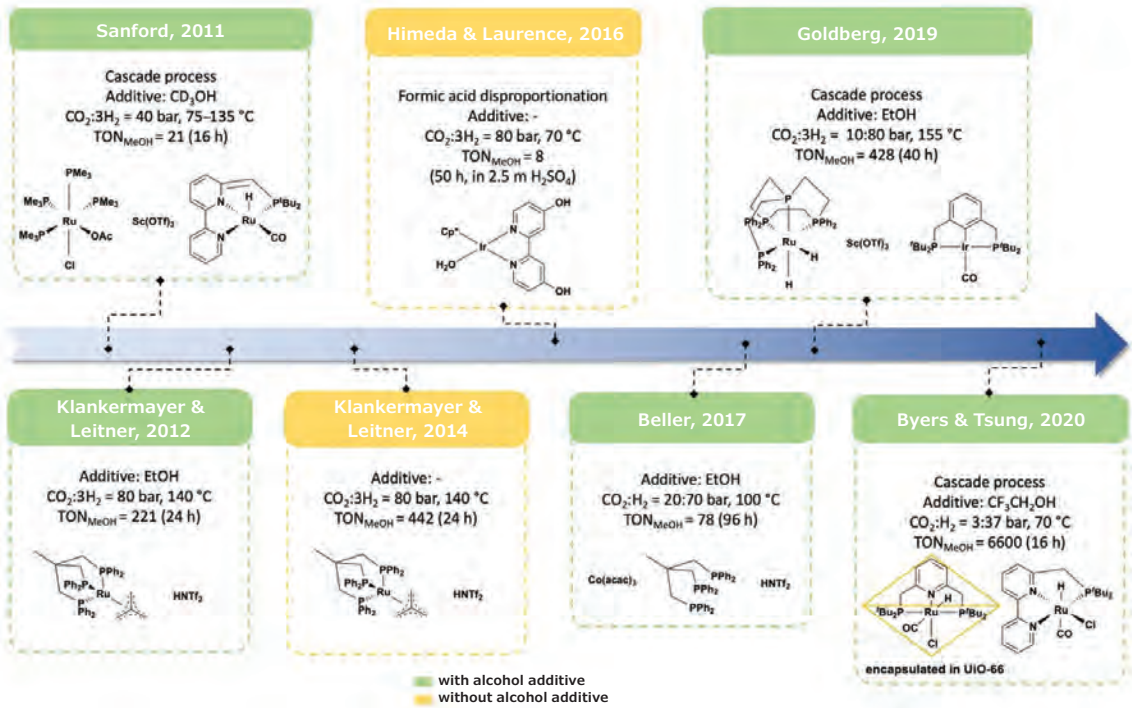

Figure 4. Timeline of Key Developments in the Alcohol-Assisted and the Direct Hydrogenation of CO_2 to Methanol.

dilute sources such as air (containing ~ 415 ppm CO_2). These capture species, without any purification and separation, are directly subjected to hydrogenative conditions in the presence of catalysts to synthesize methanol. The highlight of these integrated systems is the elimination of the large energy and cost penalties associated with the desorption and compression steps in the extraction of pure CO_2 that are a part of the conventional carbon capture and storage or utilization processes.[128,132]

4.1. CO_2 Capture by Amines and Conversion to Methanol

CO_2 utilization under low pressure (1–3 bar) and conversion to methanol was demonstrated by Milstein and co-workers in 2015 (**Scheme 3**).[133] First, CO_2 reacts with amino alcohols in the presence of Cs_2CO_3 as catalyst to form oxazolidinones. These are then subjected to Milstein's Ru-PNN hydrogenation catalyst to synthesize methanol. While this report was a pivotal step towards integration of CO_2 capture and CO_2 utilization processes, the requirement of a high temperature (150 °C) for CO_2 to form oxazolidinones presented considerable challenges in the context of CO_2 capture under ambient conditions.

4.1.1. Proof of Concept

Since amines have been well-studied for CO_2 capture and are commercially used to scrub CO_2 from industrial gas streams, our group envisaged the first example of an integrated system in which CO_2 can be readily captured by bubbling it through aqueous amine solutions at room temperature and atmospheric pressure.[109] The captured species, namely ammonium carbamates and bicarbonates, are directly hydrogenated to methanol in the presence of H_2 gas and a homogeneous hydrogenation catalyst such as Ru-MACHO®-BH (**Scheme 4**).[109] Pentaethylenehexamine (PEHA); an inexpensive, readily available, and high-boiling polyamine with a low vapor pressure; was found to be highly efficient for both the capture and hydrogenation steps, and was regenerated concurrently with methanol formation. A similar reduction of ammonium carbamates to methanol had previously been reported by Sanford and co-workers.[107]

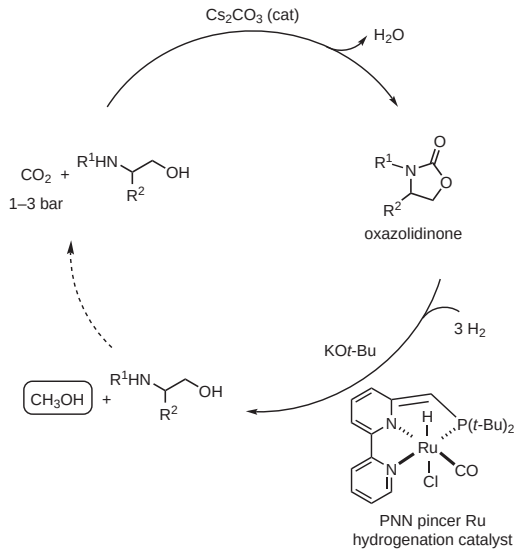

Scheme 3. Milstein's Low-Pressure CO_2 Combined Capture and Utilization. *(Ref. 133)*

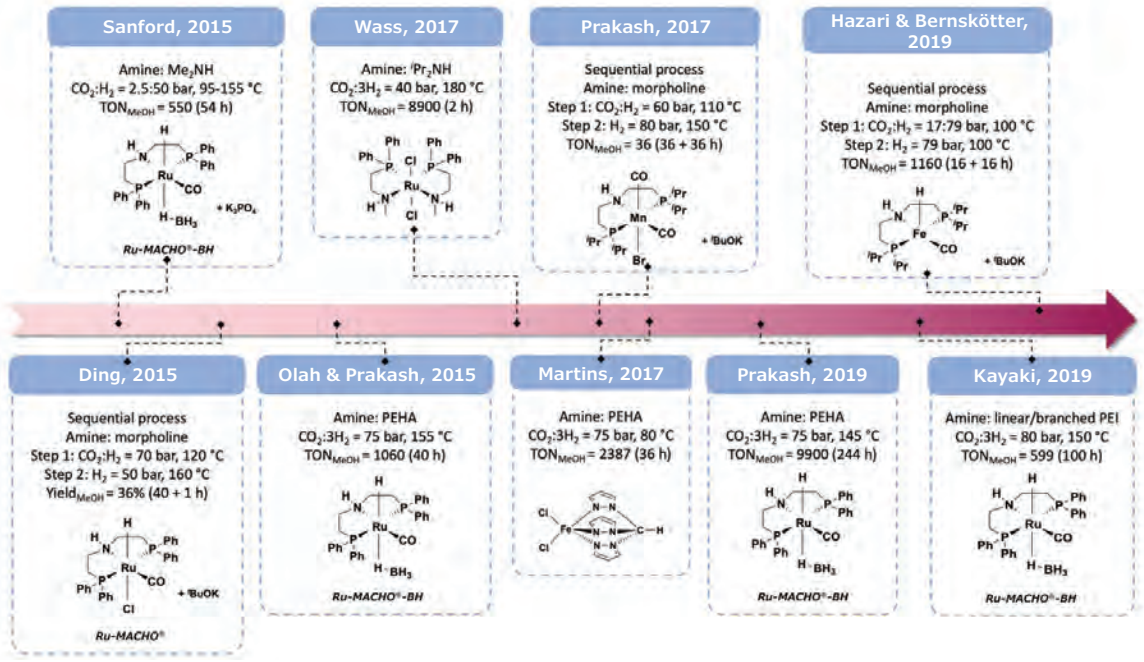

Figure 5. Timeline of Key Developments in the Amine-Assisted CO_2 Hydrogenation to Methanol

4.1.2. Recycling Studies

For the purpose of large-scale applications of such a system, effective recycling of the active components, principally the base and the catalyst, is highly desirable. In this context, we developed a biphasic solvent system to demonstrate the recyclability of our process (**Figure 6**, Part (A)).[134] First, CO_2 is captured by amines in the aqueous phase to form soluble carbamates and/or bicarbonate salts. Next, the catalyst is dissolved in a water-immiscible organic phase such as 2-MTHF (2-methyltetrahydrofuran) and then added to the aqueous phase. This results in a biphasic system for the captured CO_2 to be efficiently hydrogenated to methanol. Following completion of the reaction, methanol is collected from the solution under reduced pressure. The catalyst can be reprocessed with the organic layer for hydrogenation, and the amine-containing aqueous solution can be reused for CO_2 capture over successive cycles. Hence, a highly recyclable integrated system was demonstrated over multiple cycles, retaining more than 90% of the initial activity of the components (Figure 6, Part (B)). Such a practical system is a critical step in implementing the proposed processes at industrial scale.

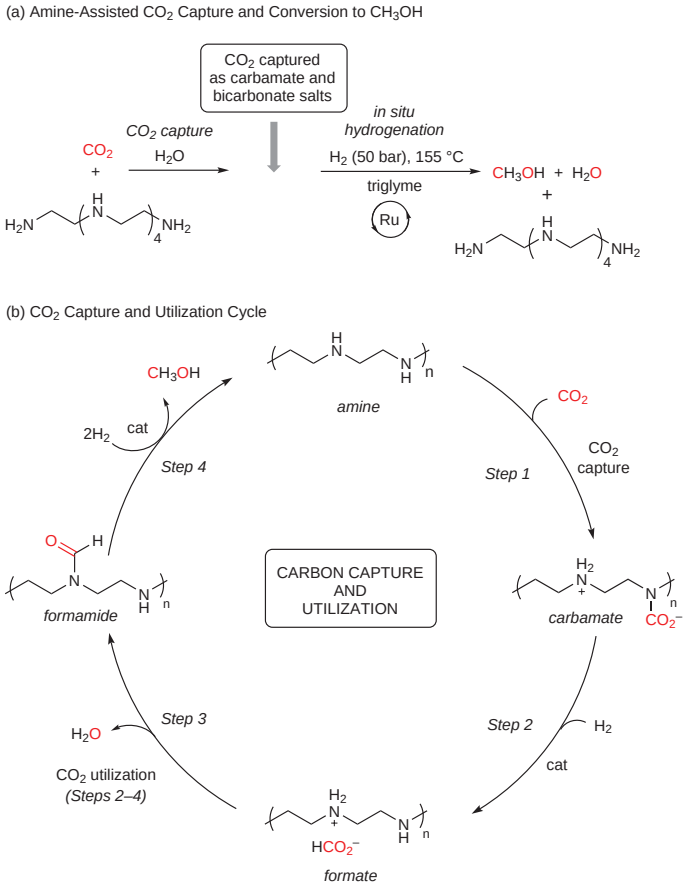

Scheme 4. Olah and Prakash's Amine-Based Integrated System for CO_2 Capture and Recycling to Methanol. *(Ref. 109)*

4.1.3. Solid-Supported Amines

We next explored the immobilization of CO_2-capturing agents, such as amines, onto solid supports (**Figure 7**).[135] It is worth noting in this context that solid-supported amines (SSAs) have been widely explored, by our group and others, for capturing CO_2 from concentrated and diffused sources such as ambient air.[11,136–140] With no solvent required, SSAs provide significant energy and economic benefits as well as high CO_2-capture efficiency. In our studies, various linear and branched polyethyleneimines were either physically impregnated or covalently anchored on nanostructured fumed silica supports. CO_2 was captured directly by the solid adsorbents. For hydrogenation, the CO_2-loaded solid adsorbents were mixed with the catalyst, dissolved in a solvent, and subjected to pressurized H_2 at 140 °C to form methanol. Following hydrogenation, the sorbent could be easily filtered from the mixture, dried, and conveniently reused in consecutive cycles. In the course of these studies, we found that the SSAs with physically bound polyamines suffered from leaching of the amine into the solvent. However, when the amine was chemically bound to silica, leaching was significantly reduced, making them potentially useful for a practical integrated capture and conversion system.

4.1.4. Effect of the Amine Molecular Structure

In CO_2 capture, primary and secondary amines or their mixtures act both as bases and as nucleophiles in reacting with CO_2 to form ammonium carbamates (**Scheme 5**, Part (a)).[134,141,142] In the presence of water, they can also form ammonium

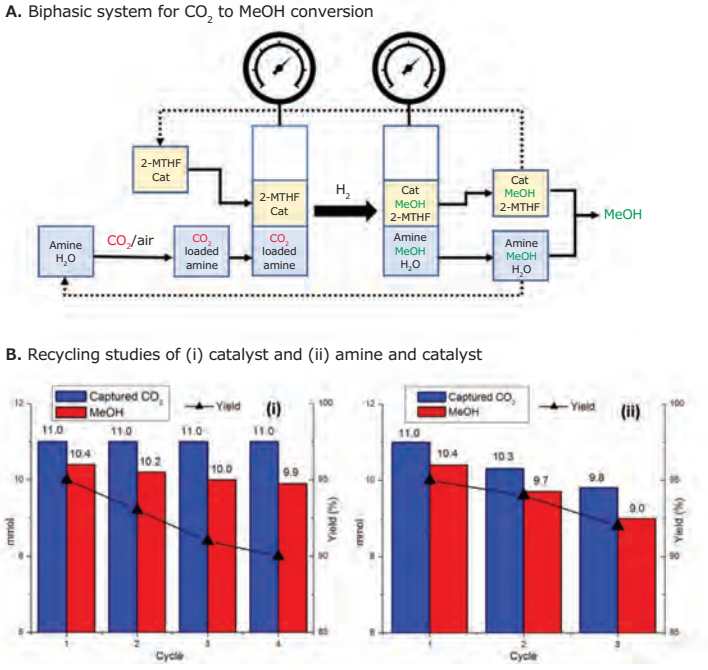

Figure 6. Prakash's Biphasic System for Recycling of Catalyst (Ru-MACHO®-BH) and Amine (Pentaethylenehexamine, PEHA). *(Adapted with permission from reference 134. © 2018, American Chemical Society)*

bicarbonate/carbonate in addition to carbamates. Theoretically, the formation of carbamates requires a CO_2-to-amine ratio of 1:2, whereas bicarbonates require a CO_2:N ratio of only 1:1. In contrast to primary and secondary amines, tertiary amines lack NH protons and, therefore, are unable to react with CO_2 by themselves. However, they can form ammonium bicarbonates/carbonates with CO_2 in the presence of water.[141,142] To this end, the use of amines with high boiling points, low volatility, and high amine content [e.g., polyamines such as PEHA and PEI (polyethyleneimine)] is highly recommended to avoid the loss of active species and the degradation for the quality of the surrounding air by amine emissions.

In the amine-assisted hydrogenation of CO_2 to methanol, amines play multiple key roles (Scheme 5, Part (b)).[107,143,144] First, amines promote dissolution of CO_2 gas, thus increasing its concentration in the solution phase, where the catalysis takes place. Following hydrogenation of CO_2 to formate, amines play a crucial part in detaching the formate from the Ru metal (Scheme 5, Part (c)). This is evident from the fact that CO_2 hydrogenation, even to formate, does not take place in the absence of amine under our reaction conditions. Finally, amines with NH protons form formamide intermediates, which are crucial for further reduction of the formate salt to methanol.

To understand the role of the amine and the effect of variations in its molecular structure on the hydrogenation of CO_2 to CH_3OH, a series of amines was systematically screened for methanol formation (**Scheme 6**).[134,143] In the presence of Ru-MACHO®-BH, the monoamines produced only traces of CH_3OH, with formates and formamides being the major products. In contrast, diamines with either primary or secondary amino groups were significantly active for methanol synthesis. The presence of a secondary amino group enhanced the CH_3OH yield marginally relative to its primary equivalent. Furthermore, polyamines such as diethylenetriamine (DETA) and pentaethylenehexamine (PEHA) performed most efficiently to yield methanol. Interestingly, diamines with even one tertiary amino group were completely inactive for producing methanol. Hence, it can be inferred that amines with 1,2-diamine substructures with exclusively primary or secondary amino groups are the most efficient in the hydrogenation of CO_2 to methanol.

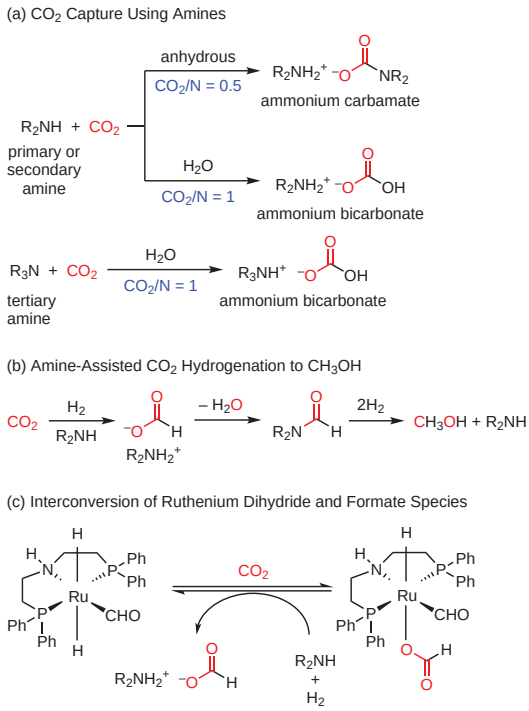

Scheme 5. Role of the Amine in CO_2 Capture and Hydrogenation to CH_3OH. *(Adapted with permission from reference 143. © 2019, American Chemical Society.)*

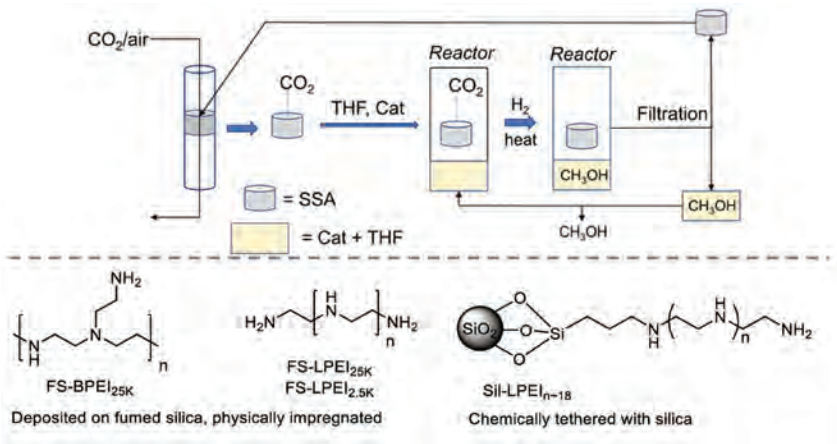

Figure 7. Recycling of Active Elements (in Integrated CO_2 Capture and Utilization) Through Immobilization of Amines onto Solid Supports (cat = Ru-MACHO®-BH; SSA = Solid-Supported Amine; FS = Fumed Silica; BPEI = Branched Polyethyleneimine; LPEI = Linear Polyethyleneimine; Sil = Silica; Subscripts Right after the Polyamine Names Are MW's in Daltons). *(Adapted with permission from reference 135. © 2019, John Wiley and Sons)*

4.1.5. Effect of the Catalyst Molecular Structure

In order to develop a practical process of methanol synthesis from CO_2 using homogeneous catalysis, one of the vital reaction parameters to maximize is turnovers (TONs and TOFs) of the catalyst. For this purpose, understanding the effect of the ligand structure around the metal center is essential. Based on the significant activity observed with Ru-MACHO®-BH in various studies, several variations of the catalyst were screened (**Scheme 7**).[143] It was observed that replacing the CO spectator ligand with NHC did not influence the catalytic activity to any great extent. Surprisingly, when the substituents on phosphorus were changed from Ph to *i*-Pr, Cy, and *t*-Bu, the methanol yields decreased drastically. Yet, all the catalysts were considerably active for the two individual steps separately: CO_2 to formamide and formamide to CH_3OH. While such an observation was contrary to our expectations, we were able to attribute it to the in situ formation of deactivating Ru–biscarbonyl complexes during the reaction (**Figure 8**, Part (A)). These catalytic species were identified and characterized by NMR, IR, and single-crystal X-ray crystallography (Figure 8, Parts (B), (C), and (D)). Furthermore, the biscarbonyl complexes could be converted into the activated dihydride species under H_2 pressure. The rate of this conversion was primarily dependent on the type of substituent on phosphorus. The presence of *i*-Pr, Cy, and *t*-Bu based electron-donating phosphines increases the electron density on the metal center and strengthens the back-bonding between the axial CO and ruthenium. As a result, lability of the axial carbonyl and the rate of conversion to the dihydride species decrease considerably. Understandably, the complexes with phenyl-substituted phosphines enhance the lability of the CO ligand and hence reversibility to the catalytically active dihydride species is observed. Hence, Ru-MACHO® and Ru-MACHO®-BH were the most active homogeneous catalysts for the hydrogenation of CO_2 to CH_3OH (see Scheme 7).

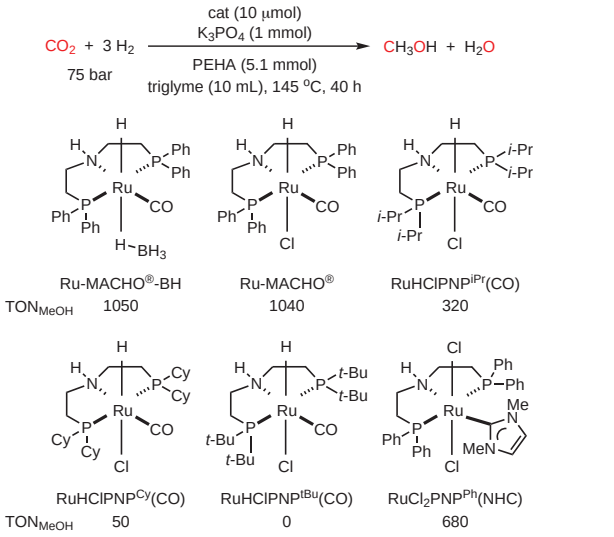

Scheme 7. Effect of Catalyst Structure on the Efficiency of CO_2-to-Methanol Conversion under Homogeneous Catalysis Conditions. *(Ref. 143)*

4.1.6. Catalytic Route

In the proposed overall mechanism for the conversion of carbon dioxide to methanol (**Scheme 8**),[128,143] the reaction sequence proceeds through initial formation of a ruthenium dihydride complex (**3**) by H_2 splitting. This step is followed by insertion of CO_2 to generate a Ru–formate species (**4**). Next, the formate ligand is detached from the metal center by an amine, leading to an ammonium formate salt, which undergoes condensation to a formamide at high temperatures, accompanied by loss of water. The formamide can be hydrogenated with the ruthenium dihydride complex (**3**) to form a hemiaminal and a ruthenium imido complex (**6**). The imido species, in a separate cycle, can then re-form the dihydride species (**3**) by splitting H_2. Concurrently, the hemiaminal dissociates to formaldehyde, and the amine is regenerated for subsequent cycles. Finally, formaldehyde is reduced by the ruthenium dihydride species (**3**) to produce methanol. In parallel, a small amount of formaldehyde can decompose to produce CO and give rise to the ruthenium biscarbonyl complex (**7**) that represents the catalyst resting state.

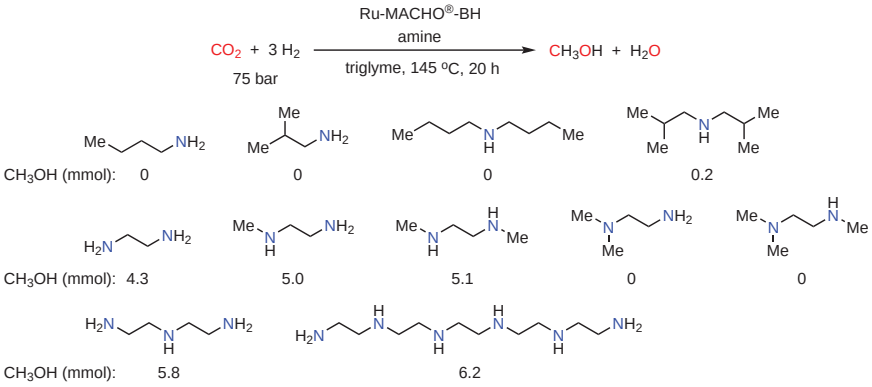

Scheme 6. Effect of the Amine Molecular Structure on the Yield of Methanol. *(Ref. 143)*

4.1.7. Tertiary-Amine-Based Integrated System

As discussed previously, tertiary amines are non-nucleophilic bases that require a protic solvent to be active for CO_2 capture (see Scheme 5, Part (a)). Compared to their secondary and primary amine analogues, tertiary amines have considerably higher boiling points and enhanced stability under oxidative conditions. Very recently, we reported a novel process for combined CO_2 capture and hydrogenation to methanol using tertiary amines in glycol solvent.[145] Once CO_2 is captured as ammonium alkyl carbonates, these species are hydrogenated in situ with Ru-MACHO®-BH as catalyst to efficiently produce methanol and regenerate the tertiary amine and glycol (**Scheme 9**).[145] Furthermore, we demonstrated that the tertiary amine based integrated system was effective in producing

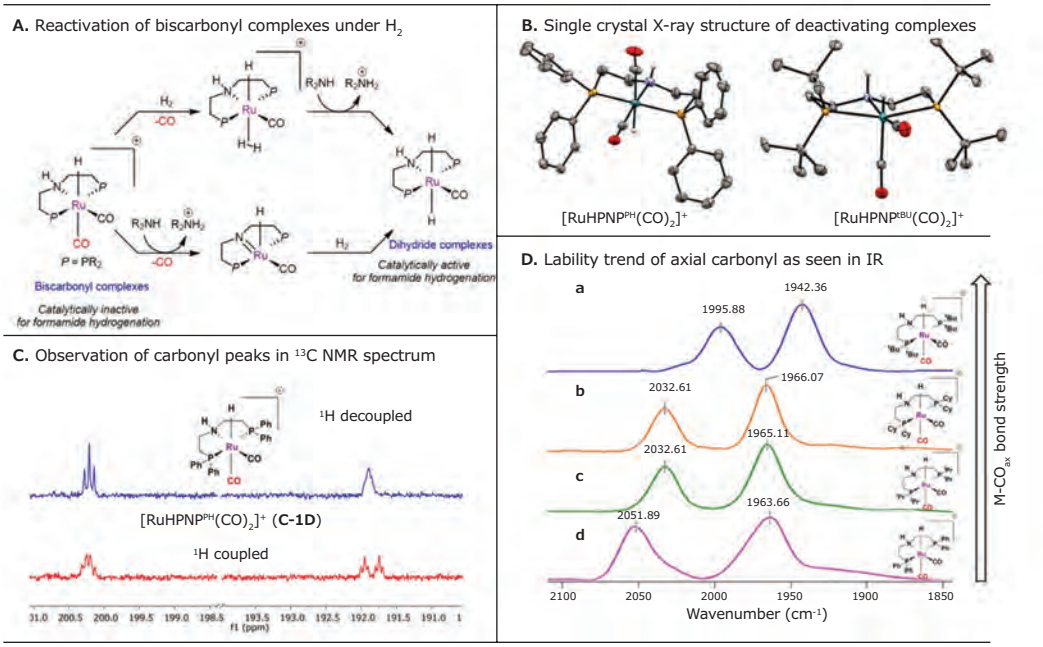

Figure 8. Insights into the Formation of Ruthenium Biscarbonyl Complexes. *(Adapted with permission from reference 143. © 2019, American Chemical Society.)*

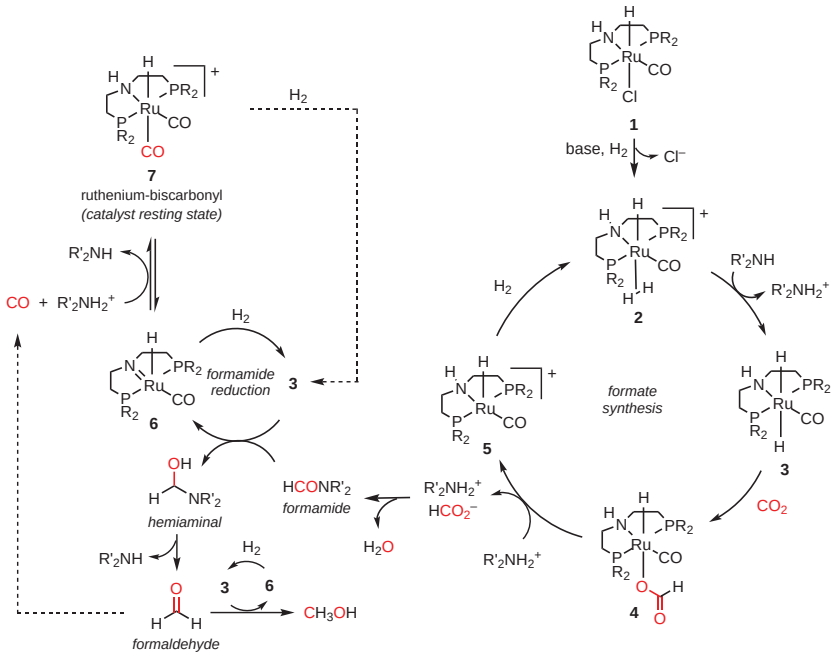

Scheme 8. The Proposed Overall Mechanism for the Conversion of CO_2 to CH_3OH Enabled by Amines. *(Ref. 128,143)*

methanol from a dilute CO_2 stream as encountered in flue gases (10% CO_2 in N_2). Hence, this system has significant potential for use in post-combustion CO_2 capture and utilization.

4.2. CO_2 Capture by Alkali Hydroxides and Conversion to Methanol

4.2.1. Hydroxides for CO_2 Capture

In addition to amines, alkali hydroxides such as NaOH, KOH, and $Ca(OH)_2$ are promising agents for CO_2 capture.[11,141] While amines and amino alcohols are more commonly employed to scrub CO_2 from industrial effluents, hydroxides offer a higher affinity for CO_2 capture from dilute CO_2 sources. Unlike most amines, these bases are stable and have a negligible vapor pressure. Moreover, even amines with high boiling points can suffer from considerable volatility issues and oxidative degradation over the long run.[146] Additionally, alkali hydroxides are relatively inexpensive and readily available through electrolysis of their salts. Pilot plants for direct CO_2 capture from air using hydroxides have already been built and are currently being tested.[147] However, larger scale deployment of hydroxide-based systems face challenges due to the highly energy-intensive and costly regeneration process.[11] Aqueous hydroxide solutions capture CO_2 to form carbonate and bicarbonate salts. Conventionally, the regeneration process of the alkali hydroxide involves multiple steps—causticization, calcination, and slaking—and requires temperatures of 700 °C and above for the calcination step (**Scheme 10**). On the other hand, the advantage of amines is that they can be regenerated at much lower temperatures (50–100 °C).

4.2.2. Hydroxide-Based Integrated System

The bicarbonate and carbonate salts obtained by CO_2 capture with alkali hydroxides in aqueous medium can be hydrogenated effectively to formate salts. This reduction has been thoroughly explored using various noble- and base-metal homogeneous catalysts.[148−155] In 2018, our group disclosed an integrated system where aqueous solutions of various alkali hydroxides were used to capture CO_2 under ambient conditions and the resulting species were hydrogenated in situ to formate salts in a biphasic system.[151] The catalyst was reused over multiple cycles with high TONs (up to 2,788) and TOFs (up to 5,420 h^{-1}) per cycle. However, the alkali formate salts could not be reduced further to methanol under similar conditions. The primary reason for the challenging formate reduction could be attributed to the findings that the formate anion can act as a strong ligand to the metal center (see **4**, Scheme 8).[128] This differs from the amine-based system, where the amine is able to detach the formate ligand from the metal.[143] Here, the formate stays attached to the metal, and is blocked from being reduced further to methanol.

In our efforts to effectively mediate the hydrogenation to methanol, we reported the first and only example to date of an integrated system for converting CO_2 to methanol using hydroxide bases (**Scheme 11**).[156] In this recent study, we surmised that replacing water with alcohols could facilitate the hydrogenation pathway to methanol through the key formate ester intermediate, similarly to the reduction of the formamide intermediates in the amine-assisted route. To validate our hypothesis, we readily achieved the hydrogenation of HCO_2K and $KHCO_3$ to CH_3OH in an alcohol solvent (ethylene glycol) with yields of >90% (Scheme 11, Part (C)). Furthermore, to develop an integrated system, we demonstrated that CO_2 can be efficiently captured by an alkali metal base in a non-aqueous, high-boiling, and highly polar ethylene glycol solvent (Scheme 11, Part (A)). Similarly to bicarbonates, the captured products, namely metal alkyl carbonates, were hydrogenated to CH_3OH in a one-pot system (Scheme 11, Part (B)). The hydroxide-glycol assisted hydrogenation seems to be more facile as compared to the amine-assisted system, with complete conversion within 20 h under similar conditions (140 °C, 70 bar H_2, 0.5 mol % Ru-MACHO®-BH). Surprisingly, the system was significantly active at temperatures as low as 100 °C.

As discussed in Section 4.2.1, regeneration of the hydroxide base is quite challenging and is associated with high energy penalties. However, with our hydroxide-based system, we achieved hydroxide base regeneration for the first time (concurrently with methanol formation) at low temperatures of 100–140 °C (**Scheme 12**).[156] Notably, a fraction of the base was deactivated during the hydrogenation reaction by an unprecedented side reaction, wherein the in situ dehydrogenation of ethylene glycol led to formation of glycolate salts.[157] While this is the only study to date demonstrating hydroxide base regeneration at mild temperatures, there is room for further improvement, particularly in minimizing side reactions and achieving complete hydroxide base regeneration to allow effective recycling.

4.3. Air as a Renewable C1 Source (Direct Air Capture and Its Integration)

At first, capturing carbon dioxide from concentrated sources such as fossil-fuel-burning power plants, industrial plants, and natural sources might be the most practical approach.[10,14,158] However, to be considered renewable and sustainable, the capturing of

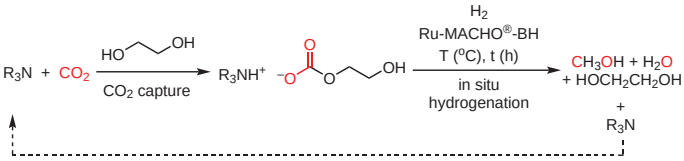

Scheme 9. Tertiary Amine–Ethylene Glycol Based Integrated System for CO_2 Capture and Recycling to Methanol. *(Ref. 145)*

$Na_2CO_3 + Ca(OH)_2$	⟶	$2NaOH + CaCO_3$	causticization
$CaCO_3$	⟶	$CaO + CO_2$	calcination
$CaO + H_2O$	⟶	$Ca(OH)_2$	slaking
$Na_2CO_3 + H_2O$	⟶	$2NaOH + CO_2$	overall

Scheme 10. Conventional Process for Regenerating NaOH from Na_2CO_3.

CO_2 will have to be increasingly from biogenic sources as well as ambient air.[159,160] Despite its relatively low concentration in air (currently ~415 ppm), CO_2 is technically recoverable from that source, and an increasing number of companies are developing so-called Direct Air Capture (DAC) technologies to render this approach economically feasible on a large scale.[11,12,16,147,161,162] DAC systems are, for the most part, based on amines, strong bases such as NaOH and KOH, or quaternary ammonium ions.[16,140,163,164] Compared to point source capture, DAC offers a number of advantages. Air constitutes an almost inexhaustible source of sustainable CO_2 that is available everywhere on earth. The DAC plants can thus operate independently of emission point sources and could be erected at any location. This would allow for the capture of CO_2 from any source—even small and distributed sources such as home and office heating and the transportation sector that would otherwise be difficult to collect from. As it is the case for CO_2 capture from other sources, the regeneration of the sorbents used in DAC to obtain pure CO_2 is very energy intensive. Integration of DAC and CO_2 conversion could thus considerably reduce the energy demand of the overall CCU process.

4.3.1. Conversion of CO_2 from Air to Methanol

In 2016, our group reported for the first time, the synthesis of methanol using air as the carbon source. In an amine-assisted integrated system, simulated air (N_2/O_2 = 80:20, containing ~410 ppm CO_2) was bubbled through an aqueous solution of PEHA at a flow rate of 200 mL/min, leading to the capture of 5.4 mmol of CO_2 after 64 h.[109] The resulting solution was directly treated with H_2 gas in the presence of Ru-MACHO®-BH in triglyme as a co-solvent, achieving a methanol yield of 79%. Later, this process was also demonstrated using a biphasic (2-MTHF/water) solvent system, leading to an 89%

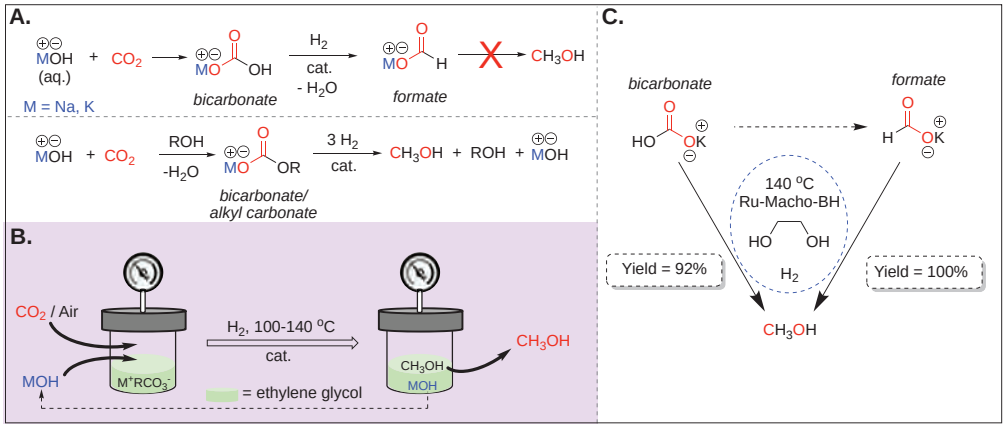

Scheme 11. (A) Alkali Hydroxide Based CO_2 Capture and Hydrogenation. (B) Schematic Representation of a One-Pot Process. (C) Proof of Concept: Hydrogenation of Bicarbonate and Formate Salts to Methanol. *(Ref. 156)*

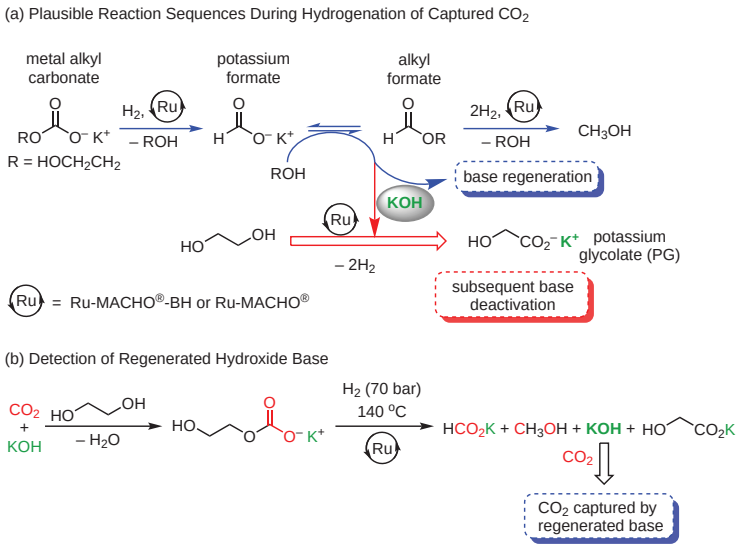

Scheme 12. Plausible Reaction Steps during Hydrogenation of Captured CO_2 and Evidence for the Regeneration of Hydroxide Base. *(Ref. 156)*

yield of methanol.[134] This year, we reported a highly efficient system using alkali hydroxides for direct air capture of CO_2 and its subsequent conversion to methanol.[156] In this case, indoor air was bubbled through a solution of KOH (5 mmol) in ethylene glycol (10 mL). After 48 h, 3.3 mmol of CO_2 had been captured as carbonate/alkyl carbonate salts. The resulting solution was directly hydrogenated with H_2 gas (70 bar) at 140 °C in the presence of Ru-MACHO®-BH, resulting in ~100% conversion to methanol after 72 h. Notably, this hydroxide-based system showed a higher affinity for CO_2 from dilute streams such as air when compared to the amine-based system.

5. Conclusion and Outlook

Mimicking nature's carbon cycle, through efficient recycling of anthropogenic CO_2 directly from the atmosphere to fuels and feedstocks such as methanol, can lead to a carbon-neutral methanol economy.[19,165,166] In the past decade, we have witnessed significant developments in the field of CO_2 hydrogenation to methanol using homogeneous catalysis under relatively mild conditions. Methanol syntheses from various CO_2 derivatives such as carbonates, urea, and carbamates were achieved. Furthermore, direct CO_2 hydrogenation to methanol has been extensively studied, often in the presence of alcohol or amine additives. Additionally, various mechanistic insights have been provided to help understand the catalytic pathways involved in the hydrogenation process. While most of the molecular catalysts employed have been based on ruthenium, such as Ru-MACHO®-BH (TON_{max} = 9,900), a handful of catalysts with first-row metals (Mn, Fe, Co) have also been studied for CO_2 hydrogenation to methanol.[23,167] While these developments are seminal, there is further need to develop efficient and robust catalysts, with high TONs, preferably using non-noble metals, to enable the cost-effective and large-scale deployment of such processes. Moreover, the effective and easy recycling of catalysts, being an important criterion for industrial processes, demands adequate attention from the research community.

In recent years, the integration of CO_2 capture and utilization has been introduced, which can bypass the energy-intensive desorption and compression steps employed in the conventional downstream utilization of the captured CO_2. Such processes allow the capture of CO_2 directly from air as the renewable carbon source and the production of methanol from the captured CO_2. In the first examples, amines were utilized for CO_2 capture from air under ambient conditions, and the capture species were directly hydrogenated to methanol in a tandem process. Importantly, recycling of the active components (amine and catalyst) was demonstrated over multiple cycles. Recently, the first example of an integrated system using alkali hydroxides as capturing agents was also reported. Furthermore, hydroxide base regeneration was observed for the first time at mild temperatures (100–140 °C). While a hydroxide-based system looks promising, it is still in its infancy. Hence, there are huge opportunities to explore the challenging hydrogenation of metal bicarbonate and formate salts to produce methanol while concurrently regenerating the alkali hydroxide efficiently. Additionally, there is a need to develop novel processes that can effectively recycle CO_2 to methanol and other feedstocks, preferably directly from air. In the future, the development of such processes should focus on making them feasible on a large scale in a cost-effective and sustainable way.

6. Acknowledgment

Support of our work by the Loker Hydrocarbon Research Institute, USC, is gratefully acknowledged.

7. References

(1) Perera, F. *Int. J. Environ. Res. Public Health* **2018**, *15*, 16.
(2) Olah, G. A.; Goeppert, A.; Prakash, G. K. S. *Beyond Oil and Gas: The Methanol Economy*, 3rd ed.; Wiley-VCH: Weinheim, Germany, 2018.
(3) Olivier, J. G. J.; Peters, J. A. H. W. *Trends in Global CO_2 and Total Greenhouse Gas Emissions: 2019 Report* (May 26, 2020); PBL Netherlands Environmental Assessment Agency, Publication No 4068: The Hague, The Netherlands, 2020.
(4) CO_2.earth: Are We Stabilizing Yet? ProOxygen Web Site. https://www.co2.earth/ (accessed Oct 27, 2020).
(5) Climate Change 2014: Synthesis Report. Contribution of Working Groups I, II, and III to the Fifth Assessment Report (AR5); The Core Writing Team, Pachauri, R. K., Meyer, L., Eds.; Intergovernmental Panel on Climate Change (IPCC): Geneva, Switzerland, 2014. https://www.ipcc.ch/site/assets/uploads/2018/02/SYR_AR5_FINAL_full.pdf (accessed Oct 27, 2020).
(6) Hansen, J.; Sato, M.; Ruedy, R.; Lo, K.; Lea, D. W.; Medina-Elizade, M. *Proc. Natl. Acad. Sci. U. S. A.* **2006**, *103*, 14288.
(7) Pan, S.; Tian, H.; Dangal, S. R. S.; Yang, Q.; Yang, J.; Lu, C.; Tao, B.; Ren, W.; Ouyang, Z. *Earth's Future* **2015**, *3*, 15.
(8) IPCC, 2014. Summary for Policymakers. In: *Climate Change 2014: Impacts, Adaptation, and Vulnerability. Part A: Global and Sectoral Aspects. Contribution of Working Group II to the Fifth Assessment Report of the Intergovernmental Panel on Climate Change*; Field, C. B., Barros, V. R., Dokken, D. J., Mach, K. J., Mastrandrea, M. D., Bilir, T. E., Chatterjee, M., Ebi, K. L., Estrada, Y. O., Genova, R. C., Girma, B., Kissel, E. S., Levy, A. N., MacCracken, S., Mastrandrea, P. R., White, L. L., Eds.; Cambridge University Press: Cambridge, U.K., and New York, NY, U.S.; pp 1–32.
(9) Krug, J. H. A. *Carbon Balance Manage.* **2018**, *13*, 1.
(10) Wang, Y.; Zhao, L.; Otto, A.; Robinius, M.; Stolten, D. *Energy Procedia* **2017**, *114*, 650.
(11) Goeppert, A.; Czaun, M.; Prakash, G. K. S.; Olah, G. A. *Energy Environ. Sci.* **2012**, *5*, 7833.
(12) Sanz-Pérez, E. S.; Murdock, C. R.; Didas, S. A.; Jones, C. W. *Chem. Rev.* **2016**, *116*, 11840.
(13) Chalmers, H. *Nat. Clim. Change* **2019**, *9*, 348.
(14) Adderley, B.; Carey, J.; Gibbins, J.; Lucquiaud, M.; Smith, R. *Faraday Discuss.* **2016**, *192*, 27.
(15) Bhattacharyya, D.; Miller, D. C. *Curr. Opin. Chem. Eng.* **2017**, *17*, 78.
(16) Keith, D. W.; Holmes, G.; St. Angelo, D.; Heidel, K. *Joule* **2018**, *2*, 1573.
(17) Bui, M.; Adjiman, C. S.; Bardow, A.; Anthony, E. J.; Boston, A.;

Brown, S.; Fennell, P. S.; Fuss, S.; Galindo, A.; Hackett, L. A.; Hallett, J. P.; Herzog, H. J.; Jackson, G.; Kemper, J.; Krevor, S.; Maitland, G. C.; Matuszewski, M.; Metcalfe, I. S.; Petit, C.; Puxty, G.; Reimer, J.; Reiner, D. M.; Rubin, E. S.; Scott, S. A.; Shah, N.; Smit, B.; Trusler, J. P. M.; Webley, P.; Wilcox, J.; Mac Dowell, N. *Energy Environ. Sci.* **2018**, *11*, 1062.

(18) White, C. M.; Strazisar, B. R.; Granite, E. J.; Hoffman, J. S.; Pennline, H. W. *J. Air Waste Manage. Assoc.* **2003**, *53*, 645.

(19) Goeppert, A.; Czaun, M.; Prakash, G. K. S.; Olah, G. A. CO_2 Capture and Recycling to Fuels and Materials: Towards a Sustainable Future. In *An Introduction to Green Chemistry Methods*; Luque, R., Colmenares, J. C., Eds.; Future Science, 2013; pp 132–146.

(20) Jones, W. D. *J. Am. Chem. Soc.* **2020**, *142*, 4955.

(21) Goeppert, A.; Czaun, M.; Jones, J.-P.; Prakash, G. K. S.; Olah, G. A. *Chem. Soc. Rev.* **2014**, *43*, 7995.

(22) Liu, Q.; Wu, L.; Jackstell, R.; Beller, M. *Nat. Commun.* **2015**, *6*, 5933.

(23) Kar, S.; Kothandaraman, J.; Goeppert, A.; Prakash, G. K. S. *J. CO_2 Util.* **2018**, *23*, 212.

(24) Li, Y.-N.; Ma, R.; He, L.-N.; Diao, Z.-F. *Catal. Sci. Technol.* **2014**, *4*, 1498.

(25) Kätelhön, A.; Meys, R.; Deutz, S.; Suh, S.; Bardow, A. *Proc. Natl. Acad. Sci. U. S. A.* **2019**, *116*, 11187.

(26) Beydoun, K.; Klankermayer, J. Recent Advances on CO_2 Utilization as C1 Building Block in C–N and C–O Bond Formation. Synthesis of *N*-Formyl Amines, *N*-Methylamines, and Dialkoxymethanes. In *Organometallics for Green Catalysis*; Dixneuf, P. H., Soulé, J.-F., Eds.; Topics in Organometallic Chemistry Series No. 63; Springer Nature Switzerland: Cham, Switzerland, 2018; pp 39–76.

(27) Stephan, D. W. *Nature* **2013**, *495*, 54.

(28) Liu, W.-C.; Baek, J.; Somorjai, G. A. *Top. Catal.* **2018**, *61*, 530.

(29) *Methanol: The Basic Chemical and Energy Feedstock of the Future—Asinger's Vision Today*; Bertau, M., Offermanns, H., Plass, L., Schmidt, F., Wernicke, H.-J., Eds.; Springer-Verlag: Berlin Heidelberg, Germany, 2014.

(30) Obama, B. *Science* **2017**, *355*, 126.

(31) George Olah Renewable Methanol Plant; First Production of Fuel from CO_2 at Industrial Scale. Carbon Recycling International Web site. https://www.carbonrecycling.is/projects#project-goplant (accessed Oct 28, 2020).

(32) Stöcker, M. Methanol to Olefins (MTO) and Methanol to Gasoline (MTG). In *Zeolites and Catalysis: Synthesis, Reactions and Applications*; Čejka, J., Corma, A., Zones, S., Eds.; Wiley-VCH: Weinheim, Germany, 2010; Volume 1, pp 687–711.

(33) Alberico, E.; Nielsen, M. *Chem. Commun.* **2015**, *51*, 6714.

(34) Owusu, P. A.; Asumadu-Sarkodie, S. *Cogent Eng.* **2016**, *3*, 1167990.

(35) Zhen, X.; Wang, Y. *Renew. Sust. Energ. Rev.* **2015**, *52*, 477.

(36) Kamarudin, S. K.; Achmad, F.; Daud, W. R. W. *Int. J. Hydrogen Energy* **2009**, *34*, 6902.

(37) Li, X.; Faghri, A. *J. Power Sources* **2013**, *226*, 223.

(38) Demirbas, A.; Balubaid, M. A.; Basahel, A. M.; Ahmad, W.; Sheikh, M. H. *Pet. Sci. Technol.* **2015**, *33*, 1190.

(39) Lee, H.; Jung, I.; Roh, G.; Na, Y.; Kang, H. *Energies* **2020**, *13*, 224.

(40) Sun, Z.; Sun, Z. *J. Cent. South Univ.* **2020**, *27*, 1074.

(41) Avgouropoulos, G.; Paxinou, A.; Neophytides, S. *Int. J. Hydrogen Energy* **2014**, *39*, 18103.

(42) Kothandaraman, J.; Kar, S.; Goeppert, A.; Sen, R.; Prakash, G. K. S. *Top. Catal.* **2018**, *61*, 542.

(43) Palo, D. R.; Dagle, R. A.; Holladay, J. D. *Chem. Rev.* **2007**, *107*, 3992.

(44) Crabtree, R. H. *Chem. Rev.* **2017**, *117*, 9228.

(45) Nielsen, M. Hydrogen Production by Homogeneous Catalysis: Alcohol Acceptorless Dehydrogenation. In *Hydrogen Production and Remediation of Carbon and Pollutants*; Lichtfouse, E., Schwarzbauer, J., Robert, D., Eds.; Environmental Chemistry for a Sustainable World Series; Springer International Publishing: Switzerland, 2015; Series Volume 6, pp 1–60.

(46) Hu, P.; Diskin-Posner, Y.; Ben-David, Y.; Milstein, D. *ACS Catal.* **2014**, *4*, 2649.

(47) Nielsen, M.; Alberico, E.; Baumann, W.; Drexler, H.-J.; Junge, H.; Gladiali, S.; Beller, M. *Nature* **2013**, *495*, 85.

(48) Rodríguez-Lugo, R. E.; Trincado, M.; Vogt, M.; Tewes, F.; Santiso-Quinones, G.; Grützmacher, H. *Nat. Chem.* **2013**, *5*, 342.

(49) Bielinski, E. A.; Förster, M.; Zhang, Y.; Bernskötter, W. H.; Hazari, N.; Holthausen, M. C. *ACS Catal.* **2015**, *5*, 2404.

(50) Andérez-Fernández, M.; Vogt, L. K.; Fischer, S.; Zhou, W.; Jiao, H.; Garbe, M.; Elangovan, S.; Junge, K.; Junge, H.; Ludwig, R.; Beller, M. *Angew. Chem., Int. Ed.* **2017**, *56*, 559.

(51) Campos, J.; Sharninghausen, L. S.; Manas, M. G.; Crabtree, R. H. *Inorg. Chem.* **2015**, *54*, 5079.

(52) Fujita, K.; Kawahara, R.; Aikawa, T.; Yamaguchi, R. *Angew. Chem., Int. Ed.* **2015**, *54*, 9057.

(53) Shen, Y.; Zhan, Y.; Li, S.; Ning, F.; Du, Y.; Huang, Y.; He, T.; Zhou, X. *Chem. Sci.* **2017**, *8*, 7498.

(54) Kothandaraman, J.; Kar, S.; Sen, R.; Goeppert, A.; Olah, G. A.; Prakash, G. K. S. *J. Am. Chem. Soc.* **2017**, *139*, 2549.

(55) Preuster, P.; Papp, C.; Wasserscheid, P. *Acc. Chem. Res.* **2017**, *50*, 74.

(56) Shao, Z.; Li, Y.; Liu, C.; Ai, W.; Luo, S.-P.; Liu, Q. *Nat. Commun.* **2020**, *11*, 591.

(57) Agapova, A.; Junge, H.; Beller, M. *Chem.—Eur. J.* **2019**, *25*, 9345.

(58) Xie, Y.; Hu, P.; Ben-David, Y.; Milstein, D. *Angew. Chem., Int. Ed.* **2019**, *58*, 5105.

(59) Roode-Gutzmer, Q. I.; Kaiser, D.; Bertau, M. *ChemBioEng Rev.* **2019**, *6*, 209.

(60) Olah, G. A.; Goeppert, A.; Prakash, G. K. S. *J. Org. Chem.* **2009**, *74*, 487.

(61) Chen, Y.-Z.; Liaw, B.-J.; Chen, B.-J. *Appl. Catal., A* **2002**, *236*, 121.

(62) Li, K.; Jiang, D. *J. Mol. Catal. A: Chem.* **1999**, *147*, 125.

(63) Dombek, B. D. *J. Am. Chem. Soc.* **1980**, *102*, 6855.

(64) Bradley, J. S. *J. Am. Chem. Soc.* **1979**, *101*, 7419.

(65) Somorjai, G. A. *Catal. Rev. Sci. Eng.* **2006**, *23*, 189.

(66) Li, B.; Jens, K.-J. *Ind. Eng. Chem. Res.* **2014**, *53*, 1735.

(67) Li, B.; Jens, K. J. *Top. Catal.* **2013**, *56*, 725.

(68) Mahajan, D. *Top. Catal.* **2005**, *32*, 209.

(69) Kar, S.; Goeppert, A.; Prakash, G. K. S. *J. Am. Chem. Soc.*

2019, *141*, 12518.
(70) Ryabchuk, P.; Stier, K.; Junge, K.; Checinski, M. P.; Beller, M. *J. Am. Chem. Soc.* **2019**, *141*, 16923.
(71) Yang, Y.; Mims, C. A.; Mei, D. H.; Peden, C. H. F.; Campbell, C. T. *J. Catal.* **2013**, *298*, 10.
(72) Fujita, S.; Usui, M.; Ito, H.; Takezawa, N. *J. Catal.* **1995**, *157*, 403.
(73) Grabow, L. C.; Mavrikakis, M. *ACS Catal.* **2011**, *1*, 365.
(74) Dang, S.; Yang, H.; Gao, P.; Wang, H.; Li, X.; Wei, W.; Sun, Y. *Catal. Today* **2019**, *330*, 61.
(75) Behrens, M.; Studt, F.; Kasatkin, I.; Kühl, S.; Hävecker, M.; Abild-Pedersen, F.; Zander, S.; Girgsdies, F.; Kurr, P.; Kniep, B.-L.; Tovar, M.; Fischer, R. W.; Nørskov, J. K.; Schlögl, R. *Science* **2012**, *336*, 893.
(76) Behrens, M. *Angew. Chem., Int. Ed.* **2014**, *53*, 12022.
(77) Tang, Q.; Shen, Z.; Huang, L.; He, T.; Adidharma, H.; Russell, A. G.; Fan, M. *Phys. Chem. Chem. Phys.* **2017**, *19*, 18539.
(78) Nguyen, H. K. D.; Dang, T. H.; Nguyen, N. L. T.; Nguyen, H. T.; Dinh, N. T. *Can. J. Chem. Eng.* **2018**, *96*, 832.
(79) Studt, F.; Sharafutdinov, I.; Abild-Pedersen, F.; Elkjær, C. F.; Hummelshøj, J. S.; Dahl, S.; Chorkendorff, I.; Nørskov, J. K. *Nat. Chem.* **2014**, *6*, 320.
(80) Martin, O.; Martín, A. J.; Mondelli, C.; Mitchell, S.; Segawa, T. F.; Hauert, R.; Drouilly, C.; Curulla-Ferré, D.; Pérez-Ramírez, J. *Angew. Chem., Int. Ed.* **2016**, *55*, 6261.
(81) Xie, S.; Zhang, W.; Jia, C.; Ong, S. S. G.; Zhang, C.; Zhang, S.; Lin, H. *J. Catal.* **2020**, *389*, 247.
(82) Kothandaraman, J.; Heldebrant, D. J. *Green Chem.* **2020**, *22*, 828.
(83) Kothandaraman, J.; Dagle, R. A.; Dagle, V. L.; Davidson, S. D.; Walter, E. D.; Burton, S. D.; Hoyt, D. W.; Heldebrant, D. J. *Catal. Sci. Technol.* **2018**, *8*, 5098.
(84) Hertrich, M. F.; Beller, M. Metal-Catalysed Hydrogenation of CO_2 into Methanol. In *Organometallics for Green Catalysis*; Dixneuf, P. H.; Soulé, J.-F., Eds.; Topics in Organometallic Chemistry Series No. 63; Springer Nature Switzerland: Cham, Switzerland, 2018; pp 1–16.
(85) Tominaga, K.; Sasaki, Y.; Watanabe, T.; Saito, M. *Bull. Chem. Soc. Jpn.* **1995**, *68*, 2837.
(86) Tominaga, K; Sasaki, Y.; Kawai, M.; Watanabe, T.; Saito, M. *J. Chem. Soc.* **1993**, 629.
(87) Balaraman, E.; Gunanathan, C.; Zhang, J.; Shimon, L. J. W.; Milstein, D. *Nat. Chem.* **2011**, *3*, 609.
(88) Gunanathan, C.; Milstein, D. *Chem. Rev.* **2014**, *114*, 12024.
(89) Piccirilli, L.; Lobo Justo Pinheiro, D.; Nielsen, M. *Catalysts* **2020**, *10*, 773.
(90) Balaraman, E.; Ben-David, Y.; Milstein, D. *Angew. Chem., Int. Ed.* **2011**, *50*, 11702.
(91) Han, Z.; Rong, L.; Wu, J.; Zhang, L.; Wang, Z.; Ding, K. *Angew. Chem., Int. Ed.* **2012**, *51*, 13041.
(92) Kaithal, A.; Hölscher, M.; Leitner, W. *Angew. Chem., Int. Ed.* **2018**, *57*, 13449.
(93) Zubar, V.; Lebedev, Y.; Azofra, L. M.; Cavallo, L.; El-Sepelgy, O.; Rueping, M. *Angew. Chem., Int. Ed.* **2018**, *57*, 13439.
(94) Kumar, A.; Janes, T.; Espinosa-Jalapa, N. A.; Milstein, D. *Angew. Chem., Int. Ed.* **2018**, *57*, 12076.
(95) Das, U. K.; Kumar, A.; Ben-David, Y.; Iron, M. A.; Milstein, D. *J. Am. Chem. Soc.* **2019**, *141*, 12962.
(96) Ferretti, F.; Scharnagl, F. K.; Dall'Anese, A.; Jackstell, R.; Dastgir, S.; Beller, M. *Catal. Sci. Technol.* **2019**, *9*, 3548.
(97) Huff, C. A.; Sanford, M. S. *J. Am. Chem. Soc.* **2011**, *133*, 18122.
(98) Chu, W.-Y.; Culakova, Z.; Wang, B. T.; Goldberg, K. I. *ACS Catal.* **2019**, *9*, 9317.
(99) Rayder, T. M.; Adillon, E. H.; Byers, J. A.; Tsung, C.-K. *Chem* **2020**, *6*, 1742.
(100) Wesselbaum, S.; vom Stein, T.; Klankermayer, J.; Leitner, W. *Angew. Chem., Int. Ed.* **2012**, *51*, 7499.
(101) Wesselbaum, S.; Moha, V.; Meuresch, M.; Brosinski, S.; Thenert, K. M.; Kothe, J.; vom Stein, T.; Englert, U.; Hölscher, M.; Klankermayer, J.; Leitner, W. *Chem. Sci.* **2015**, *6*, 693.
(102) Schieweck, B. G.; Jürling-Will, P.; Klankermayer, J. *ACS Catal.* **2020**, *10*, 3890.
(103) Scharnagl, F. K.; Hertrich, M. F.; Neitzel, G.; Jackstell, R.; Beller, M. *Adv. Synth. Catal.* **2019**, *361*, 374.
(104) Schneidewind, J.; Adam, R.; Baumann, W.; Jackstell, R.; Beller, M. *Angew. Chem., Int. Ed.* **2017**, *56*, 1890.
(105) Sordakis, K.; Tsurusaki, A.; Iguchi, M.; Kawanami, H.; Himeda, Y.; Laurenczy, G. *Chem.—Eur. J.* **2016**, *22*, 15605.
(106) Wang, T.; Hovland, J.; Jens, K. J. *J. Environ. Sci.* **2015**, *27*, 276.
(107) Rezayee, N. M.; Huff, C. A.; Sanford, M. S. *J. Am. Chem. Soc.* **2015**, *137*, 1028.
(108) Zhang, L.; Han, Z.; Zhao, X.; Wang, Z.; Ding, K. *Angew. Chem., Int. Ed.* **2015**, *54*, 6186.
(109) Kothandaraman, J.; Goeppert, A.; Czaun, M.; Olah, G. A.; Prakash, G. K. S. *J. Am. Chem. Soc.* **2016**, *138*, 778.
(110) Everett, M.; Wass, D. F. *Chem. Commun.* **2017**, *53*, 9502.
(111) Yoshimura, A.; Watari, R.; Kuwata, S.; Kayaki, Y. *Eur. J. Inorg. Chem.* **2019**, 2375.
(112) Kar, S.; Goeppert, A.; Kothandaraman, J.; Prakash, G. K. S. *ACS Catal.* **2017**, *7*, 6347.
(113) Lane, E. M.; Zhang, Y.; Hazari, N.; Bernskötter, W. H. *Organometallics* **2019**, *38*, 3084.
(114) Ribeiro, A. P. C.; Martins, L. M. D. R. S.; Pombeiro, A. J. L. *Green Chem.* **2017**, *19*, 4811.
(115) Courtemanche, M.-A.; Légaré, M.-A.; Maron, L.; Fontaine, F.-G. *J. Am. Chem. Soc.* **2013**, *135*, 9326.
(116) Riduan, S. N.; Zhang, Y.; Ying, J. Y. *Angew. Chem., Int. Ed.* **2009**, *48*, 3322.
(117) Barton, E. E.; Rampulla, D. M.; Bocarsly, A. B. *J. Am. Chem. Soc.* **2008**, *130*, 6342.
(118) Wu, J.; Huang, Y.; Ye, W.; Li, Y. *Adv. Sci.* **2017**, *4*, 1700194.
(119) Kuwabata, S.; Nishida, K.; Tsuda, R.; Inoue, H.; Yoneyama, H. *J. Electrochem. Soc.* **1994**, *141*, 1498.
(120) Boston, D. J.; Xu, C.; Armstrong, D. W.; MacDonnell, F. M. *J. Am. Chem. Soc.* **2013**, *135*, 16252.
(121) Amao, Y.; Watanabe, T. *Chem. Lett.* **2004**, *33*, 1544.
(122) El-Zahab, B.; Donnelly, D.; Wang, P. *Biotechnol. Bioeng.* **2008**, *99*, 508.
(123) Obert, R.; Dave, B. C. *J. Am. Chem. Soc.* **1999**, *121*, 12192.
(124) Dibenedetto, A.; Stufano, P.; Macyk, W.; Baran, T.; Fragale, C.;

Costa, M.; Aresta, M. *ChemSusChem* **2012**, *5*, 373.
(125) Giesbrecht, P. K.; Herbert, D. E. *ACS Energy Lett.* **2017**, *2*, 549.
(126) Kobayashi, T.; Takahashi, H. *Energy Fuels* **2004**, *18*, 285.
(127) Ohya, S.; Kaneco, S.; Katsumata, H.; Suzuki, T.; Ohta, K. *Catal. Today* **2009**, *148*, 329.
(128) Kar, S.; Goeppert, A.; Prakash, G. K. S. *Acc. Chem. Res.* **2019**, *52*, 2892.
(129) Leclaire, J.; Heldebrant, D. J. *Green Chem.* **2018**, *20*, 5058.
(130) Olah, G. A.; Prakash, G. K. S.; Goeppert, A. *J. Am. Chem. Soc.* **2011**, *133*, 12881.
(131) Lao, D. B.; Galan, B. R.; Linehan, J. C.; Heldebrant, D. J. *Green Chem.* **2016**, *18*, 4871.
(132) Koelbl, B. S.; van den Broek, M.; van Ruijven, B.; van Vuuren, D. P.; Faaij, A. P. C. *Energy Procedia* **2013**, *37*, 7537.
(133) Khusnutdinova, J. R.; Garg, J. A.; Milstein, D. *ACS Catal.* **2015**, *5*, 2416.
(134) Kar, S.; Sen, R.; Goeppert, A.; Prakash, G. K. S. *J. Am. Chem. Soc.* **2018**, *140*, 1580.
(135) Kar, S.; Goeppert, A.; Prakash, G. K. S. *ChemSusChem* **2019**, *12*, 3172.
(136) Goeppert, A.; Zhang, H.; Sen, R.; Dang, H.; Prakash, G. K. S. *ChemSusChem* **2019**, *12*, 1712.
(137) Goeppert, A.; Meth, S.; Prakash, G. K. S.; Olah, G. A. *Energy Environ. Sci.* **2010**, *3*, 1949.
(138) Zhang, H.; Goeppert, A.; Prakash, G. K. S.; Olah, G. *RSC Adv.* **2015**, *5*, 52550.
(139) Goeppert, A.; Zhang, H.; Czaun, M.; May, R. B.; Prakash, G. K. S.; Olah, G. A.; Narayanan, S. R. *ChemSusChem* **2014**, *7*, 1386.
(140) Goeppert, A.; Czaun, M.; May, R. B.; Prakash, G. K. S.; Olah, G. A.; Narayanan, S. R. *J. Am. Chem. Soc.* **2011**, *133*, 20164.
(141) Heldebrant, D. J.; Kothandaraman, J. Solvent-based Absorption. In *Carbon Capture and Storage*; Bui, M., Mac Dowell, N., Eds.; Energy and Environment Series No. 26; The Royal Society of Chemistry, 2020; Chapter 3, pp 36–68.
(142) Kothandaraman, J.; Goeppert, A.; Czaun, M.; Olah, G. A.; Prakash, G. K. S. *Green Chem.* **2016**, *18*, 5831.
(143) Kar, S.; Sen, R.; Kothandaraman, J.; Goeppert, A.; Chowdhury, R.; Munoz, S. B.; Haiges, R.; Prakash, G. K. S. *J. Am. Chem. Soc.* **2019**, *141*, 3160.
(144) Cabrero-Antonino, J. R.; Adam, R.; Papa, V.; Beller, M. *Nat. Commun.* **2020**, *11*, 3893.
(145) Sen, R.; Koch, C. J.; Goeppert, A.; Prakash, G. S. *ChemSusChem* **2020**, Accepted Author Manuscript, DOI: 10.1002/cssc.202002285.
(146) Jahandar Lashaki, M.; Khiavi, S.; Sayari, A. *Chem. Soc. Rev.* **2019**, *48*, 3320.
(147) We Believe Humanity Can Solve Climate Change. Carbon Engineering Ltd Web site. https://carbonengineering.com (accessed Oct 30, 2020).
(148) Bertini, F.; Mellone, I.; Ienco, A.; Peruzzini, M.; Gonsalvi, L. *ACS Catal.* **2015**, *5*, 1254.
(149) Coufourier, S.; Gaillard, S.; Clet, G.; Serre, C.; Daturi, M.; Renaud, J.-L. *Chem. Commun.* **2019**, *55*, 4977.
(150) Dai, Z.; Luo, Q.; Cong, H.; Zhang, J.; Peng, T. *New J. Chem.* **2017**, *41*, 3055.
(151) Kar, S.; Goeppert, A.; Galvan, V.; Chowdhury, R.; Olah, J.; Prakash, G. K. S. *J. Am. Chem. Soc.* **2018**, *140*, 16873.
(152) Kothandaraman, J.; Czaun, M.; Goeppert, A.; Haiges, R.; Jones, J.-P.; May, R. B.; Prakash, G. K. S.; Olah, G. A. *ChemSusChem* **2015**, *8*, 1442.
(153) Marcos, R.; Xue, L. Q.; Sánchez-de-Armas, R.; Ahlquist, M. S. G. *ACS Catal.* **2016**, *6*, 2923.
(154) Zhu, F.; Zhu-Ge, L.; Yang, G.; Zhou, S. *ChemSusChem* **2015**, *8*, 609.
(155) Ziebart, C.; Federsel, C.; Anbarasan, P.; Jackstell, R.; Baumann, W.; Spannenberg, A.; Beller, M. *J. Am. Chem. Soc.* **2012**, *134*, 20701.
(156) Sen, R.; Goeppert, A.; Kar, S.; Prakash, G. K. S. *J. Am. Chem. Soc.* **2020**, *142*, 4544.
(157) Kar, S.; Goeppert, A.; Sen, R.; Kothandaraman, J.; Prakash, G. K. S. *Green Chem.* **2018**, *20*, 2706.
(158) Bhown, A. S.; Freeman, B. C. *Environ. Sci. Technol.* **2011**, *45*, 8624.
(159) Keith, D. W. *Science* **2009**, *325*, 1654.
(160) Lackner, K. S. *Eur. Phys. J. Spec. Top.* **2009**, *176*, 93.
(161) Let's Reverse Climate Change. Climeworks Web site. http://www.climeworks.com/ (accessed Oct 30, 2020).
(162) Global Thermostat Adds New Support for Its Carbon Removal Technology. Global Thermostat Web site. http://www.globalthermostat.com/ (accessed Oct 30, 2020).
(163) Stolaroff, J. K.; Keith, D. W.; Lowry, G. V. *Environ. Sci. Technol.* **2008**, *42*, 2728.
(164) Wang, T.; Lackner, K. S.; Wright, A. *Environ. Sci. Technol.* **2011**, *45*, 6670.
(165) Goeppert, A.; Olah, G. A.; Prakash, G. K. S. Toward a Sustainable Carbon Cycle: The Methanol Economy. In *Green Chemistry*; Török, B., Dransfield, T., Eds.; Elsevier, 2018; Chapter 3.26, pp 919–962.
(166) Olah, G. A. *Angew. Chem., Int. Ed.* **2005**, *44*, 2636.
(167) Bernskötter, W. H.; Hazari, N. *Acc. Chem. Res.* **2017**, *50*, 1049.

About the Authors

Raktim Sen received his B.Sc. degree (Honors) in 2015 from St. Stephen's College, University of Delhi, and his M.Sc. degree in 2017 from the Indian Institute of Technology (IIT) Delhi. He was an S. N. Bose Fellow in the summer of 2016 with Prof. G. K. Surya Prakash at the University of Southern California (USC). In 2017, he joined USC as a Ph.D. student in the group of Prof. Prakash. His research focuses on novel techniques for direct air capture of CO_2, integrated CO_2 capture and utilization, and liquid hydrogen carrier systems.

Alain Goeppert obtained his Ph.D. degree in 2002 from the University of Strasbourg. He is currently a Research Scientist in the Prakash group at the Loker Hydrocarbon Research Institute, USC. His research focuses on methane and CO_2 activation and catalytic transformation to value-added products, including methanol, methyl formate, formic acid, and dimethyl ether. He

is also involved in research on the catalytic decomposition of formic acid to hydrogen and CO_2 as well as the development of regenerative sorbents for CO_2 separation and capture from various sources, including air. He is a coauthor, with G. A. Olah and G. K. S. Prakash, of the book *Beyond Oil and Gas: The Methanol Economy*.

G. K. Surya Prakash received his B.Sc. degree (Honors) in 1972 from Bangalore University, his M.Sc. degree in 1974 from IIT Madras, and his Ph.D. degree in 1978 from USC. He joined the USC faculty in 1981 and is currently a Professor in the Department of Chemistry and Director of the Loker Hydrocarbon Research Institute, holding the Olah Nobel Laureate Chair in Hydrocarbon Chemistry. He is also the chair of the USC Chemistry Department. His research interests include fluorination and synthetic methods, mechanistic studies, superacid chemistry, electrochemistry, and the methanol economy. He is a prolific author, with 815 publications, 110 issued patents, and 14 books, and has received three ACS national awards. He is a co-proponent of the methanol economy concept with the late Prof. Olah, for which he shared with Prof. Olah the 2013 Eric and Sheila Samson Prime Minister's Prize for Alternative Fuels for Transportation from the State of Israel.

Designing Renewable, High-Performance Solvents with Improved Toxicity Profiles


Dr. J. Sherwood


Dr. H. E. Buist


Dr. B. v. d. Burg


Dr. F. P. Byrne


Dr. J. E. Camp


Dr. T. J. Farmer


Dr. E. D. Kroese


Ms. M. Y. Meima

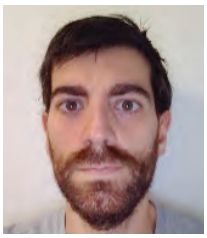
Dr. D. Méndez Sevillano


Dr. A. Puente


Dr. B. M. A. v. Vugt-Lussenburg


Prof. J. H. Clark

James Sherwood,[a] Harrie E. Buist,[b] Bart van der Burg,[c] Fergal P. Byrne,[a] Jason E. Camp,[d] Thomas J. Farmer,[a] E. Dinant Kroese,[b] Marie Y. Meima,[b] David Méndez Sevillano,[e] Ángel Puente,[f] Barbara M. A. van Vugt-Lussenburg,[c] and James H. Clark*[,a]

[a] Green Chemistry Centre of Excellence
Department of Chemistry
The University of York
Heslington, York YO10 5DD, U.K.
[b] TNO
Princetonlaan 6
3584 CB Utrecht, The Netherlands
[c] BioDetection Systems BV
Science Park 406
1098XH Amsterdam, The Netherlands
[d] Circa Sustainable Chemicals Ltd
1 Hassacarr Close
Dunnington, York YO19 5SN, U.K.
[e] Process Design Center BV
Catharinastraat 21F
4811 XD Breda, The Netherlands
[f] nova-Institut GmbH
50354 Hürth, Germany
Email: james.clark@york.ac.uk

Keywords. bioassay; bio-based; Cyrene™; extraction; synthesis; polarity; polymerization; solvent; tetramethyloxolane.

Abstract. The ReSolve project brought together expertise from chemistry, engineering, toxicology, techno-economics, and life cycle assessment in order to develop safer, bio-based solvents. This article summarizes findings from the project including the further development of Cyrene™ and 2,2,5,5-tetramethyloxolane (TMO) as replacements for *N*-methylpyrrolidone (NMP) and toluene, respectively.

Outline

1. Introduction

Solvents are ubiquitous in synthetic chemistry and are used to dissolve reactants, stabilize activated complexes, and modify equilibria, among others.[1] In the European Union (EU), approximately 5 million metric tonnes of solvents are utilized annually, with paints and coatings being the largest industrial sector where they are used.[2] Most organic solvents are derived from petrochemicals and, therefore, their production is directly linked to the consumption of finite resources and climate change. It is also important to minimize the risks solvents pose to human health and the environment. Toluene and *N*-methylpyrrolidone

(NMP) typify the challenges of contemporary solvent use. Toluene is a commodity solvent with a wide variety of uses. While NMP is a speciality solvent, it is still utilized in high tonnage to produce wire coatings and agrochemical formulations and for petrochemical separations. Both solvents have further applications in organic synthesis. However, EU regulations have set conditions on the use of toluene and NMP due to their chronic toxicity hazards (**Table 1**).[3]

The utility of toluene and NMP justify their substitution with safer alternatives. Recent work is addressing the issues created by traditional solvents by introducing new alternatives designed for lower hazards and lower environmental impact. Dihydrolevoglucosenone (also known as Cyrene™) and 2,2,5,5-tetramethyloxolane (TMO) are two examples. Cyrene™ is an alternative to NMP,[4] prepared by the hydrogenation of levoglucosenone, and TMO is an ether designed as a replacement for toluene.[5] A relatively recent minireview of the preparation and applications of Cyrene™ has been published.[6]

This article charts the development of replacements for toluene and NMP that was recently undertaken by the ReSolve project consortium (http://resolve-bbi.eu/). The principle that chemically dissimilar compounds are preferable as substitute solvents was adopted, because structural similarities can be linked to the same hazards. Often compounds with multiple functional groups, such as Cyrene™, are desirable in order to approximate the intermolecular interactions of functional groups to be avoided (e.g., *N*-methylamides) or with steric hindrance that is introduced to mask the influence of new functionality (as is true of the di-tertiary ether TMO). Following this principle, it is unlikely that a single substitute solvent will be found that incorporates all the desirable properties of the solvent it is replacing. Therefore, a diverse portfolio of greener alternative solvents is developing as research continues. In particular, bio-based solvents offer new functionality distinct from those derived from petrochemicals,[7] and these solvents are recognized as key contributors to the bio-based economy.[8]

The alternative solvents studied by ReSolve are obtainable from cellulosic agricultural and forestry residues. This bridges different sectors of the bio-based economy to yield solvents with an appropriate cost, while also aligning with the goals of the circular economy whereby waste is a resource.[9] The emerging bio-based industry is already producing—either intentionally or as a byproduct of lignocellulosic biorefineries—a number of "new" platform chemicals that ReSolve drew upon as intermediates.

The production of some bio-based solvents has been claimed to release less greenhouse gas emissions compared to fossil equivalents.[10] However, it cannot be assumed, simply because a solvent is bio-derived, that it is automatically green or sustainable. It was thus a priority of the ReSolve project to design novel solvents, not only by considering their toxicity and functionality, but also by their production in an industrial setting, their market competitiveness, and their environmental impact. In this respect, the choice of novel solvent candidates was supported by early-stage process designs, techno-economic, and environmental evaluations in order to guide the process development in a sustainable and integrated manner.

Table 1. Comparing Toluene and *N*-Methylpyrrolidone (NMP).

Category	Toluene	NMP
Price and Source	Historically \$0.6–1.2/kg,[a] directly dependent on the price of crude oil[b]	Decreased from \$3.2/kg,[c] to current values of \$2.0–2.3/kg,[d] due to the falling price of its precursor 1,4-butanediol[e]
EU Demand	>500,000 tonnes per year[f]	>10,000 tonnes per year[g]
Chronic Toxicity Hazards and Response in Regulation	Suspected of damaging the unborn child; may cause damage to organs through prolonged or repeated exposure; restricted to <0.1% in adhesives and spray paints intended for the public[h]	May damage the unborn child; its presence in products and in manufacturing is restricted to <0.3% unless exposure is below 14.4 mg/m^3 (by inhalation) and 4.8 mg/kg/day (dermal)[i]
Environmental Impacts	Harmful to aquatic life, with long-lasting effects	Environmental hazards insufficient for labelling

(a) U.S. Grains Council. Ethanol Market and Pricing Data – September 10, 2019. https://grains.org/ethanol_report/ethanol-market-and-pricing-data-september-10-2019/ (accessed 22nd June 2020). (b) Straathof, A. J. J.; Bampouli, A. *Biofuels, Bioprod. Biorefin*. **2017**, *11*, 798. (c) AMEC Environment & Infrastructure UK Limited. Annex XV Restriction Report – Proposal for a Restriction, Version 2.0. August 9, 2013. https://echa.europa.eu/documents/10162/13641/nmp_annex_xv_report_en.pdf (accessed 22nd June 2020). (d) ZAUBA Technologies Pvt Ltd. Appendix A, Section 2.2, page 18, 2018. www.zauba.com (accessed 22nd June 2020). (e) Everchem Specialty Chemicals. Butanediol Price Hike Announcement. BASF Seeks to Raise North American BDO in July. The Urethane Blog, June 1, 2016. https://everchem.com/butanediol-price-hike-announcement/ (accessed 22nd June 2020). (f) Independent Commodity Intelligence Services (ICIS), Reed Business Information Ltd. Toluene Uses and Market Data. March 7, 2008. https://www.icis.com/explore/resources/news/2007/11/07/9076550/toluene-uses-and-market-data/ (accessed 22nd June 2020). (g) European Chemicals Agency (ECHA). Substance Infocard: 1-Methyl-2-pyrrolidone. https://echa.europa.eu/substance-information/-/substanceinfo/100.011.662 (accessed 22nd June 2020). (h) European Chemicals Agency (ECHA). Substances Restricted under REACH, Annex XVII: Toluene. https://echa.europa.eu/substances-restricted-under-reach/-/dislist/details/0b0236e1807e2c14 (accessed 22nd June 2020). (i) European Chemicals Agency (ECHA). Substances Restricted under REACH, Annex XVII: 1-Methyl-2-pyrrolidone. https://echa.europa.eu/substances-restricted-under-reach/-/dislist/details/0b0236e1827f617f (accessed 22nd June 2020).

2. Prediction of Solvent Properties

2.1. Property-Led Solvent Design

Solvent design and selection is an active area of research, and numerous computer-aided methodologies have been developed by which to identify potentially greener or higher-performance solvents.[11–13] In this project, the testing schedule previously proposed by Jin et al. was adopted (**Figure 1**).[14] This series of investigative steps sequentially reduces the potential number of candidate solvents with a thorough understanding of solvent properties, safety, suitability towards scale-up and manufacturing, and environmental impact in the research and development phase. The methodical approach makes a robust case for commercial development if the results are favorable. Perhaps more importantly, it also identifies failings (e.g., poor performance or toxicity) at an early stage before further investment of time and money is made.

Alternatives to toluene and NMP were sought by surveying the known transformations of key intermediates (e.g., levoglucosenone) and evaluating whether the synthetic protocol and functionality of the product were suitable.[15,16] To predict the properties of solvent candidates, group contribution methods are available for the quick calculation of volatility, viscosity, density, and other properties. Polarity is perhaps the most crucial property to understand, as it governs solubility, reaction kinetics, and equilibria. There are many scales of solvent polarity, each appropriate for different circumstances. The Hansen solubility parameters relate to the solubility of solutes.[17] Dispersion forces (δ_D), dipolarity (δ_P), and hydrogen bonding (δ_H) are accounted for in the form of cohesive energy densities (units of $MPa^{½}$). The identification of Cyrene™ and TMO as valuable alternative solvents was guided by the similarity of their Hansen solubility parameters to those of NMP and toluene, respectively (**Figure 2**).[4,5,18] The Hansen solubility parameters can be rapidly calculated using appropriate software;[18] however the calculated properties must be interpreted with caution, appreciating the accuracy of the model and anticipating unexpected phenomena. An example of such phenomena arises from the combination of Cyrene™ and water, resulting in a geminal diol hydrate that can co-exist with Cyrene™. This has been exploited to control the solubility of small molecules.[19,20]

Another set of polarity measurements that are invaluable in solvent substitution are the Kamlet–Abboud–Taft (KAT) solvatochromic parameters.[21] The three KAT parameters of hydrogen-bond donating ability (α, zero for aprotic solvents including toluene and NMP), hydrogen-bonding accepting ability (β), and polarizability/dipolarity (π^*) can be correlated to rates of reaction and equilibrium constants. A method for calculating KAT solvatochromic parameters was developed for ReSolve (**Figure 3**).[22] This reduced the need to synthesize solvents and test polarity experimentally and consequently accelerated the solvent discovery pathway.

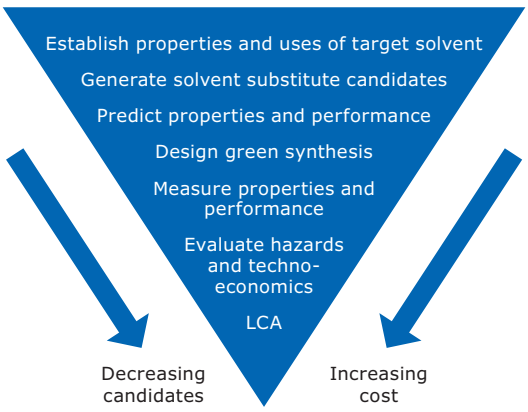

Figure 1. Hunt's Suggested Stages of New Solvent Development (LCA = Life Cycle Analysis). *(Ref. 14)*

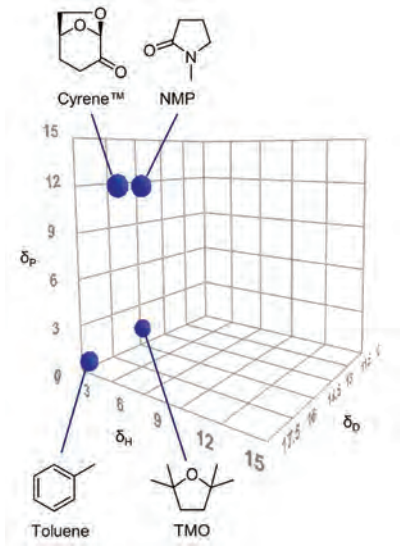

Figure 2. The Hansen Solubility Parameters of Cyrene™ and NMP (High Polarity), TMO and Toluene (Low Polarity). δ_D = Dispersion Forces, δ_P = Dipolarity, and δ_H = Hydrogen Bonding *(Ref. 4,5,18)*

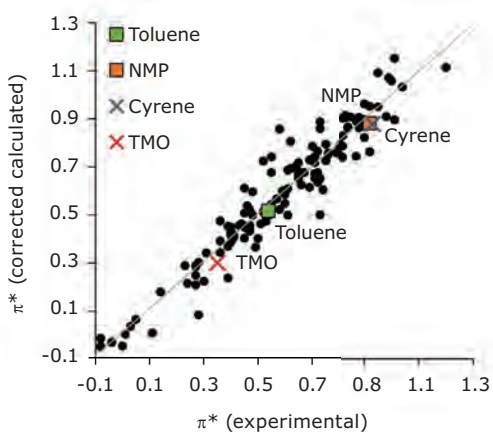

Figure 3. Calculation of the Polarizability/Dipolarity (π^*) KAT Parameter for Common Solvents, with Correction Factors Applied and Selected Solvents Overlaid. *(Ref. 22)*

Abraham's solvation parameter model uses a different approach by characterizing solutes according to the interactions they have with a solvent.[23] This approach was used in particular to understand the potential of TMO as a substitute for toluene. It revealed that, although TMO and toluene are generally similar, experimental partitioning of solutes in organic solvent–water systems demonstrated a more favorable extraction of alcohols and phenols into TMO due to its ability to accept hydrogen bonds from such solutes.[24,25] The properties of several hundred prospective solvents were calculated and the most promising synthesized for testing. Some of these solvents are discussed in this article and are shown in **Figure 4**.[4,15,16,26]

2.2. Toxicological Assessment

As an example of toxicological assessment, a series of succindiamides were designed to investigate whether these novel structures avoid the chronic toxicity of typical amide solvents.[26] *N*,*N*,*N*′,*N*′-tetra(*n*-butyl)succindiamide (TBSA), *N*,*N*′-diethyl-*N*,*N*′-di(*n*-butyl)succindiamide (EBSA), and *N*,*N*′-dimethyl-*N*,*N*′-di(*n*-butyl)succindiamide (MBSA) were synthesized and analyzed using an integrated approach of in silico and in vitro assessments (**Table 2**).[26] These assessments provide complementary information based on the notion that the in silico models use structural alerts of chemicals to predict biological behavior, whereas the in vitro methods use biological pathways to assess chemical behavior.

The in silico approach consisted of gathering any available adequate experimental toxicity data from ECHA's database,[27] performing quantitative structure–activity relationship (QSAR) model-based predictions,[28,29] and exploring read-across from similar structures with adequate experimental toxicity data or available QSAR predictions for the prioritized health endpoints of carcinogenicity, mutagenicity, reproductive toxicity, and skin sensitization.[30] The in vitro approach utilized the CALUX® battery of 18 reporter gene assays. These human cell-based assays provide information on the possibility of a test compound triggering certain molecular events that could result in adverse health effects.[31–35] The in silico predictions and data suggested that none of the succindiamides were likely to exhibit carcinogenicity, reproduction toxicity, or skin sensitization properties. For mutagenicity, neither data nor confident model predictions could be retrieved (see Table 2).

The in vitro tests also showed no convincing indications of toxicity, but rather induction of a detoxification pathway (PXR). Moreover, the bioassay activation profile of the succindiamides compared favorably with that of NMP. In the ReSolve project, this early-stage integrated safety assessment approach has been effectively employed as a fast, cost-effective, and animal-free method to help guide solvent development choices in this and similar examples.[26]

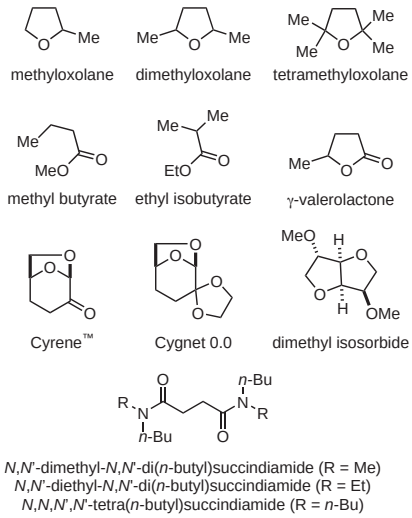

Figure 4. Some of the Most Promising Solvents Synthesized for Testing and Discussed in This Article. *(Ref. 4,15,16,26)*

Table 2. Results of the in Silico and in Vitro Assessment of Succindiamides. Key (in Silico): Absence of Property (-), Presence of Property (+), No Prediction Possible (?), Conclusion Based on Reliable Experimental Data (exp). In Vitro Assay Results Are Presented as "Lowest Effect Level" Concentrations (LogM) with Blank Entries Indicating No Effect Was Observed Up to the Highest Test Concentration. *(Ref. 26)*

	NMP	MBSA	EBSA	TBSA
in silico				
carcinogenicity	- (exp)	-	-	-
mutagenicity	- (exp)	?	?	?
reprotox	+ (exp)	-	-	-
skin sens	- (exp)	-	-	-
in vitro				
cytotox	-1.4	-2.3	-3.1	-3.4
PXR	-	-3.9	-5.0	-6.1
ERα	-	-	-	-
AR-anti	-	-	-	-
PR-anti	-	-	-	-
GR-anti	-	-	-	-
TRβ	-	-	-	-
TRβ-anti	-	-	-	-
AhR	-2.0	-	-	-
PPARα	-	-	-	-
PPARδ	-2.2	-	-	-
PPARγ	-	-	-	-
TCF	-2.5	-	-	-
AP1	-1.5	-	-	-
ESRE	-	-2.4	-	-
Nrf2	-	-2.9	-	-
p21	-2.0	-	-	-
p53	-	-	-	-

3. Applications of Solvents

Polyesters have been produced in THF, 2-MeTHF, 2,5-Me_2THF, and 2,2,5,5-tetramethyltetrahydrofuran (TMO) with catalysis by *Candida antarctica lipase B* (CaLB), and the results compared to those in the conventional solvent toluene.[36] Monomer conversions were superior in the ethers compared to toluene, and achievable at lower temperatures. TMO permitted the synthesis of poly(1,4-butylene adipate) with a M_n of >2000 Da at 50 °C, whereas reactions in toluene needed to be conducted at 85 °C over 6 hours to match monomer conversions and polymer molecular masses.

The radical polymerization of acrylates is also commonly performed in toluene. Ether solvents susceptible to α-proton abstraction prematurely terminate the reaction. Polymers with molecular weights equivalent to those prepared in toluene can be obtained in TMO (which lacks any α protons), methyl butyrate, and ethyl isobutyrate.[5,16]

Succindiamide solvents were evaluated for suitability for polymer processing, where a dipolar aprotic solvent is ordinarily used, by dissolving polyvinylidene fluoride (PVDF), polyethersulfone (PES), and polyamideimides (PAIs).[26] MBSA, EBSA, and TBSA could dissolve PVDF and PAIs, but only MBSA could fully dissolve PES. Based on this result, the successful fabrication of a PES membrane was carried out using MBSA. Unlike traditional dipolar aprotic solvents, the three succindiamides are immiscible with water, a property that could be advantageous in other applications.

The Suzuki–Miyaura coupling between phenylboronic acid and 4-bromotoluene, using [1,1′-bis(diphenylphosphino)ferrocene]-dichloropalladium(II) as a precatalyst, had been previously optimized, primarily through the quantity of water added, for the solvents Cyrene™ and dimethyl isosorbide.[37,38] Using an intermediate quantity of water (25 vol %), conversions to 4-phenyltoluene were 96% in dimethyl isosorbide and similar to those in NMP when the reaction was performed in γ-valerolactone and Cyrene™ (**Scheme 1**).[39]

A significant limitation of Cyrene™ is that it generally has poor stability towards inorganic bases, and may decompose at elevated temperatures.[40] An example of synthetic chemistry where stability at high temperatures in the presence of a base is necessary was attempted with the reaction of 4-bromoacetophenone and *N*-methylpyrrole at 150 °C (**Scheme 2**).[41] Cyrene™ and dimethyl isosorbide appeared to decompose shortly upon initiation of the reaction, and the desired product was not observed. However, Cygnet 0.0 (84% conversion) matched the performance of NMP.[41] Although it is a solid at room temperature, Cygnet 0.0 is appropriate for high-temperature, base-activated chemistry.[15]

4. Future Opportunities

The growing governmental support for bio-based products, coupled with the stringent regulations imposed on VOC emissions and other hazardous air pollutants, is creating opportunities for designing newer and greener solvents. Bio-based alternatives that meet the criteria of low toxicity and low VOC are likely to be considered as valid alternatives provided they meet the functional requirements of the fossil fuel derived equivalents. Moreover, the independence from fossil-fuel sources and potential biodegradability or compostability add value to bio-based solvents.

However, the perception of high production costs and the uncertainties about feedstock availability and future regulations could hamper the development of renewable solvents. To address this, a new EU funded project, ReSolute, will build on the success of ReSolve and develop the first commercial plant in Europe to scale up production of Cyrene™. The plant is expected to reach a production capacity of 1,000 tonnes per annum, using feedstock from non-food renewable biomass. The economy of scale provided by increased production will accelerate the use of Cyrene™ in a variety of applications where bio-derived alternatives to dipolar aprotic solvents are needed. Work has also begun on the large-scale synthesis and purification of TMO to demonstrate the feasibility of producing this solvent at a scale suitable for commercial activity.

5. Acknowledgments

This project has received funding from the Bio-Based Industries Joint Undertaking (JU) under the European Union's Horizon 2020 research and innovation programme under agreement No 745450. This article reflects only the authors' views and the JU is not responsible for any use that may be made of the information it contains.

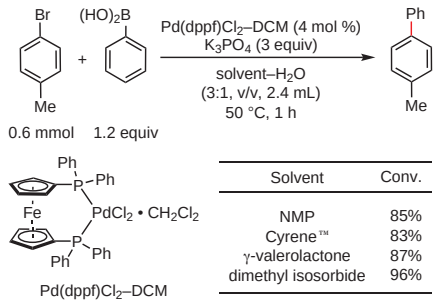

Scheme 1. Conversions in the Suzuki–Miyaura Coupling in the Model Reaction of 4-Bromotoluene with Phenylboronic Acid. *(Ref. 39)*

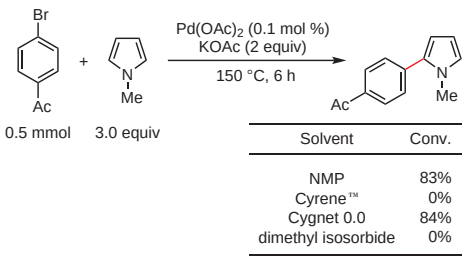

Scheme 2. Solvent Performance in the α-Arylation of *N*-Methylpyrrole. (*Ref. 41*)

6. References

(1) *Solvents and Solvent Effects in Organic Chemistry*, 4th ed.; Reichardt, C, Welton, T., Eds.; Wiley-VCH: Weinheim, 2011; Chapters 4 and 5, pp 107–357.
(2) ESIG, 2020. https://www.esig.org/wp-content/uploads/2020/01/ESIG-advocacy-document-triptic_WEB-2020February-2.pdf (accessed 18th September 2020).
(3) Sherwood, J.; Farmer, T. J.; Clark, J. H. *Chem* **2018**, *4*, 2010.
(4) Sherwood, J.; De bruyn, M.; Constantinou, A.; Moity, L.; McElroy, C. R.; Farmer, T. J.; Duncan, T.; Raverty, W.; Hunt, A. J.; Clark, J. H. *Chem. Commun.* **2014**, *50*, 9650.
(5) Byrne, F.; Forier, B.; Bossaert, G.; Hoebers, C.; Farmer, T. J.; Clark, J. H.; Hunt, A. J. *Green Chem.* **2017**, *19*, 3671.
(6) Camp, J. E. *ChemSusChem* **2018**, *11*, 3048.
(7) Lie, Y.; Ortiz, P.; Vendamme, R.; Vanbroekhoven, K.; Farmer, T. J. *Ind. Eng. Chem. Res.* **2019**, *58*, 15945.
(8) Ad-hoc Advisory Group for Bio-based Products in the framework of the European Commission's Lead Market Initiative. In *Taking Bio-Based from Promise to Market, Measures to Promote the Market Introduction of Innovative Bio-Based Products*; European Commission Publications Office of the European Union, November 3, 2009 (DOI: 10.2769/34881).
(9) Sherwood, J. *Bioresour. Technol.* **2020**, *300*, 122755.
(10) Hermann, B. G.; Blok, K.; Patel, M. K. *Environ. Sci. Technol.* **2007**, *41*, 7915.
(11) Moity, L.; Molinier, V.; Benazzouz, A.; Barone, R.; Marion, P.; Aubry, J. -M. *Green Chem.* **2014**, *16*, 146.
(12) Austin, N. D.; Sahinidis, N. V.; Konstantinov, I. A.; Trahan, D. W. *AIChE J.* **2018**, *64*, 104.
(13) Struebing, H.; Obermeier, S.; Siougkrou, E.; Adjiman, C. S.; Galindo, A. *Chem. Eng. Sci.* **2017**, *159*, 69.
(14) Jin, S.; Byrne, F.; McElroy, C. R.; Sherwood, J.; Clark, J. H.; Hunt, A. J. *Faraday Discuss.* **2017**, *202*, 157.
(15) Alves Costa Pacheco, A.; Sherwood, J.; Zhenova, A.; McElroy, C. R.; Hunt, A. J.; Parker, H. L.; Farmer, T. J.; Constantinou, A.; De bruyn, M.; Whitwood, A. C.; Raverty, W.; Clark, J. H. *ChemSusChem* **2016**, *9*, 3503.
(16) Byrne, F. P.; Forier, B.; Bossaert, G.; Hoebers, C.; Farmer, T. J.; Hunt, A. J. *Green Chem.* **2018**, *20*, 4003.
(17) *Hansen Solubility Parameters: A User's Handbook*, 2nd ed.; Hansen, C. M., Ed.; CRC Press: Boca Raton, FL, 2007; pp 4–17.
(18) Hansen Solubility Parameters in Practice (HSPiP), 2020. Hansen Solubility Parameters and HSPiP Software Web Site. https://www.hansen-solubility.com/HSPiP/ (accessed 22nd June 2020).
(19) De bruyn, M.; Budarin, V. L.; Misefari, A.; Shimizu, S.; Fish, H.; Cockett, M.; Hunt, A. J.; Hofstetter, H.; Weckhuysen, B. M.; Clark, J. H.; Macquarrie, D. J. *ACS Sustainable Chem. Eng.* **2019**, *7*, 7878.
(20) Bousfield, T. W., Pearce, K. P. R.; Nyamini, S. B.; Angelis-Dimakis, A.; Camp, J. E. *Green Chem.* **2019**, *21*, 3675.
(21) Kamlet, M. J.; Abboud, J.-L. M.; Abraham, M. H.; Taft, R. W. *J. Org. Chem.* **1983**, *48*, 2877.
(22) Sherwood, J.; Granelli, J.; McElroy, C. R.; Clark, J. H. *Molecules* **2019**, *24*, 2209.
(23) Abraham, M. H.; Ibrahim, A.; Zissimos, A. M. *J. Chromatogr. A* **2004**, *1037*, 29.
(24) Byrne, F. P.; Hodds, W. M.; Shimizu, S.; Farmer, T. J.; Hunt, A. J. *J. Cleaner Prod.* **2019**, *240*, 118175.
(25) Churchill, B.; Acree, W. E.; Abraham, M. H. *Phys. Chem. Liq.* **2019**, DOI: 10.1080/00319104.2019.1675161.
(26) Byrne, F. P.; Nussbaumer, C. M.; Savin, E. J.; Milescu, R. A.; McElroy, C. R.; Clark, J. H.; van Vugt-Lussenburg, B. M. A.; van der Burg, B.; Meima, M. Y.; Buist, H. E.; Kroese, E. D.; Hunt, A. J.; Farmer, T. J. *ChemSusChem* **2020**, *13*, 3212.
(27) Registered Substances, 2020. European Chemicals Agency (ECHA) Web Site. https://echa.europa.eu/information-on-chemicals/registered-substances (accessed 22nd June 2020).
(28) Vega Hub, 2020. Istituto di Ricerche Farmacologiche Mario Negri IRCCS Web Site. https://www.vegahub.eu/about-vegahub/ (accessed 22nd June 2020).
(29) Danish (Q)SAR Database Web Site. http://qsar.food.dtu.dk/ (accessed 22nd June 2020).
(30) Guidance on Grouping of Chemicals, 2nd ed.; OECD Series on Testing and Assessment No. 194, April 14, 2014; OECD Environment, Health and Safety Publications. http://www.oecd.org/officialdocuments/publicdisplaydocumentpdf/?cote=env/jm/mono(2014)4&doclanguage=en (accessed 2nd September 2020)
(31) Piersma, A. H.; Bosgra, S.; van Duursen, M. B. M.; Hermsen, S. A. B.; Jonker, L. R. A.; Kroese, E. D.; van der Linden, S. C.; Man, H.; Roelofs, M. J. E.; Schulpen, S. H. W.; Schwarz, M.; Uibel, F.; van Vugt-Lussenburg, B. M. A.; Westerhout, J.; Wolterbeek, A. P. M.; van der Burg, B. *Reprod. Toxicol.* **2013**, *38*, 53.
(32) Schenk, B.; Weimer, M.; Bremer, S.; van der Burg, B.; Cortvrindt, R.; Freyberger, A.; Lazzari, G.; Pellizzer, C.; Piersma, A.; Schäfer, W. R.; Seiler, A.; Witters, H.; Schwarz, M. *Reprod. Toxicol.* **2010**, *30*, 200.
(33) Van der Burg, B.; Pieterse, B.; Buist, H.; Lewin, G.; van der Linden, S. C.; Man, H.; Rorije, E.; Piersma, A. H.; Mangelsdorf, I.; Wolterbeek, A. P. M.; Kroese, E. D.; van Vugt-Lussenburg, B. *Reprod. Toxicol.* **2015**, *55*, 95.
(34) Van der Burg, B.; van der Linden, S.; Man, H.; Winter, R.; Jonker, L.; van Vugt-Lussenburg, B.; Brouwer, A. A Panel of Quantitative Calux® Reporter Gene Assays for Reliable High-Throughput Toxicity Screening of Chemicals and Complex Mixtures. In *High-Throughput Screening Methods in Toxicity Testing*; Steinberg, P., Ed.; Wiley: Hoboken, NJ, 2013; pp 519–532.
(35) Van der Burg, B.; Wedebye, E. B.; Dietrich, D. R.; Jaworska, J.; Mangelsdorf, I.; Paune, E.; Schwarz, M.; Piersma, A. H.; Kroese, E. D. *Reprod. Toxicol.* **2015**, *55*, 114.
(36) Pellis, A.; Byrne, F. P. Sherwood, J.; Vastano, M.; Comerford, J. W.; Farmer, T. J. *Green Chem.* **2019**, *21*, 1686.
(37) Wilson, K. L.; Murray, J.; Jamieson, C.; Watson, A. J. B. *Synlett* **2018**, *29*, 650.
(38) Wilson, K. L.; Murray, J.; Sneddon, H. F.; Jamieson, C.; Watson, A. J. B. *Synlett* **2018**, *29*, 2293.
(39) Sherwood, J. *Beilstein J. Org. Chem.* **2020**, *16*, 1001.
(40) Wilson, K. L.; Kennedy, A. R.; Murray, J.; Greatrex, B.; Jamieson, C.; Watson, A. J. B. *Beilstein J. Org. Chem.* **2016**, *12*, 2005.
(41) Bensaid, S.; Doucet, H. *Comptes Rendus Chimie* **2014**, *17*, 1184.

Trademarks. CALUX® (Xenobiotic Detection Systems International, Inc.); Cyrene™ (Circa Group Pty Ltd).

About the Authors

James Sherwood is a postdoctoral research associate at the Green Chemistry Centre of Excellence, University of York. His research interests include solvent effects in organic synthesis and bio-based solvents.

Harrie E. Buist is a senior toxicological risk assessor at the Netherlands Organisation for Applied Scientific Research (TNO). His key areas of expertise include the risk assessment of pesticides, industrial chemicals, and nanoparticles as well as the application of in silico hazard assessment methods.

Bart van der Burg is the Director of Innovation at BioDetection Systems (BDS). Until 2002, he was a senior scientific staff member at the Hubrecht Institute of the Royal Netherlands Academy of Sciences in Utrecht, working on the mechanism of action of steroid hormones, after which he joined BDS as Director of Innovation. He has ample experience in open innovation and as a leader of academic and industrial research and innovation groups of varying composition. Bart has also served as a coordinator of various large-scale collaborative research projects.

Fergal P. Byrne is a postdoctoral research associate at the Green Chemistry Centre of Excellence, University of York. His research focuses on green solvent design and synthesis.

Jason E. Camp is the Chief Technology Officer of Circa Group. He has over 10 years of experience as an independent academic at various U.K. universities during which he conducted research and published extensively in the areas of green chemistry and sustainable solvents, including Cyrene™.

Thomas J. Farmer's research covers the development and application of greener synthetic methods, including heterogeneous catalysis and microwave, ultrasound, and flow reactors. He has also published extensively around the topic of bio-derived platform molecules and their use in the synthesis of polymers, chelators, surfactants, and solvents. Tom led the work on application testing in the ReSolve project, while also being involved in the development of TMO and the derivatization of levoglucosenone to form polar aprotic solvents.

E. Dinant Kroese is senior scientist at TNO. He has over 30 years of experience in risk assessment of chemicals with a focus on chemical carcinogens. The development and validation of new-approach methodologies in risk assessment is his more recent area of interest.

Marie Y. Meima holds a master's degree in toxicology and environmental health and is employed at TNO as a junior scientist. Her research is focused on human-risk assessment of chemicals based on the scientific literature and the application of various in silico hazard assessment tools.

David Méndez Sevillano holds a master's degree in chemical engineering from the University of Valladolid (Spain) with training at the Budapest University of Technology and Economics (Hungary). He earned his Ph.D. degree from Delft University of Technology (The Netherlands), where he also did postdoctoral training in biochemical engineering. He has worked as a process engineer for more than 3 years with the Process Design Centre (The Netherlands), helping to design (bio)processes with a special emphasis on phase extraction (LLE or SLE) and performing conceptual designs and techno-economical evaluations.

Ángel Puente holds a master's degree in synthetic, industrial, and applied chemistry and a Ph.D. degree in organic chemistry from the University of the Basque Country (UPV-EHU) in Spain. His Ph.D. dissertation was based on the design and synthesis of novel organic catalysts and their application in new catalytic and enantioselective reactions. In particular, he investigated the suitability of new organic catalysts for water-containing systems. He is currently involved in various projects on the circular economy as a consultant and Life Cycle Assessments (LCA) analyst.

Barbara M. A. van Vugt-Lussenburg is a senior researcher at BDS. Her key areas of expertise include hepatic metabolism, robotics, and the development and automation of high-throughput, cell-based assays.

James H. Clark is Professor of Chemistry at the University of York and is a founding director of the Green Chemistry Centre of Excellence and the Bio-renewables Development Centre. He was recently appointed Chair Professor at Fudan University in China, and he holds Visiting Professorships in South Africa and China. He started the award-winning company Starbons Ltd, and is now involved in the commercialization of other green technologies. He was a founding scientific editor of the journal *Green Chemistry* and is editor in chief of the RSC Green Chemistry book series. His research involves the application of green chemical technologies to waste or low-value feedstocks, notably biomass, to create new green and sustainable supply chains for chemicals and materials. His research work and his educational work have led to numerous awards, including honorary doctorates from universities in Belgium, Germany, and Sweden as well as prizes from the RSC, SCI, ACS, and EU. In 2018, he won the RSC Green Chemistry Prize. He has published over 500 articles (*h*-index of 77) and written or edited over 20 books.

Greener Alternatives Platform

MilliporeSigma's Commitment to Advancing Scientific Research on the Basis of Green Chemistry Principles

Awareness of the importance of protecting and preserving the natural environment and of the need for sustainable development has grown significantly in the second half of the 20th century and the first two decades of this century. Throughout this whole time, the spotlight has been focused on the industrial-scale use and disposal of chemicals, in particular hazardous ones, in the environment, since the uncontrolled use and irresponsible disposal of such can have a profound effect on the health of all living organisms. Societies and institutions worldwide are demanding that safeguards be put in place to ensure that chemicals are used and disposed of in a responsible manner that minimizes or eliminates their adverse effects on ecosystems.

The need to develop benign and sustainable production processes has contributed to the rise of what has become known as "Green Chemistry", which aims to ensure that the generation of chemicals, materials, and energy are sustainable and safe. Green chemistry has been defined as the design, invention, and application of chemical products to reduce or eliminate the use and generation of hazardous substances.[1] The practice of green chemistry is beneficial environmentally, socially, and economically. If this approach is not adopted by industry, industrial chemistry would not be sustainable in the long run. In their seminal book, *Green Chemistry: Theory and Practice*, Paul T. Anastas and John C. Warner set the raison d'être of this approach when they articulated the 12 principles of green chemistry (**Figure 1**).[1] These principles can light the way for chemists to fulfill their unique and vital role in achieving sustainable development.

Figure 1. Graphical Summary of the Twelve Principles of Green Chemistry. *(Ref. 1)*

1. Greener Alternatives

MilliporeSigma has been committed to advancing scientific research on the basis of the 12 principles of green chemistry. The result has been a growing, uncompromising, and diverse portfolio of greener alternative products that the researcher can take advantage of to reduce the environmental impact of his or her research. The portfolio consists of four categories of products: re-engineered, enabling, 12-principles-aligned, and design-for-sustainability (DfS) developed products.[2]

1.1. Re-engineered Products

Re-engineered products are those that are prepared through re-engineering or modification of an existing synthetic process by utilizing fewer resources, less hazardous reactants, or by simply applying green chemistry principles. To evaluate the relative greenness of a process, the DOZN™ 2.0 tool can be employed to obtain confirmatory documentation validating the green characteristics of the process and helping to enhance its overall sustainability.[3] In DOZN™ 2.0 matrix calculation, a synthetic process receives an aggregate score on a scale of 0 to 100, with 0 being the most sustainable and thus most desirable. A small selection of re-engineered products exhibiting a dramatic drop in DOZN™ score is featured in **Table 1**.[4] The drop indicates

Table 1. Examples of Products Re-engineered for Better Alignment with Green Chemistry Principles. *(Ref. 4)*

		Process DOZN™ Score		
Prod. No.	Prod. Name	Old	Re-engineered	%Δ
A7005	β-Amylase from sweet potato Type I-B	57	1	98%
656453	1,3,5-Tris(4-iodophenyl)-benzene	100	16	84%
694460	3,3′′′-Dihexyl-2,2′:5′,2′′:5′′,2′′′-quaterthiophene	82	24	71%
N7004	β-Nicotinamide adenine dinucleotide hydrate	56	20	64%
A3940	1-Aminobenzotriazole	93	46	51%
N2132	4-Nitrophenyl β-D-xylopyranoside	100	51	49%
705977	2-Methyloxazole-4-carboxaldehyde	94	54	43%
324612	(*S*)-(−)-3-Chloro-1-phenyl-1-propanol	100	62	38%

that the new process is more sustainable, since it is better aligned with green chemistry principles relating to minimization of waste, the use of more benign solvents and auxiliaries, and to designing for energy efficiency.

1.2. Twelve-Principles-Aligned Products

Examples in this group include biorenewable solvents such as acetone and 1-butanol, greener chromatography solvents such as heptane, greener substitute solvents such as Cyrene™, catalysts, and biodegradable surfactants (**Table 2**).[5,6]

1.3. Enabling Products

These are products that empower research on alternative energy and make greener alternatives possible through enabling technologies. They are typically used for energy generation and storage and for boosting efficiency; they belong to two categories—materials science enabling products and other enabling products (**Table 3**).[7-9] For example, lithium phosphate monobasic and lithium manganese oxide are materials science enabling products used in the fabrication of rechargeable lithium-ion batteries as electrolytic and electrode materials.[7] Other materials science enabling products include carbonaceous materials employed as anodes in lithium-ion batteries and iodide- and bromide-based alkylated halides utilized as precursors in the fabrication of perovskites for photovoltaic (solar) cells.[8] Other enabling products include enzymes and reagents employed in biofuel research such as biodiesel and ethanol fuel research.

1.4. Design-for-Sustainability Products

Design-for-sustainability (DfS) developed products enable a sustainable development that meets the needs of the current generation without compromising the ability to meet the needs of future generations. According to Elkington's "triple bottom line" (3BL or TBL),[10] the three sustainability components are (i) economic prosperity, (ii) environmental quality, and (iii) social justice. Presently, these are referred to as the "triple P" (3P): profit, planet, and people. Examples of DfS products include Stericup® E and Steritop® E filtration systems (**Table 4**).[11] These new filters demonstrate significant sustainability characteristics in comparison to traditional Stericup® and Steritop® sterile filters, since a considerable reduction in the use of plastic and packaging materials is achieved. Stericup® E sterile filter eliminates the need for disposable filter funnels, whereas Steritop® E sterile filter eliminates both the disposable filter funnel and the receiver bottle, thus reducing the environmental impact in multiple ways.

2. References

(1) Anastas, P. T.; Warner, J. C. *Green Chemistry: Theory and Practice*; Oxford University Press: Oxford, U.K., 1998.

(2) For a full listing of the products within the greener alternatives portfolio, see https://www.sigmaaldrich.com/chemistry/greener-alternatives.html.

Table 3. Examples of Enabling Products. *(Ref. 7–9)*

Prod. No.	Prod. Name	Type	Class	Category
442682	Lithium phosphate monobasic	Enabling Product	Electrolyte	Materials Science
765201	Lithium manganese oxide	Enabling Product	Electrolyte	Materials Science
805971	Acetamidinium iodide	Enabling Product	Perovskite Precursor	Materials Science
806196	Benzylammonium iodide	Enabling Product	Perovskite Precursor	Materials Science

Table 4. Examples of Design-for-Sustainability (DfS) Developed Products. *(Ref. 11)*

Prod. No.	Prod. Name	Type	Class	Category
SEGPU1145	Stericup® E-GP 1,000 mL, 0.2 µm, 45 mm	DfS Product	Sterile Filter	Waste Reduction
SEGPT0045	Steritop® E-GP 150-1,000 mL, 0.2 µm, 45 mm	DfS Product	Sterile Filter	Waste Reduction

Table 2. Examples of Products Aligned with One or More of the Twelve Principles of Green Chemistry. *(Ref. 5,6)*

Prod. No.	Prod. Name	Type	Class	Principle
904082	Acetone	Biorenewable	Solvent	5 and 7
901351	1-Butanol	Biorenewable	Solvent	5 and 7
592579	Heptane	Chromatography	Solvent	5
807796	Cyrene™	Greener Substitute	Solvent	4
901235	TBS-DHG Catalyst	Regenerable & Reusable	Catalyst	9
STS0006	ECOSURF™ EH-9, non-ionic surfactant	Biodegradable	Surfactant	10
STS0001	TERGITOL™ 15-S-30, non-ionic surfactant	Biodegradable	Surfactant	10
STS0005	Triton™ CG-110, non-ionic surfactant	Biodegradable	Surfactant	10

(3) DeVierno Kreuder, A.; House-Knight, T.; Whitford, J.; Ponnusamy, E.; Miller, P.; Jesse, N.; Rodenborn, R.; Sayag, S.; Gebel, M.; Aped, I.; Sharfstein, I.; Manaster, E.; Ergaz, I.; Harris, A.; Grice, L. N. *ACS Sustainable Chem. Eng.* **2017**, *5*, 2927.
(4) To view the full list of re-engineered products, see https://www.sigmaaldrich.com/chemistry/chemistry-products.html?TablePage=119262232.
(5) To view the full list of twelve-principles-aligned products, see https://www.sigmaaldrich.com/chemistry/chemistry-products.html?TablePage=119262253.
(6) Prat, D.; Pardigon, O.; Flemming, H.-W.; Letestu, S.; Ducandas, V.; Isnard, P.; Guntrum, E.; Senac, T.; Ruisseau, S.; Cruciani, P.; Hosek, P. *Org. Process Res. Dev.* **2013**, *17*, 1517.
(7) Goodenough, J. B.; Park, K.-S. *J. Am. Chem. Soc.* **2013**, *135*, 1167.
(8) Kalyanasundaram, K.; Zakeeruddin, S. M.; Grätzel, M. *Mater. Matters* **2016**, *11* (1), 3.
(9) To view the full list of enabling products, visit https://www.sigmaaldrich.com/chemistry/chemistry-products.html?TablePage=119262252.
(10) Elkington, J. *Calif. Manage. Rev.* **1994**, *36*, (2), 90 (DOI: 10.2307/41165746).
(11) To view the full list of design-for-sustainability (DfS) developed products, visit https://www.sigmaaldrich.com/chemistry/chemistry-products.html?TablePage=127560657.

Sigma-Aldrich®
Lab & Production Materials

MilliporeSigma

Biodegradable Greener Surfactants

Minimize Your Environmental Footprint

We believe that green chemistry will contribute to a better tomorrow. With a growing portfolio of greener alternatives, there are now more choices to reduce the ecological impact of your research while still delivering quality and efficacy so your results are not compromised.

To help aid you in reducing the environmental footprint of your research, we offer numerous chemically stable products that break down into innocuous degradation products and do not persist in the environment at the end of their function.

These products are aligned with the “Design for Degradation” principle of The 12 Principles of Greener Chemistry to meet your research and production needs.

TERGITOL™ 15-S and ECOSURF™ surfactants are readily biodegradable per OECD 301F (>60% biodegradation within 28 days).

Biodegradable without compromised quality

Catalog No.	Product Name
15S7	TERGITOL™ 15-S-7
15S9	TERGITOL™ 15-S-9
STS0001	TERTIGOL™ 15-S-30
STS0002	TERGITOL™ 15-S-40
STS0003	TERGITOL™ 15-S-40 solution
STS0005	Triton™ CG-110
STS0006	ECOSURF™ EH-9
STS0007	ECOSURF™ SA-9
STS0012	ECOSURF™ EH-9 solution 90% in water
STS0013	TERGITOL™ 15-S-5
STS0014	TERGITOL™ 15-S-15
STS0015	ECOSURF™ EH-3
STS0016	ECOSURF™ EH-6
STS0017	ECOSURF™ SA-4
STS0018	ECOSURF™ SA-7
STS0019	TERGITOL™ 15-S-3
STS0020	TERGITOL™ 15-S-12
STS0021	TERGITOL™ 15-S-20 solution

Explore our complete range of greener alternatives at:

SigmaAldrich.com/greenchemistry

The life science business of Merck KGaA, Darmstadt, Germany operates as MilliporeSigma in the U.S. and Canada.

MilliporeSigma

Exceptional variety.
Quick delivery.

NOW!

All you need to keep your discoveries moving forward. Breakthrough ideas require access to the basics. That's why we remain committed to providing you with an unmatched chemical and biochemical portfolios, with many products shipping the same day your order is placed.

Visit, SigmaAldrich.com/Chemistry to order SCIENCESATIONAL

Sigma-Aldrich®
Lab & Production Materials

MilliporeSigma
P.O. Box 14508
St. Louis, MO 63178
USA

Acta Archive Indexes

The Acta Archive Indexes document provides easy searching of all of the Acta content; 1968 to the present.

The volumes, issues, and content are sorted as follows:

- Chronological
- Authors
- Titles
- Affiliations
- Painting Clues (by volume)

Using the sorted sections, you can locate reviews by various authors or author affiliation. Additionally, the content is fully searchable, allowing you to look for a particular key word from the various data available. Once you identify a topic and which volume/issue it is in, you can access it via the archive table.

To access the index, **click here**.

2017-02521
11/2018